Palladium and Platinum Dithioacetylacetonates and their Structural Analogues

Joan H. Leslie

Ph.D. Thesis
University of Edinburgh
1983

Declaration

Except where specific reference is made to other sources, the work presented in this thesis is the original work of the author. It has not been submitted, in whole or in part, for any other degree. Certain of the results presented have already been published.

Joan H. Leslie

To Derek

Acknowledgments

I wish to thank Dr. G.A. Heath for his help and encouragement throughout this work. I also wish to thank Mrs Mina Sharma for her contribution to the $[Co(SacSac)_2]$ study and to Dr. L.J. Yellowlees for her invaluable help with O.T.T.L.E. work. In addition, I am grateful to Mr. J.R.A. Millar and Dr. I.H. Sadler for recording N.M.R. spectra, and to the latter for useful discussion, and to Mr. M. Grunbaum for performing microanalytical measurements. I am deeply indebted to the S.E.R.C. for their financial support and the University of Edinburgh for the use of facilities. Finally, my thanks to Miss A. Erskine for typing this thesis.

Abstract

Chapter 1 briefly discusses the stereochemical effect of replacing oxygen with sulphur as donor atoms, with particular reference to the β-diketonate complexes and their thio-analogues.

Chapter 2 describes the synthetic procedures applied to extend the range of planar dithio-β-diketonate complexes of palladium and platinum, their subsequent characterisation by a number of spectroscopic techniques and comparison with the analogous nickel complexes.

Chapter 3 discusses the electrochemical behaviour of the Ni, Pd and Pt dithio-β-diketonates. The complexes undergo two successive one-electron reductions, with a marked tendency for the monoanion to undergo a rearrangement reaction. Reduction potentials are strongly influenced by the inductive nature of ligand substituent groups, and comparison with related systems suggests the redox-active orbital of the 1,3-dithio complexes is of largely ligand character. Our study was extended to include a number of isostructural palladium β-diketonate complexes and preliminary work concerning nickel monothio-β-diketonates.

Chapter 4 presents a detailed kinetic study of the rearrangement of the one-electron reduced species by cyclic voltammetry, showing it to be a dimerisation reaction. Measurements over a temperature range yield activation parameters which are also in line with a bimolecular reaction.

Chapter 5 describes the synthesis and electrochemical characterisation of a number of cobalt(II) dithio-β-diketonates. A concentration study of $[Co(SacSac)_2]$ shows anomalous behaviour when using mercury as a working electrode. Reversible reaction with dioxygen is also discussed briefly.

List of Contents

		Page
Chapter 1	Relative effects of oxygen and sulphur donor atoms in transition metal complexes	1
	References	9
Chapter 2	The dithio-β-diketonate complexes of nickel, palladium and platinum: synthesis and characterisation	10
	2.1 Introduction	11
	2.2 Synthesis and Characterisation	16
	2.3 Experimental	27
	References	38
Chapter 3	Electrochemical studies of palladium and platinum bis-dithio-acetylacetonates and their structural analogues	40
	3.1 Introduction	41
	3.2 Voltammetry of $[M(SacSac)_2]$ complexes	45
	3.3 The substituted complexes	48
	3.4 Comparison with the oxo system	63
	3.5 Experimental	68
	References	75

		Page
Chapter 4	The monoanion rearrangement:- A kinetic study	77
	4.1 Introduction	78
	4.2 Qualitative study of the $[M(SacSac)_2]^{1-}$ rearrangement reaction	91
	4.3 Kinetic and activation parameter analysis for monoanion rearrangements	102
	4.4 Implications of the kinetic analysis	117
	4.5 Experimental	124
	References	130
Chapter 5	Cobalt(II)bis(dithio-β-diketonates)	133
	5.1 Introduction	134
	5.2 The substituted Co(II)bis(dithio-β-diketonates)	143
	5.3 Complexities in the voltammetry of $[Co(SacSac)_2]$ - Electrode adsorption phenomena (concentration dependence at the d.m.e.)	150
	5.4 Reaction with dioxygen	155
	5.5 Experimental	158
	References	162

List of Figures

		Page
Figure 2.1	^{1}H n.m.r. of $[Pt(SacSac)_2]$, showing ^{195}Pt satellites	18
2.2	^{13}C n.m.r. spectrum of $[Pt(SacSac)_2]$	19
2.3	Infrared spectra of $[M(S_2C_3CF_3HCH_3)_2]$	21
2.4	Infrared spectra of $[Pd(SOC_3PhHPh)_2]$ and $[Pd(S_2C_3PhHPh)_2]$	25
3.1	Schematic π-molecular orbital energy level diagram	43
3.2	Complementary a.c., d.c. and C.V. data for $[Pd(SacSac)_2]$	47
3.3	Cyclic voltammogram of $[Ni(SacSac)_2]$ in CH_2Cl_2 showing oxidation to $[S_2C_3CH_3HCH_3]^+$ and its subsequent reduction	49
3.4	Electrochemical behaviour of $[Pd(S_2C_3CF_3HCH_3)_2]$	50
3.5	Reduction potential *vs*. Taft parameter for the $[M(S_2C_3RHR')_2]$ complexes	53
3.6	Electrochemical production of $[S_2C_3CF_3HCH_3]^+$ by the irreversible oxidation of $[Ni(S_2C_3CF_3HCH_3)_2]$, and its subsequent reduction	60
3.7	Substituent sensitivity for delocalised organosulphur systems	62
3.8	Reduction potential/substituent effect correlations for $[Pd(X_2C_3RHR')_2]$ systems, (X = O, S)	67

		Page
Figure 3.9	D.c. voltammogram of $[Pd(S_2C_3CF_3HCH_3)_2]$ using r.p.e., showing two reduction waves of equal height	70
3.10	Frequency dependence (a.c. measurements, first and second reductions) for $[Pd(S_2C_3CF_3HCH_3)_2]$	72
4.1	Variation of anodic current with switching potential	83
4.2	Cyclic voltammetry of $[M(SacSac)_2]$	93
4.3	C.V. of $[Pd(SacSac)_2]$ showing temperature dependence	95
4.4	Electronic spectra of $[Pt(SacSac)_2]$ and its electrogenerated dimer	98
4.5	O.T.T.L.E. generated spectra of $[Pt(SacSac)_2]^{1-}$ dimerisation in the visible region, showing isosb estic points	99
4.6	Variation of ia/ic with kinetic parameter for a dimerisation reaction (with $\emptyset$ = zero and $a\tau$ = 4)	104
4.7	Typical cyclic a.c. voltammogram for the one-electron reduction of $[Pt(SacSac)_2]$	114
4.8	The determination of activation parameters for the $[Pt(SacSac)_2]^{1-}$ dimerisation reaction	119
4.9	Variation of the diffusion-limited current with changing temperature	121

Page

Figure 4.10 The variation of ia/ic with ω, for $\emptyset$ = zero 127

4.11 Cyclic voltammogram defining the parameters $(ic)_o$, $(is)_o$ and $(ia)_o$ used to determine the ratio ia/ic 129

5.1 The use of C.V. to monitor the reaction of $[Co(SacSac)_2]^{1-}$ with MeI 141

5.2 Electrode potential/substituent effect for the $[Co(S_2C_3RHR')_2]$ complexes 148

5.3 Electrochemical behaviour of $[Co(SacSac)_2]$ in the a.c. mode, showing effects of changing working electrode 151

5.4 Variation of current response with changing concentration for the adsorption wave of $[Co(SacSac)_2]$ at the d.m.e. 152

List of Tables

		Page
Table 2.1	Principal infrared assignments for the $[M(S_2C_3RHR')_2]$ complexes	23
3.1	Electrode potentials for the complexes $[M(S_2C_3RHR')_2]$	52
3.2	Substituent inductive parameters	55
3.3	Linear E^o/inductive parameter correlations in $[M(X_2C_3RHR')_2]$	57
3.4	Electrode potentials for the electrochemically derived 1,2-dithiolylium ions	59
3.5	Electrode potentials for diketonato and monothio-diketonato complexes	66
4.1	Rate constant determination of $[Pt(SacSac)_2]^{1-}$ dimerisation: Variation of concentration	106
4.2	Rate constant determination of $[Pt(SacSac)_2]^{1-}$ dimerisation: Variation of scan rate	108
4.3	Rate constant determination using a single cyclic voltammogram	109
4.4	Calculated rate constants for the $[Pt(SacSac)_2]$ complex	110
4.5	Rate constants for the dimerisation of $[M(SacSac)_2]^{1-}$ at 293 Kelvin	112
4.6	Comparison of activation energies for bimolecular reactions	116

Page

Table 5.1 Comparison of reduction potentials for the series $[M(S_2C_3RHR')_2]$, where M = nickel and cobalt 146

5.2 Linear E^o/inductive parameter correlations in $[M(S_2C_3RHR')_2]$, where M = nickel and cobalt 147

CHAPTER 1

Relative Effects of Oxygen and Sulphur Donor Atoms in Transition Metal Complexes

Over the past fifteen years there has been a considerable resurgence of interest in the area of sulphur ligand chemistry. Ligand systems with sulphur donor atoms are chemically very versatile, forming a wide variety of stable compounds with transition metal ions, which display interesting, and often novel, properties and structures. In addition, the importance of metal-sulphur systems in biochemical contexts has prompted the study of various compounds as possible models for biological activity.

Much work has centred around the systematic investigation of compounds formed by substitution of oxygen by sulphur, in order to establish a better understanding of the effects of donor atom variation. Livingstone provided an early review of complexes containing sulphur, selenium and tellurium donor atoms[1], attempting to compare the coordinating ability of oxygen and sulphur donors with such fundamental parameters as ionization energies, electronegativities, polarizabilities, dipole moments and π-bonding effects. While this presented a number of useful qualitative generalisations, later discoveries have led to new, sometimes striking, observations on the effect of sulphur coordination in particular contexts, and especially in unsaturated, resonance-stabilized systems.

A systematic study, more relevant to the present work, was accomplished by Holm et al[2-5] on the stereochemical and electronic effects of sulphur donor

substitution in a variety of structurally related chelate ligands (i).

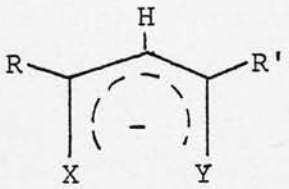

(i)

(a) X = Y = O; β-diketonate

(b) X = O, Y = S; monothio-β-diketonate

(c) X = O, Y = NR; β-ketoamine

(d) X = S, Y = NR; β-aminothione

By the detailed comparison of complexes, identical in constitution except for their donor atom sets, the particular stereochemical consequences were assessed. Thus, sulphur tends to stabilize the planar form of monomeric complexes, particularly of Ni(II) and Co(II). These trends can be ideally illustrated by the following examples.

To examine the effect of donor atom variation on stereochemistry, consider the Ni(II) mixed donor complexes of (i) c and (i)d, <u>i.e.</u> [Ni(β-ketoamine)$_2$] and [Ni(β-aminothione)$_2$][4,5]. Both types exhibit planar $\rightleftharpoons$ tetrahedral equilibria. The higher proportion of the planar isomer at equilibrium for the β-aminothione complex than for the β-ketoamine, directly illustrates the greater tendency for sulphur to stabilize the planar geometry than oxygen.

By measuring the temperature dependence of ΔG for the planar-tetrahedral conversion, a complete set of thermodynamic data was collected. Analysis shows that the differences in stereochemical populations are due to enthalpy rather than entropy considerations[4]. The greater stability of the planar stereochemistry for the β-aminothiones is attributed to the larger extent of ligand/metal/ligand π-bonding superimposed on the approximately equal σ bond strength in a particular geometry.

The second important structural consequence is the tendency of sulphur to stabilize the monomeric complexes. For example, sterically unencumbered Ni(II) β-diketonates are trimeric in the solid state[6] and in solution[7], with the nickel centre being octahedrally coordinated. $[Pd(acac)_2]$ and $[Pt(acac)_2]$, however, are both planar and monomeric[8]. This illustrates the competing factors of coordinative saturation and ligand field stabilization energy, LFSE. In the latter two complexes, the extreme ligand field splittings, Δ, in 2nd and 3rd row metals help stabilize the planar form, whereas in $[Ni(acac)_2]_3$, the drive to obtain coordinative saturation over-rides LFSE considerations. (Typically in first row transition metal complexes, LFSE is only 10% of the total bond formation energies). However, the effect of sulphur substitution on the nickel complex is dramatic. Analogous NiO_2S_2 (ii)[9,10], $NiOS_3$ (iii)[11], NiS_4 (iv)[11,12]

compounds are, without exception, planar. Similarly, $[Co(acac)_2]$ is tetrameric[13,14] but CoO_2S_2[2] and CoS_4[11,12] complexes are monomeric.

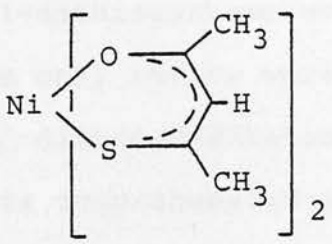

(ii)

$[Ni(Sacac)_2]$

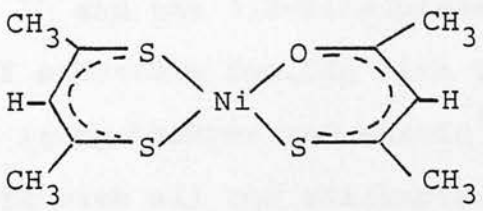

(iii)

[Ni(SacSac)(Sacac)]

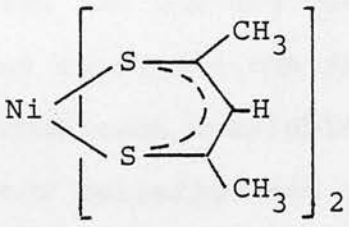

(iv)

$[Ni(SacSac)_2]$

Note, the abbreviations used above for monothio- ($Sacac^-$) and dithio- ($SacSac^-$) acetylacetonate anions are an extension of the traditional $acac^-$ abbreviation for the acetylacetonate anion.

This again reflects the ability of the sulphur donor atoms to interact in extended co-planar π-bonding (since their ligand field splittings, Δ, are only moderate) thus overcoming the strong tendency for coordinative saturation of the nickel and cobalt complexes.

The resurgence of interest in transition metal-sulphur complexes has prompted the compilation of some notable review articles, principally concerning the 1,1-dithiocarbamates[15,16] and the 1,2-dithiolenes[17]. The only review worthy of attention dealing with the dithio-β-diketonates is by Lockyer and Martin[18]. This comprehensively deals with all the available data concerning the dithio-β-diketonates and related compounds, and in so doing tends to illuminate the areas which have been relatively neglected (this is especially the case for the 2nd and 3rd row elements). With this in mind we set out to extend the range of planar dithio-β-diketonate complexes available, with particular attention to preparing new palladium and platinum dithio-β-diketonate compounds (Chapter 2).

Sulphur chelates of transition metals frequently display facile and reversible redox behaviour in which several members of a series are related by the transfer of one electron. For example, 1,2-dithio chelates such as (v) undergo successive reductions involving both the

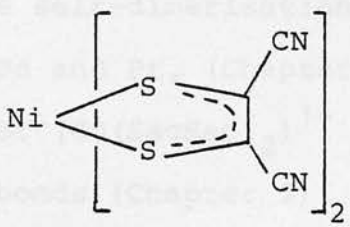

(v)

ligand array (principally) and ultimately the metal centre, as indicated:

$$[Ni(II)(mnt)_2]^{0} \Longleftrightarrow [Ni(II)(mnt)_2]^{1-} \Longleftrightarrow [Ni(II)(mnt)_2]^{2-} \Longleftrightarrow [Ni(I)(mnt)_2]^{3-}$$

Metal complexes of the 1,3-dithio chelates are also redox-active, with the planar bis-dithioacetylacetonates of the divalent metals (M = Co, Ni, Pd, Pt) exhibiting two consecutive, reversible one-electron reductions.

$$[M(SacSac)_2]^{0} \Longleftrightarrow [M(SacSac)_2]^{1-} \Longleftrightarrow [M(SacSac)_2]^{2-}$$

However, the nature of the redox-active orbital was in some doubt.

We have made a detailed study of the effect of changing the ligand substituent groups on the characteristic electrode potentials, and, by comparison with a range of related systems, determined unambiguously that both electron transfers are essentially ligand based (Chapter 3).

We have also established that the one-electron reduced species are prone to further reaction, and have identified two distinct situations, depending on the metal centre, (a) the self-dimerisation of $[M(SacSac)_2]^{1-}$, where M = Ni, Pd and Pt, (Chapter 4) and (b) the nucleophilic attack of $[Co(SacSac)_2]^{1-}$ on alkyl halides, to form Co(III) alkyl bonds (Chapter 5).

Thus by extending the variety of available planar dithio-β-diketonate complexes, and by applying extensive electrochemical and spectroscopic methods over the whole family, we have increased our understanding of the

complexes in their normal oxidation states and generated new redox-activ ated species, whose structures and reactions merit careful attention.

References (Chapter 1)

1. S.E. Livingstone, Quarterly Revs., 1965, 19, 386.
2. D.H. Gerlach and R.H. Holm, Inorg.Chem., 1969, 8, 2292.
3. D.H. Gerlach and R.H. Holm, Inorg.Chem., 1970, 9, 588.
4. D.H. Gerlach and R.H. Holm, J.Am.Chem.Soc., 1969, 91, 3457.
5. R.H. Holm, D.H. Gerlach, J.G. Gordon and M.G. McNamee, J.Am.Chem.Soc., 1968, 90, 4184.
6. G.J. Bullen, R. Mason and P. Pauling, Inorg.Chem., 1965, 4, 456.
7. A.W. Addison and D.P. Graddon, Aust.J.Chem., 1968, 21, 2003.
8. J.P. Fackler, Prog.Inorg.Chem., 1966, 7, 361.
9. M. Cox and J. Darken, Coord.Chem.Rev., 1971, 7, 29.
10. S.E. Livingstone, Coord.Chem.Rev., 1971, 7, 59.
11. C.G. Barraclough, R.L. Martin and I.M. Stewart, Aust.J.Chem., 1969, 22, 891.
12. R. Beckett and B.F. Hoskins, J.C.S. Dalton, 1974, 622.
13. F.A. Cotton and R.H. Soderberg, Inorg.Chem., 1964, 3, 1.
14. F.A. Cotton and R.C. Elder, Inorg.Chem., 1965, 4, 1145.
15. J. Willemse, J.A. Cras, J.J. Steggerda and C.P. Keijzers, Structure and Bonding, 1976, 28, 83.
16. D. Coucouvanis, Prog.Inorg.Chem., 1970, 11, 233.
17. J.A. McCleverty, Prog.Inorg.Chem., 1968, 10, 49.
18. T.N. Lockyer and R.L. Martin, Prog.Inorg.Chem., 1980, 27, 224.

CHAPTER 2

The dithio-β-diketonate complexes of nickel, palladium and platinum: synthesis and characterisation

2.1 Introduction

ß-diketonate complexes have been reported for all the non-radioactive metallic and metalloid elements in the periodic table[1-3]. The acetylacetonate anion ($acac^-$) normally functions by coordination of both oxygen atoms to the metal to give a wide range of neutral complexes, $[M(acac)_n]$. Divalent metal cations, with coordination number of four, can adopt either tetrahedral, e.g. $[Be(acac)_2]$ or square-planar geometry, e.g. $[Cu(acac)_2]$ and $[Pd(acac)_2]$.

Repeated attempts to prepare dithioacetylacetone by the reaction of acacH with H_2S in HCl solution resulted in the isolation of a colourless, crystalline solid of the correct stoichiometry[4]. However, subsequent characterisation showed a tetrathia-adamantane type dimer (i)[5]. where the C-S-C links confer stability, resulting in its inert chemical behaviour.

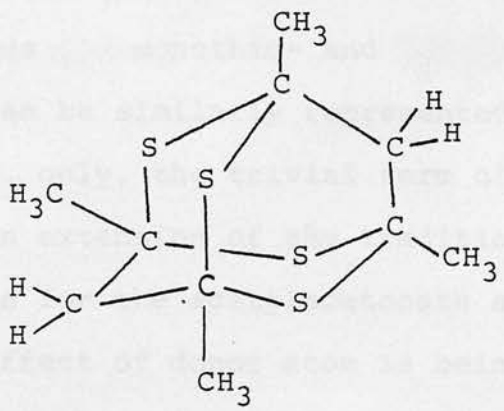

(i)

Although the acacH-H_2S reaction did not yield a simple dithio-β-diketone species, isolation of the dimer, did, however, establish that both oxygen atoms can be replaced by sulphur under these reaction conditions.

By carrying out the same reaction in the presence of various metal ions (M(II) = Ni, Pd, Pt, Co), Martin and Stewart trapped the unknown dithioacetylacetone ligand in the form of its metal complexes (ii), where R = R ' = CH_3 [6].

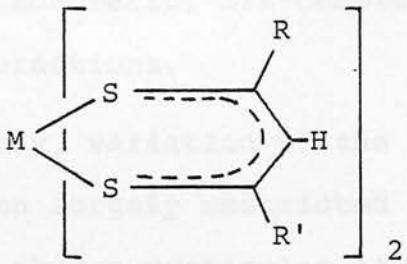

(ii)

This seems an appropriate time to explain the nomenclature applied throughout this thesis. The dithio-compound (ii) is abbreviated to $[M(S_2C_3RHR')_2]$. The analogous monothio- and diketonate complexes can be similarly represented. However, when R = R' = CH_3 only, the trivial term of $SacSac^-$ is employed (an extension of the traditional $acac^-$ abbreviation for the acetylacetonate anion). At points where the effect of donor atom is being considered, but otherwise the constitution of the complex remains unaltered, then only the immediate coordination sphere of the metal will be represented, i.e. MS_4, MO_2S_2 and MO_4.

The stereochemical consequences of changing the ligand donor atom from oxygen to sulphur leads to suppression of oligomerisation and a tendency to stabilize the planar geometry (Chapter 1). Thus, although $[Ni(acac)_2]$ and $[Co(acac)_2]$ are trimeric and tetrameric in the solid state respectively, with each metal atom having a coordination number of six (the $acac^-$ ligands acting as bridging groups between two metal centres), the sterically unencumbered $SacSac^-$ ligand forms planar, monomeric, bis-complexes, with an incapacity for axial interactions.

Previously, variation of the dithio-β-diketonate ligand has been largely restricted to the nickel complexes[7], thus a particular aim of our work has been to extend the number of M(II) bis(dithio-β-diketonate) complexes available, by the synthesis of a range of usefully substituted palladium and platinum compounds and to record their physical properties, together with those of their nickel analogues, in a systematic manner.

The preparation of the series of nickel complexes, however, has established three distinct synthetic routes. It should be noted that the parent (protonated) dithio-ligand itself is unstable in virtually all cases, and attempts to isolate the unco-ordinated 1,3-dithio-diketonate ligand, derived from the appropriate 1,3——diketone, generally lead to dimer formation.

Method 1

Generalisation of the original Martin and Stewart reaction involves the direct sulphuration of the appropriate β-diketonate ligand, by H_2S in ethanolic-HCl medium, generally using the metal chloride as a source of M(II) ions[8,9] (Equation [1]).

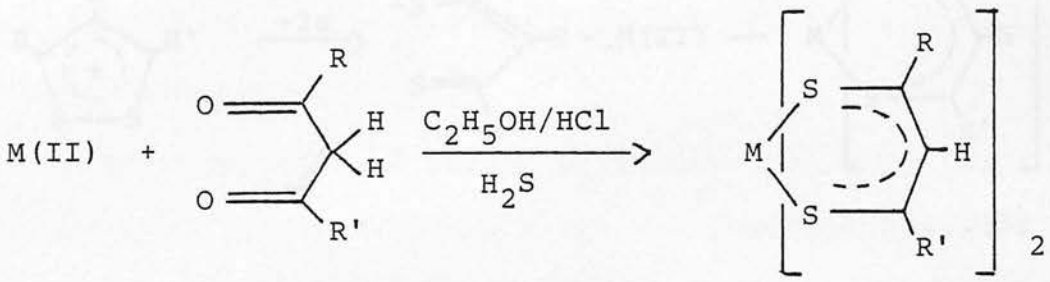

.....[1]

Method 2

The monothio- ligands are well-known, stable, species which react with a wide variety of metal ions to give the corresponding monothio-β-diketonate complex[10,11]. Treatment with H_2S in an ethanolic-HCl medium yields the fully sulphurated complex[12] (Equation [2]).

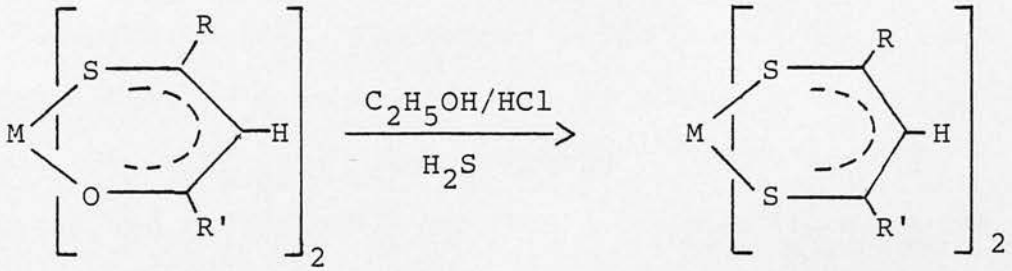

....[2]

Method 3

This involves the reduction of a 1,2-dithiolylium cation in the presence of a metal ion; thus treatment of a 1,2-dithiolylium tetrahalo-metallate salt with $NaBH_4$ affords the corresponding dithio-β-diketonate complex[13,14] (Equation [3]).

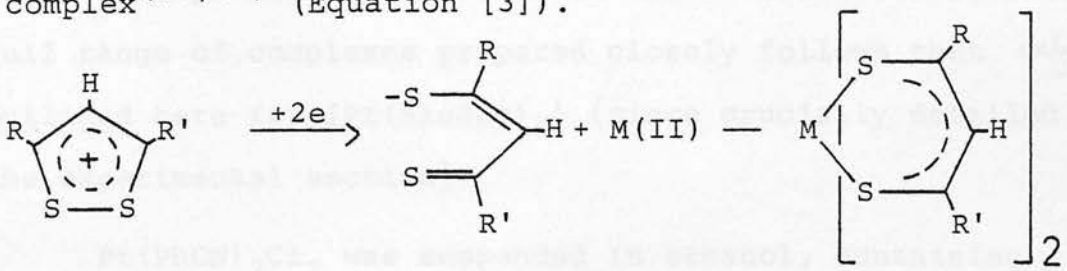

...[3]

No generally applicable synthetic route is available and, indeed, it will become apparent from the following discussion that, by changing the reaction conditions, a substantial improvement in yield and the minimisation of unwanted by-products can result.

2.2 Synthesis and Characterisation

A number of new palladium and platinum bis-(dithio-β-diketonates) (ii) have been prepared, (where M = Pd or Pt; R,R' = ^{t}Bu, CH_3, Ph or CF_3, not all possible combinations).

The synthetic procedure and characterisation of the full range of complexes prepared closely follows that only outlined here for $[Pt(SacSac)_2]$ (since crucially detailed in the experimental section).

$Pt(PhCN)_2Cl_2$ was suspended in ethanol, containing an excess of acetylacetone, which was degassed then cooled. Maintaining a slight flow of N_2 to act as a carrier gas, hydrogen chloride, HCl(g), followed by hydrogen sulphide, H_2S(g), were bubbled through the solution. The reaction mixture was allowed to return slowly to room temperature, then stand under N_2 for 24 hours. The purple solid was collected by filtration and washed with ethanol. Recrystallisation under N_2 from 1:1 ethanol, methylene chloride gave the pure microcrystalline purple product.

A variety of techniques were employed routinely for characterisation. The purple solid proved to be non-conducting in a number of organic solvents, e.g. $CHCl_3$, acetone, C_6H_6 etc. Both infrared[15] (KBr disk and nujol mull) and U.V./visible studies[16] showed spectra analogous to those previously reported, with no traces of residual $Pt(PhCN)_2Cl_2$ starting material apparent in the infrared. Mass spectrometry shows a parent-ion peak at m/e 457, along with a much stronger peak at m/e 131 due to $[C_5H_7S_2]^+$ [6]. The spectrum is dominated by the fragmentation of this ion.

The ^{1}H n.m.r. spectrum shows two singlet resonances at δ7.26 and 2.12 ppm, with an integral ratio of 1:6, assigned to the methine ring and methyl group protons respectively[17]. The equivalence of the methyl groups and the high frequency position of the ring C-H absorption is consistent with a π-bonded aromatic type ring current within the metal-sulphur framework. Closer examination shows doublet signals arising from coupling of ^{195}Pt ($I = \frac{1}{2}$) to the ligand protons (Figure 2.1). The coupling constants have been determined (see Experimental Section).

The $^{13}C-\{^{1}H\}$ spectrum was also obtained, showing three resonances at δ34.2, 135.2 and 174.2 ppm (Figure 2.2). By expansion we can determine Pt-C coupling constants, and by retaining proton coupling, the ^{13}C spectrum can be assigned.

All the physical data confirmed a successful, high yield synthesis of platinum(II)bis(dithioacetylacetonate). Analytical data were consistent with the formulation $[Pt(SacSac)_2]$.

We find that for the palladium and platinum complexes, $M(PhCN)_2Cl_2$ is a more convenient source of M(II) than the more commonly used MCl_2, proving to be more soluble in the ethanolic-HCl reaction medium, with the added advantage of PhCN being a better leaving group than Cl^-. This results in yields for $[M(SacSac)_2]$ being consistently greater than 60%.

Figure 2.1 ^{1}H n.m.r. spectrum of $[Pt(SacSac)_2]$, showing ^{195}Pt satellites

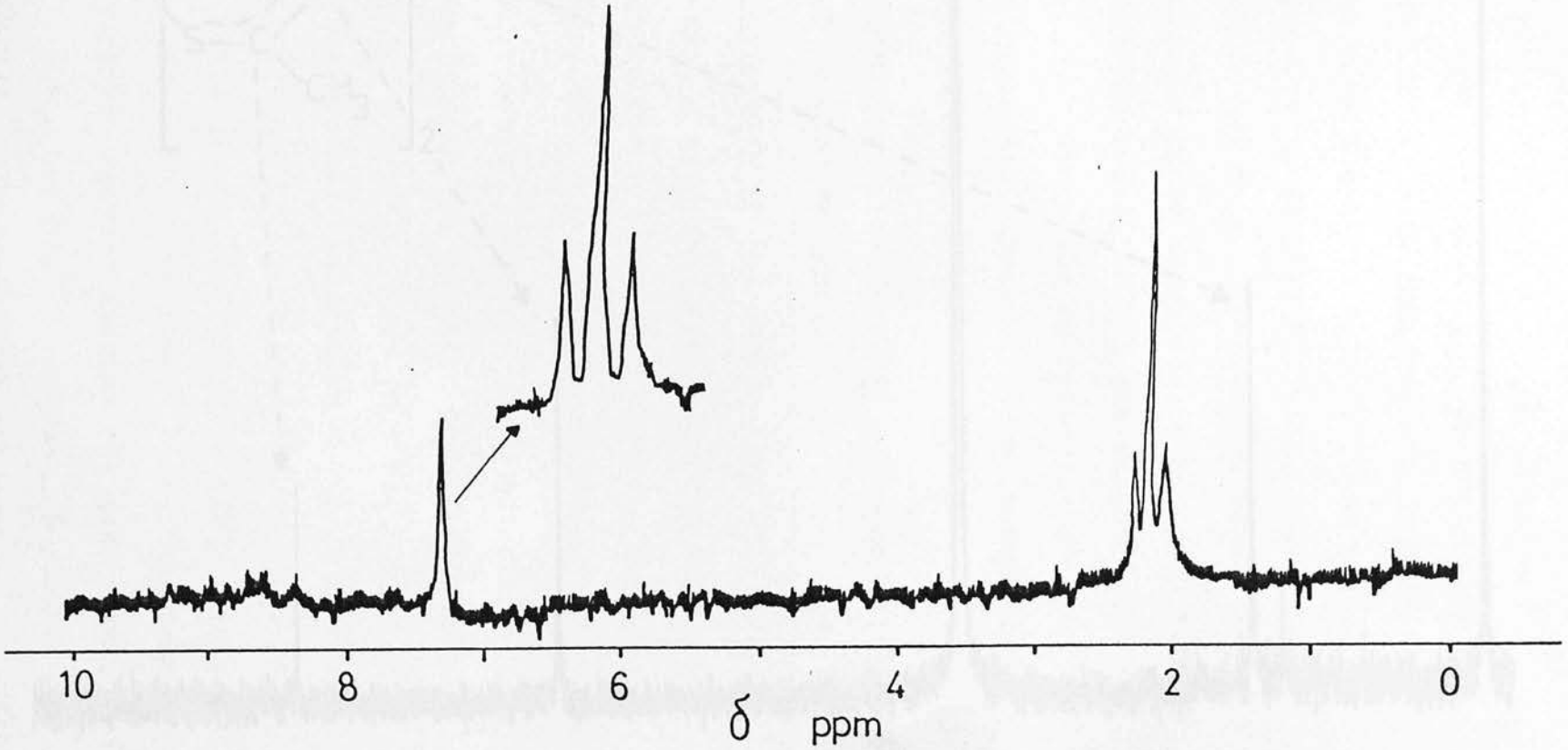

Figure 2.2 ^{13}C n.m.r. spectrum of [Pt(SacSac)$_2$]

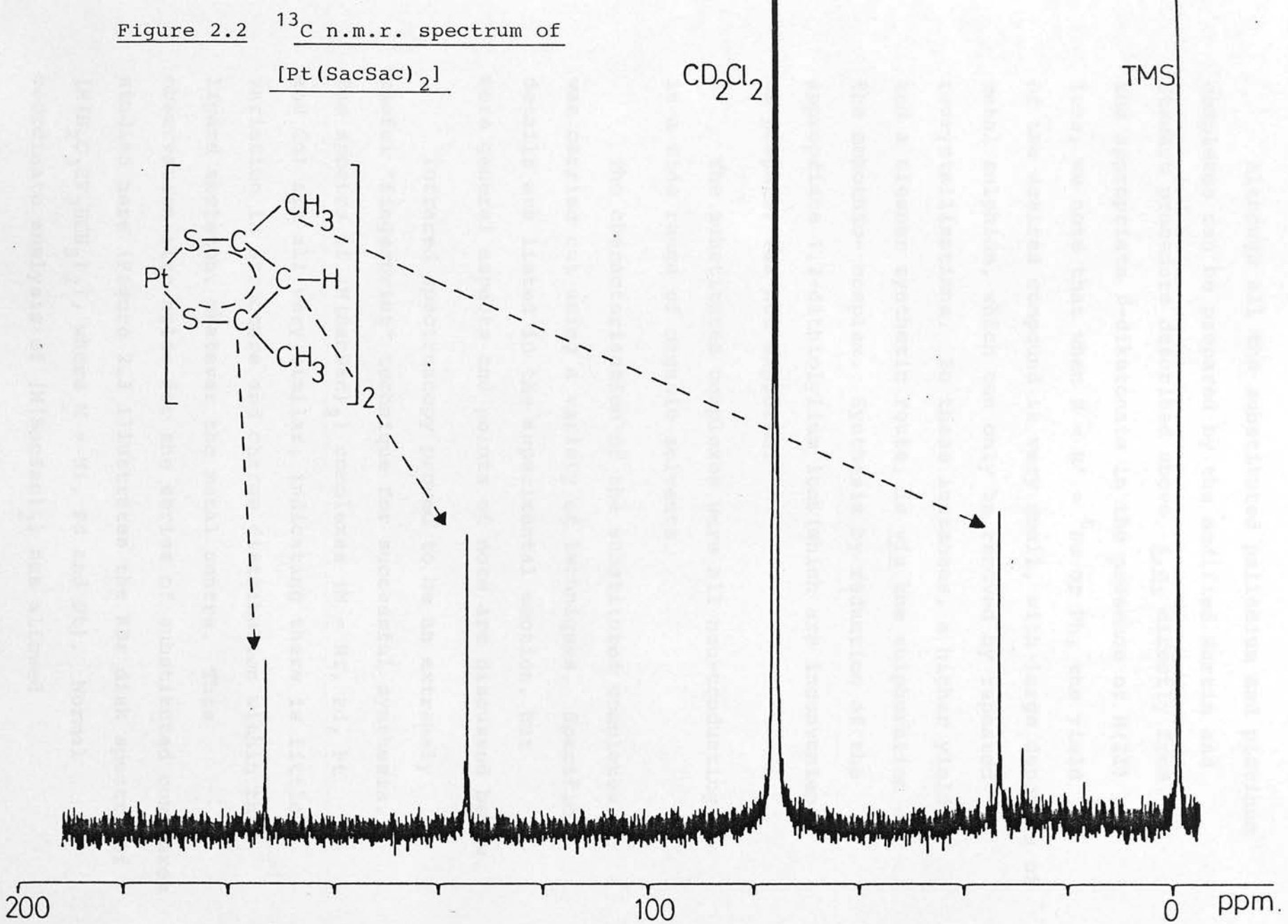

Although all the substituted palladium and platinum complexes can be prepared by the modified Martin and Stewart procedure described above, i.e. directly from the appropriate β-diketonate in the presence of M(II) ions, we note that when R = R' = ^{t}Bu or Ph, the yield of the desired compound is very small, with large deposits of metal sulphide, which can only be removed by repeated recrystallisations. In these instances, a higher yield, and a cleaner synthetic route, is via the sulphuration of the monothio- complex. Synthesis by reduction of the appropriate 1,2-dithiolylium ions (which are inconvenient to prepare) was not explored.

The substituted complexes were all non-conducting in a wide range of organic solvents.

The characterisation of the substituted complexes was carried out using a variety of techniques. Specific details are listed in the experimental section, but more general aspects and points of note are discussed below.

Infrared spectroscopy proved to be an extremely useful "fingerprint" technique for successful synthesis. The spectra of $[M(SacSac)_2]$ complexes (M = Ni, Pd, Pt and Co) are all very similar, indicating there is little variation in structure and charge distribution within the ligand skeleton, whatever the metal centre. This observation also holds for the series of substituted complexes studied here (Figure 2.3 illustrates the KBr disk spectra of $[M(S_2C_3CF_3HCH_3)_2]$, where M = Ni, Pd and Pt). Normal coordinate analysis of $[M(SacSac)_2]$ has allowed

Figure 2.3 Infrared spectra of $[M(S_2C_3CF_3HCH_3)_2]$ (KBr disks)

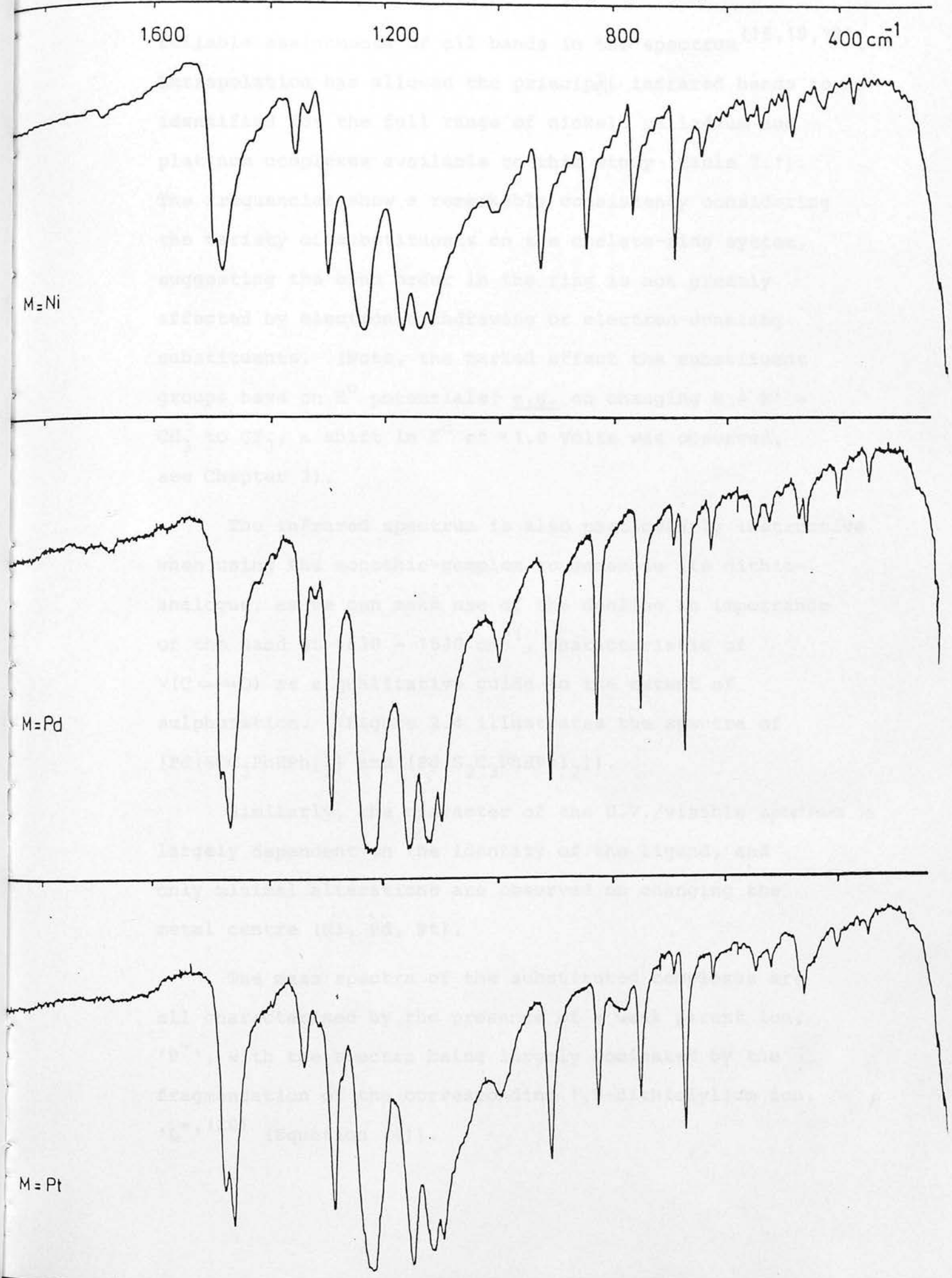

reliable assignments of all bands in the spectrum[15,18,19]. Extrapolation has allowed the principal infrared bands to be identified for the full range of nickel, palladium and platinum complexes available to this study (Table 2.1). The frequencies show a remarkable consistency considering the variety of substituents on the chelate-ring system, suggesting the bond order in the ring is not greatly affected by electron-withdrawing or electron-donating substituents. (Note, the marked effect the substituent groups have on E^{o} potentials; e.g. on changing R = R' = CH_3 to CF_3, a shift in E^{o} of $\simeq$ 1.0 Volts was observed, see Chapter 3).

The infrared spectrum is also particularly instructive when using the monothio-complex to generate its dithio-analogue, as we can make use of the decline in importance of the band at 1630 - 1530 cm^{-1}, characteristic of ν(C=O) as a qualitative guide to the extent of sulphuration. (Figure 2.4 illustrates the spectra of $[Pd(SOC_3PhHPh)_2]$ and $[Pd(S_2C_3PhHPh)_2]$).

Similarly, the character of the U.V./visible spectrum is largely dependent on the identity of the ligand, and only minimal alterations are observed on changing the metal centre (Ni, Pd, Pt).

The mass spectra of the substituted complexes are all characterised by the presence of a weak parent ion, 'P^+', with the spectra being largely dominated by the fragmentation of the corresponding 1,2-dithiolylium ion, 'L^+',[20] (Equation [4]).

Table 2.1 Principal infrared assignments for the $[M(S_2C_3RHR')_2]$ complexes (KBr disks, cm^{-1})

Compound	$\nu C{=\!=\!=}C$ + $\delta C-H$	$\nu C{=\!=\!=}C$	$\delta C-H$	$\pi C-H$	$\nu C{=\!=\!=}S$
$[Ni(S_2C_3{}^tBuH{}^tBu)_2]$	1490	1340	1314	825	630
$[Pd(S_2C_3{}^tBuH{}^tBu)_2]$	1495	1340	1320	825	630
$[Ni(SacSac)_2]$	1495	1355	1318	830	703
			1295		
$[Pd(SacSac)_2]$	1480	1350	1325	830	705
			1305		
$[Pt(SacSac)_2]$	1490	1350	1320	830	708
			1305		
$[Ni(S_2C_3PhHCH_3)_2]$	1480	1350	1308	840	690
			1295		
$[Pd(S_2C_3PhHCH_3)_2]$	1475	1350	1315	840	690
			1280		
$[Pt(S_2C_3PhHCH_3)_2]$	1470	1350	1318	840	690
			1308		

Table 2.1 (contd.)

Compound	$\nu C{=\!=\!=}C$ + $\delta C-H$	$\nu C{=\!=\!=}C$	$\delta C-H$	$\pi C-H$	$\nu C{=\!=\!=}S$
$[Ni(S_2C_3PhHPh)_2]$	1475	1350	1302	840	688
			1289		
$[Pd(S_2C_3PhHPh)_2]$	1470	1340	1315	840	688
			1307		
$[Ni(S_2C_3CF_3HCH_3)_2]$	1492	1365	1320	850	695
			1309		
$[Pd(S_2C_3CF_3HCH_3)_2]$	1490	1365	1315	850	695
$[Pt(S_2C_3CF_3HCH_3)_2]$	1490	1365	1315	850	695
$[Ni(S_2C_3CF_3HPh)_2]$	1495	1370	1305	860	695
$[Pd(S_2C_3CF_3HPh)_2]$	1500	1370	1325	860	695
			1310		
$[Pt(S_2C_3CF_3HPh)_2]$	1490	1370	1328	850	695
			1310		
$[Pd(S_2C_3CF_3HCF_3)_2]$	1500	1370	-	860	730

Figure 2.4. Infrared spectra of $[Pd(SOC_3PhHPh)_2]$ and $[Pd(S_2C_3PhHPh)_2]$ (KBr disk)

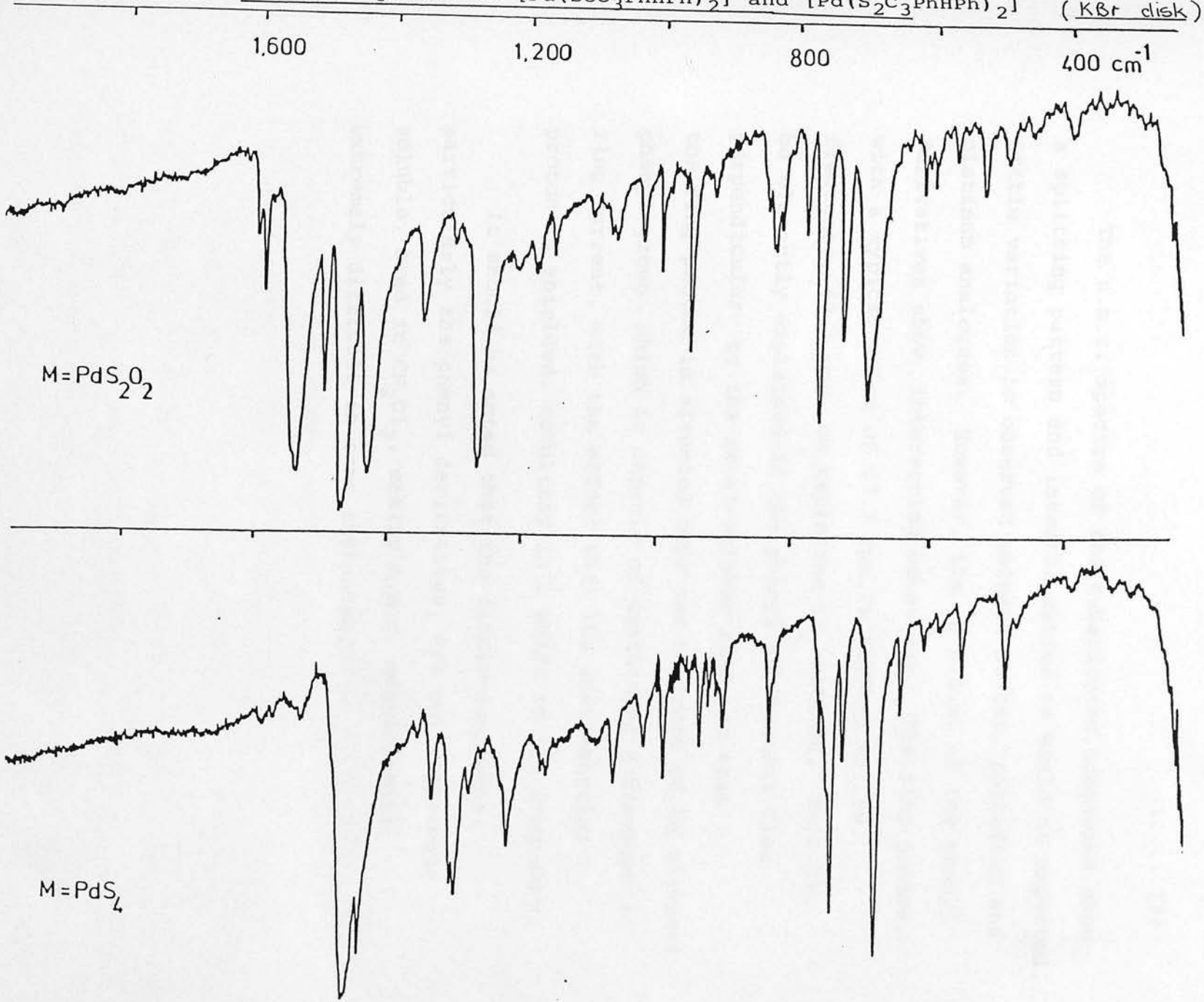

$$[M(S_2C_3RHR')_2]^+ \longrightarrow [S_2C_3RHR']^+ \xrightarrow{-HS} L - 33 \longrightarrow \underline{etc}.$$

..... [4]

The n.m.r. spectra of the substituted complexes show a splitting pattern and integral ratios as would be expected. Little variation is observed between nickel, palladium and platinum analogues. However, the ^1H n.m.r. of the phenyl derivatives show interesting behaviour. The ring proton, with a typical value of δ7.2 ppm, is shifted to low frequency, δ2.1 ppm, on replacing CH_3 with Ph. This can be elegantly explained if the phenyl substituent lies perpendicular to the metal-sulphur ring, so that the ring proton is situated over the centroid of an adjacent phenyl group which is capable of sustaining a diamagnetic ring current, with the effect that the intra-annular proton is shielded, resulting in a shift to low frequency.

It should be noted that the dithio-complexes, particularly the phenyl derivatives, are only sparingly soluble, even in CH_2Cl_2, making n.m.r. measurements extremely difficult in some instances.

2.3 Experimental

(i) Materials

Preparations of complexes are as detailed below. Dry ethanol was prepared by refluxing over magnesium turnings, with a few crystals of iodine added, followed by distillation immediately prior to use. HCl was generated by dropping concentrated sulphuric acid onto concentrated hydrochloric acid with vigorous stirring. The HCl gas was dried by bubbling through concentrated H_2SO_4. Generation of H_2S was *via* a modified Kipps apparatus, by dropping a 1:1 concentrated HCl:water mixture onto ferrous sulphide. The H_2S was then bubbled through a water spray trap, then dried by passing through three anhydrous $CaCl_2$ towers. $NiCl_2$ (commercial grade) was dried *in vacuo* at 353 Kelvin. $Pd(PhCN)_2Cl_2$ and $Pt(PhCN)_2Cl_2$ were prepared by literature methods[21]. The appropriate β-diketonate ligand was obtained commercially and used without further purification.

Although the $[Ni(S_2C_3RHR')_2]$ complexes have been previously prepared[8,9,12], the data are presented here for clarity and to enable ease of comparison between the analogous palladium and platinum complexes.

In addition, $[Ni(SOC_3RHR')_2]$[10,11] and $[Pd(O_2C_3RHR')_2]$[1-3] complexes, necessary for synthetic purposes (see below) and/or electrochemical studies (see Section 3.4) were prepared by literature methods.

Principal infrared bands and assignments for the complexes $[M(S_2C_3RHR')_2]$, where M = Ni, Pd and Pt, are to be found in Table 2.1.

Nickel(II)bis(dithio-2,2,6,6-tetramethyl-3,5-heptanedionate) $[Ni(S_2C_3{}^tBuH{}^tBu)_2]$

This was best prepared from the monothio-complex. $[Ni(SOC_3{}^tBuH{}^tBu)_2]$ (0.4 g) was suspended in ethanol (10 ml) at 323 Kelvin. After flushing with nitrogen, HCl is bubbled through the reaction mixture followed by H_2S (30 and 120 minutes respectively), maintaining a positive pressure of N_2 throughout. The reaction mixture was allowed to cool, and stand for 24 hours under N_2. The product was collected by filtration and washed with ethanol. The product was recrystallised from a 1:1 mixture of ethanol and methylene chloride. Yield (recrystallised material) 0.24 g (55%) Analysis: Found %C 53.8, %H 7.6, Calculated for $NiC_{22}H_{38}S_4$ %C 54.0, %H 7.8. Electronic spectrum (50,000 to 11,500 cm^{-1} in CH_2Cl_2): 17,860 cm^{-1} ($\log \varepsilon = 3.46$), 29,240 cm^{-1} (4.41), 36,630 cm^{-1} (4.70), 42,735 cm^{-1} (4.28), 45,250 cm^{-1} (4.32) Mass Spectrum: m/e 489, $[Ni(S_2C_3{}^tBuH{}^tBu)_2]^+$; m/e 215, $[S_2C_3{}^tBuH{}^tBu]^+$. N.M.R.: ^1H in $CDCl_3$, two singlets at δ7.45 and 1.26 ppm, assigned to methine ring proton and ^{t}butyl group respectively.

Ni(II)bis(dithioacetylacetonate) $[Ni(SacSac)_2]$

$NiCl_2$ (0.4 g) was dissolved in ethanol (10 ml) containing an excess of acetylacetone (2 ml). Upon cooling to 273 Kelvin, the mixture was first flushed with nitrogen, then HCl followed by H_2S are bubbled through (30 and 120 minutes respectively), maintaining a positive pressure

of N_2 throughout. Isolation at this stage yields only large quantities of the monothio-complex $[Ni(Sacac)_2]$. However, when the temperature was elevated to 333 Kelvin, and the passage of H_2S continued (60 minutes) the desired dithio-compound was obtained. The solid was collected by filtration, washed with ethanol, then recrystallised from 1:1 mixture of ethanol and methylene chloride. Yield 0.64 g (65%) Analysis: Found %C 37.6, %H 4.5 Calculated for $NiC_{10}H_{14}S_4$ %C 37.4, %H 4.4. Electronic spectrum (50,000 to 11,500 cm^{-1} in CH_2Cl_2): 17,990 cm^{-1} (log ε = 3.34), 24,390 cm^{-1} (sh), 29,760 cm^{-1} (4.35), 37,035 cm^{-1} (4.68), 41,670 cm^{-1} (4.33). Mass spectrum: m/e 321 $[Ni(SacSac)_2]^+$; m/e 131, $[S_2C_3CH_3HCH_3]^+$. N.M.R.: ^1H in CD_2Cl_2, two singlets at δ7.15 and 2.35 ppm, assigned to the methine ring and methyl group protons respectively.

Nickel(II)bis(dithio-1-benzoylacetonate) $[Ni(S_2C_3PhHCH_3)_2]$

$NiCl_2$ (0.4 g) was dissolved in ethanol containing excess 1-benzoylacetone (1 g). The solution was cooled to 203 Kelvin, flushed with nitrogen, then HCl followed by H_2S were bubbled very rapidly through the solution (15 and 30 minutes respectively), maintaining a positive pressure of N_2 throughout. The solution was returned slowly to room temperature, then allowed to stand overnight under N_2, to yield precipitate, which was collected by filtration, washed with ethanol, and recrystallised from a 1:1 mixture of ethanol and methylene chloride. Yield 0.82 g (60%).

Analysis: Found %C 53.4, %H 4.1. Calculated for $NiC_{20}H_{18}S_4$ %C 53.9, %H 4.0. Mass spectrum: m/e 445 $[Ni(S_2C_3PhHCH_3)_2]^+$; m/e 193 $[S_2C_3PhHCH_3]^+$. Electronic Spectrum (50,000 to 11,500 cm^{-1} in CH_2Cl_2): 17,240 cm^{-1} ($\log \varepsilon = 3.52$), 22,935 cm^{-1} (3.86), 28,985 cm^{-1} (4.56), 33,785 cm^{-1} (4.52), 40,000 cm^{-1} (4.45).
N.M.R.: ^1H in CD_2Cl_2, two singlets at δ2.13 and 2.46 ppm assigned to the methine ring and methyl group protons respectively, plus phenyl resonances between δ7.35 - 7.7 ppm.

Nickel(II)bis(dithiodibenzoylmethanate) $[Ni(S_2C_3PhHPh)_2]$

This was prepared by the same method as $[Ni(S_2C_3{}^tBuH{}^tBu)_2]$ described above, using $[Ni(SOC_3PhHPh)_2]$ (0.4 g) as starting material. Yield 0.1 g (20%). Analysis: Found %C 63.2, %H 4.0. Calculated for $NiC_{30}H_{22}S_4$ %C 63.4, %H 3.9. Mass Spectrum: m/e 568, $[Ni(S_2C_3PhHPh)_2]^+$; m/e 225, $[S_2C_3PhHPh]^+$. Electronic Spectrum (50,000 to 11,500 cm^{-1} in CH_2Cl_2): 15,430 cm^{-1}, ($\log \varepsilon = 3.53$), 21,550 cm^{-1} (3.87), 27.780 cm^{-1} (4.55), 32,050 cm^{-1} (4.51), 37.595 cm^{-1} (4.58)
N.M.R.: ^1H in CD_2Cl_2, singlet at 2.05 ppm assigned to the methine ring proton, plus phenyl resonances between δ7.4 - 7.85 ppm.

Nickel(II)bis(dithiotrifluoroacetylacetonate)

$[Ni(S_2C_3CF_3HCH_3)_2]$

The synthetic procedure was the same as $[Ni(S_2C_3PhHCH_3)_2]$ using $NiCl_2$ (0.4 g) and 1,1,1-trifluoroacetylacetone (1 ml) as ligand. Yield 0.6 g (45%) Analysis: Found %C 28.9, %H 1.9. Calculated for $NiC_{10}H_8F_6S_4$ %C 28.0, %H 1.9 Mass Spectrum: m/e 429, $[Ni(S_2C_3CF_3HCH_3)_2]^+$; m/e 185, $[S_2C_3CF_3HCH_3]^+$. Electronic Spectrum (50,000 to 11,500 cm^{-1} in CH_2Cl_2): 16,890 cm^{-1} ($\log \varepsilon = 3.30$), 22,255 cm^{-1} (sh), 29,760 cm^{-1} (4.33), 36,765 cm^{-1} (4.74), 41,670 cm^{-1} (4.11). N.M.R.: ^1H in CD_2Cl_2, two singlets at δ7.56 and 2.47 ppm assigned to the methine ring and methyl group protons respectively.

Nickel(II)bis(dithiobenzoyl-1,1,1-trifluoroacetonate)

$[Ni(S_2C_3PhHCF_3)_2]$

This was prepared in the same manner as $[Ni(S_2C_3PhHCH_3)_2]$, using $NiCl_2$ (0.4 g) and benzoyl-1,1,1-trifluoroacetone (1 g). Yield 0.68 g (40%) Analysis: Found %C 42.5, %H 2.2. Calculated for $NiC_{20}H_{12}F_6S_4$ %C 43.4, %H 2.2. Mass Spectrum: m/e 553, $[Ni(S_2C_3PhHCF_3)_2]^+$; m/e 247, $[S_2C_3PhHCF_3]^+$. Electronic Spectrum (50,000 to 11,500 cm^{-1} in CH_2Cl_2): 15,625 cm^{-1} ($\log \varepsilon = 3.34$), 22,125 cm^{-1} (3.91), 27,625 cm^{-1} (4.53), 32,895 cm^{-1} (4.35), 37,880 cm^{-1} (4.42). N.M.R.: ^1H in CD_2Cl_2, singlet at δ2.07 ppm assigned to the methine ring proton, phenyl resonances between δ7.45 - 7.9 ppm.

Palladium(II)bis(dithio-2,2,6,6-tetramethyl-3,5-heptanedionate) $[Pd(S_2C_3{}^tBuH{}^tBu)_2]$

This was prepared by the same procedure as the analogous nickel complex, using $[Pd(SOC_3{}^tBuH{}^tBu)_2]$ (0.15 g) as starting material. Yield 0.02 g (10%) Analysis: Found %C 48.5, %H 7.3. Calculated for $PdC_{22}H_{38}S_4$ %C 49.2, %H 7.1. Mass Spectrum: m/e 536 $[Pd(S_2C_3{}^tBuH{}^tBu)_2]^+$; m/e 215, $[S_2C_3{}^tBuH{}^tBu]^+$. Electronic spectrum (50,000 to 11,500 cm^{-1} in CH_2Cl_2): 19,380 cm^{-1} ($\log \varepsilon = 3.77$), 28,250 cm^{-1} (3.88), 32,895 cm^{-1} (4.43), 39,370 cm^{-1} (4.79), 40,985 cm^{-1} (sh).

Palladium(II)bis(dithioacetylacetonate) $[Pd(SacSac)_2]$

This was prepared using the same method as $[Ni(S_2C_3PhHCH_3)_2]$, using $Pd(PhCN)_2Cl_2$ (0.15 g) in place of $NiCl_2$ and acetylacetone (2 ml) as ligand. Yield 0.094 g (65%) Analysis: Found %C 32.4, %H 3.7. Calculated for $PdC_{10}H_{14}S_4$ %C 32.6, %H 3.8. Mass spectrum: m/e 368, $[Pd(SacSac)_2]^+$; m/e 131, $[S_2C_3CH_3HCH_3]^+$. Electronic spectrum (50,000 to 11,500 cm^{-1} in CH_2Cl_2): 19,800 cm^{-1} ($\log \varepsilon = 3.40$), 22,220 cm^{-1} (sh), 28,250 cm^{-1} (3.66), 33,560 cm^{-1} (4.28), 39,060 cm^{-1} (4.76), 46,985 cm^{-1} (sh). N.M.R.: ^1H in CD_2Cl_2, two singlets at δ7.22 and 2.46 ppm assigned to the methine ring and the methyl group protons respectively. $^{13}C-\{^1H\}$ in CD_2Cl_2 yields three resonances at δ33.7, 133.0 and 185.3 ppm, which, by retaining the proton coupling, can be definitively assigned to $-CH_3$, -C-H and -C-Me carbons respectively.

Palladium(II)bis(dithio-1-benzoylacetonate)

$[Pd(S_2C_3PhHCH_3)_2]$

This was prepared using the same method as the $[Ni(S_2C_3PhHCH_3)_2]$ complex, again using $Pd(PhCN)_2Cl_2$ (0.15 g) as a source of Pd(II) and 1-benzoylacetone (1 g) as ligand. Yield 0.05 g (25%) Analysis: Found %C 48.7, %H 3.5 Calculated for $PdC_{20}H_{18}S_4$, %C 48.8, %H 3.7. Mass Spectrum: m/e 492, $[Pd(S_2C_3PhHCH_3)_2]^+$; m/e 193 $[S_2C_3PhHCH_3]^+$. Electronic Spectrum (50,000 to 11,500 cm^{-1} in CH_2Cl_2): 18,690 cm^{-1} ($\log \varepsilon = 3.79$), 27,470 cm^{-1} (4.32), 31,645 cm^{-1} (4.47), 37,880 cm^{-1} (4.61), 40,320 cm^{-1} (4.59). N.M.R.: ^1H in CD_2Cl_2, two singlets at δ2.15 and 2.62 ppm, assigned to the methine ring and methyl group protons respectively, plus phenyl group resonances between δ7.4 and 7.88 ppm.

Palladium(II)bis(dithiodibenzoylmethanate) $[Pd(S_2C_3PhHPh)_2]$

This was prepared by the same procedure as $[Ni(SOC_3{}^tBuH{}^tBu)_2]$ using $[Pd(SOC_3PhHPh)_2]$ (0.15 g) as starting material. Yield 0.03 g (15%) Analysis: Found %C 58.1, %H 3.5 Calculated for $PdC_{30}H_{22}S_4$, %C 58.4, %H 3.6. Mass Spectrum: m/e 616, $[Pd(S_2C_3PhHPh)_2]^+$; m/e 255 $[S_2C_3PhHPh]^+$. Electronic Spectrum (50,000 to 11,500 cm^{-1} in CH_2Cl_2): 17,985 cm^{-1} ($\log \varepsilon = 3.63$), 27,025 cm^{-1} (4.32), 30,300 cm^{-1} (4.41), 34,720 cm^{-1} (4.39), 41,670 cm^{-1} (4.44).

Palladium(II)bis(dithiotrifluoroacetylacetonate)

$[Pd(S_2C_3CF_3HCH_3)_2]$

This was synthesised by the same procedure as the $[Ni(S_2C_3PhHCH_3)_2]$ complex, using $Pd(PhCN)_2Cl_2$ (0.15 g) and 1,1,1-trifluoroacetylacetone (1 ml). Yield 0.08 g (45%) Analysis: Found %C 25.1, %H 1.6. Calculated for $PdC_{10}H_8F_6S_4$ %C 25.2, %H 1.7. Mass Spectrum: m/e 476, $[Pd(S_2C_3CF_3HCH_3)_2]^+$; m/e 185, $[S_2C_3CF_3HCH_3]^+$. Electronic Spectrum (50,000 to 11,500 in CH_2Cl_2): 18,590 cm^{-1} ($\log \varepsilon = 3.45$), 27,175 cm^{-1} (3.56), 33,110 cm^{-1} (4.08), 39,530 cm^{-1} (4.55), 44,645 cm^{-1} (3.75). N.M.R.: ^1H in CD_2Cl_2, shows two singlets at δ7.55 and 2.62 ppm, assigned to the methine ring and the methyl group protons respectively.

Palladium(II)bis(dithiobenzoyl-1,1,1-trifluoroacetonate)

$[Pd(S_2C_3PhHCF_3)_2]$

This was again prepared by the same method as the $[Ni(S_2C_3PhHCH_3)_2]$ complex, using $Pd(PhCN)_2Cl_2$ (0.15 g) and benzoyl-1,1,1-trifluoroacetone (1 g). Yield 0.15 g (65%) Analysis: Found %C 39.4, %H 2.1 Calculated for $PdC_{20}H_{12}F_6S_4$ %C 40.0, %H 2.0. Mass Spectrum: m/e 600, $[Pd(S_2C_3PhHCF_3)_2]^+$; m/e 247, $[S_2C_3PhHCF_3]^+$. Electronic Spectrum (50,000 to 11,500 cm^{-1} in CH_2Cl_2): 17,795 cm^{-1} ($\log \varepsilon = 3.54$), 25,910 cm^{-1} (4.24), 32,260 cm^{-1} (4.16), 39,680 cm^{-1} (4.47), 43,860 cm^{-1} (4.18). N.M.R.: ^1H in CD_2Cl_2, singlet resonance at δ2.13 ppm assigned to the methine ring proton, plus phenyl resonances between δ7.45 and 7.9 ppm.

Palladium(II)bis(dithiohexafluoroacetylacetonate)

$[Pd(S_2C_3CF_3HCF_3)_2]$

This was synthesised by the same method used to prepare $[Ni(S_2C_3PhHCH_3)_2]$ using $Pd(PhCN)_2Cl_2$ (0.1 g) and hexafluoroacetylacetone (1 ml). Yield 0.08 g (50%) Analysis: Found %C 21.0, %H 0.4. Calculated for $PdC_{10}H_2F_{12}S_4$ %C 20.5, %H 0.3. Mass Spectrum: m/e 584, $[Pd(S_2C_3CF_3HCF_3)_2]^+$; m/e 239, $[S_2C_3CF_3HCF_3]^+$.

Platinum(II)bis(dithioacetylacetonate) $Pt(SacSac)_2$

This was again prepared by the same method as $[Ni(S_2C_3PhHCH_3)_2]$, using $Pt(PhCN)_2Cl_2$ (0.15 g) as a source of Pt(II) and acetylacetone (2 ml) as ligand. Yield 0.1 g (70%) Analysis: Found %C 26.1, %H 3.3 Calculated for $PtC_{10}H_{14}S_4$ %C 26.3, %H 3.6. Mass Spectrum: m/e 457, $[Pt(SacSac)_2]^+$; m/e 131 $[S_2C_3CH_3HCH_3]^+$. Electronic Spectrum (50,000 to 11,500 cm^{-1} in CH_2Cl_2): 17,545 cm^{-1} ($\log \varepsilon = 3.59$), 29,940 cm^{-1} (4.08), 35,210 cm^{-1} (4.20), 37,860 cm^{-1} (4.32), 41,320 cm^{-1} (4.52). N.M.R.: ^1H in CD_2Cl_2 shows two singlets at δ7.26 and 2.12 ppm, assigned to the methine ring and the methyl group protons respectively (Figure 2.1) complicated by ^{195}Pt satellites (33% abundance; $I = \frac{1}{2}$). Coupling constant for the methyl proton interaction, $^4J_{Pt-CH_3}$, is 8.18 Hz. The ring proton coupling constant, $^4J_{Pt-CH}$, is 8.5 Hz. $^{13}C-\{^1H\}$ n.m.r. in CD_2Cl_2 exhibits three resonances at chemical shift values of δ34.2, 135.6 and 174.1 ppm. By expansion of the spectrum we can determine the Pt-C couplings of

$^{3}J_{Pt-C}$ = 30 Hz; $^{3}J_{Pt-C}$ = 40 Hz; $^{2}J_{Pt-C}$ = 15 Hz, respectively. By retaining the proton coupling the following assignments can be made: $-CH_3$ (δ34.2 ppm), C-H (δ135.6 ppm) and S-C-Me (δ174.1 ppm).

Platinum(II)bis(dithio-1-benzoylacetonate) $[Pt(S_2C_3PhHCH_3)_2]$

This was prepared by the same procedure as the analogous nickel complex, using $Pt(PhCN)_2Cl_2$ (0.05 g) as source of Pt(II) and 1-benzoylacetone (1 g) as ligand. Yield 0.01 g (15%) Analysis: Found %C 40.5, %H 3.0 Calculated for $PtC_{20}H_{18}S_4$, %C 41.3, %H 3.1. Mass Spectrum: m/e 581, $[Pt(S_2C_3PhHCH_3)_2]^+$; m/e 193, $[S_2C_3PhHCH_3]^+$.

Platinum(II)bis(dithiotrifluoroacetylacetonate) $[Pt(S_2C_3CF_3HCH_3)_2]$

This was again prepared by the same method as the $[Ni(S_2C_3PhHCH_3)_2]$ complex using $Pt(PhCN)_2Cl_2$ (0.05 g) and 1,1,1-trifluoroacetylacetone (1 ml). Yield 0.015 g (25%) Analysis: Found %C 21.0, %H 1.5. Calculated for $PtC_{10}H_8F_6S_4$ %C 21.2, %H 1.4. Mass Spectrum: m/e 565, $[Pt(S_2C_3CF_3HCH_3)_2]^+$; m/e 185, $[S_2C_3CF_3HCH_3]^+$. Electronic spectrum (50,000 to 11,500 cm^{-1} in CH_2Cl_2): 15,725 cm^{-1} ($\log \varepsilon$ = 3.84), 29,070 cm^{-1} (4.04), 37,315 cm^{-1} (4.29), 41,670 cm^{-1} (4.56). N.M.R.: ^{1}H in CD_2Cl_2, shows two resonances at δ7.46 and 2.12 ppm, assigned to the methine ring and the methyl group protons respectively. No ^{195}Pt satellites observed.

Platinum(II)bis(dithiobenzoyl-1,1,1-trifluoroacetonate) $[Pt(S_2C_3PhHCF_3)_2]$

This was prepared by the same method as discussed previously for $[Ni(S_2C_3PhHCH_3)_2]$ using $Pt(PhCN)_2Cl_2$ (0.05 g) and benzoyl-1,1,1-trifluoroacetone (1 g) as ligand. Yield 0.015 g (20%). Analysis: Found %C 34.1, %H 1.9 Calculated for $PtC_{20}H_{12}F_6S_4$ %C 34.7, %H 1.7. Mass Spectrum: m/e 689, $[Pt(S_2C_3PhHCF_3)_2]^+$; m/e 247, $[S_2C_3PhHCF_3]^+$ Electronic Spectrum (50,000 to 11,500 cm^{-1} in CH_2Cl_2): 14,880 cm^{-1} ($\log \varepsilon = 3.54$), 23,530 cm^{-1} (4.17), 27,250 cm^{-1} (4.30), 32,260 cm^{-1} (4.24), 40,490 cm^{-1} (4.53), 43,670 cm^{-1} (4.49). N.M.R.: ^1H in CD_2Cl_2 shows a singlet resonance at δ1.62 ppm assigned to the methine ring proton, phenyl resonances observed between δ7.2 and 7.8 ppm.

(ii) Instrumentation

Microanalyses were carried out by the University of Edinburgh Chemistry Department. Infrared spectra were recorded in the 4,000 to 200 cm^{-1} region on a Perkin-Elmer 457 grating spectrometer using nujol mulls on caesium iodide plates and potassium bromide disks. U.V./visible spectra were recorded in the 50,000 to 11,500 cm^{-1} region on a Pye-Unicam SP8-400 spectrophotometer, using 1 mm matched quartz cells. Mass spectra were measured on an A.E.I. MS9 spectrometer. Hydrogen-1 n.m.r. spectra were recorded on Varian Associates HA-100 and Bruker WP-200 spectrometers. Carbon-13 n.m.r. spectra were recorded on a Bruker WH-360 spectrometer.

References (Chapter 2)

1. J.P. Fackler, Prog.Inorg.Chem., 1966, 7, 361.
2. W.C. Fernelius and B.E. Bryant, Inorg.Syn., 1957, 7, 105.
3. R.H. Holm and M.J. O'Connor, Prog.Inorg.Chem., 1971, 14, 241.
4. E. Fromm and P. Ziersch, Chem.Ber., (1906), 39, 3599.
5. A. Fredga and A. Brändström, Ark. Kemi., 1950, 1, 197.
6. R.L. Martin and I.M. Stewart, Nature, 1966, 210, 522.
7. T.N. Lockyer and R.L. Martin, Prog.Inorg.Chem., 1980, 27, 224 and references therein.
8. A. Ouchi, M. Nakatani and Y. Takahashi, Bull.Chem.Soc., Japan, 1968, 41, 2044.
9. Y. Takahashi, M. Nakatani and A. Ouchi, Bull.Chem.Soc., Japan, 1969, 42, 274.
10. S.E. Livingstone, Coord.Chem.Revs., 1971, 7, 59.
11. M. Cox and J. Darken, Coord.Chem.Revs., 1971, 7, 29.
12. C. Blejean, Inorg.Nucl.Chem.Lett., 1971, 7, 1011.
13. A. Furuhashi, S. Kawai, K. Watanuki and A. Ouchi, Sci.Pap.Coll.Gen.Educ. Tokyo Univ., 1969, 19, 183; Chem.Abs., 1970, 73, 41412.
14. K. Knauer, P. Hemmerich and J.D.W. van Voorst, Angew.Chem., 1967, 6, 262.
15. O. Siiman and J. Fresco, Inorg.Chem., 1969, 8, 1846.
16. O. Siiman and J. Fresco, J.Am.Chem.Soc., 1970, 92, 2652.
17. G.A. Heath and R.L. Martin, J.C.S. Chem.Comm., 1969, 951.

18. C.G. Barraclough, R.L. Martin and I.M. Stewart, Aust.J.Chem., 1969, 22, 891.

19. V. Agarwala and P.B. Rao, Appl.Spectrosc., 1969, 23, 224.

20. C.G. MacDonald, R.L. Martin and A.F. Masters, Aust.J.Chem., 1976, 29, 257.

21. F.R. Hartley, "The Chemistry of Platinum and Palladium", Applied Science Publishers Ltd., London, 1973.

CHAPTER 3

Electrochemical Studies of Palladium and Platinum bis-Dithio-acetylacetonates and their Structural Analogues

3.1 Introduction

Over the past few years, a large range of bis-alkyl-substituted 1,1-dithiocarbamate (i) and 1,2-dithiolene (ii) transition metal complexes have been prepared and characterised using a wide range of techniques, including electrochemical methods[1,2,3].

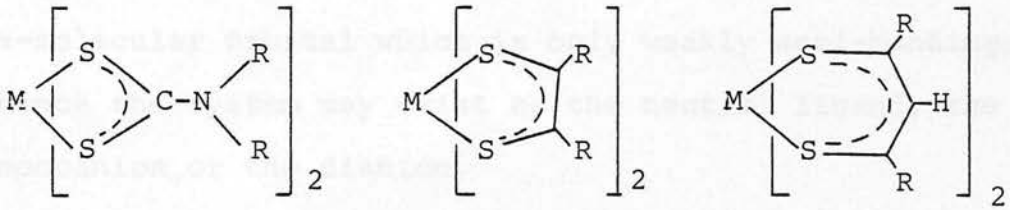

(i) (ii) (iii)

The metal-1,2-dithiolenes have made a significant contribution to the recognition of ligand-based charge transfer processes of co-ordination complexes[4]. The 1,1-dithio complexes are in turn generally believed to show substantially metal-based redox couples[5-8]. McCleverty originally suggested that the 1,3 dithio-β-diketonate complexes (iii) might posses similar redox properties to the 1,2-dithiolenes[3]. Schrauzer, however, drew attention to the important topological distinction between "even" (1,2-dithio) and "odd" (1,1-dithio and 1,3-dithio) resonance-stabilized ligands, and predicted that the chelates of the latter would not possess the unusual chemical properties associated with the dithiolenes[9].

The "odd" unsaturated ligand systems tend to exist as monoanions due to the presence of the non-bonding, singly occupied π-molecular orbital in its neutral energy level scheme (see Figure 3.1). Since no low-lying π-molecular orbitals are available, the "odd" ligands do not usually accept additional electrons beyond the monoanion. The "even" ligands, however, have a lowest unoccupied π-molecular orbital which is only weakly anti-bonding; hence the system may exist as the neutral ligand, the monoanion, or the dianion.

None the less, the planar dithioacetylacetonates $[M(SacSac)_2]$ (where M = Ni, Pd, Pt; R = R' = CH_3) were soon shown to undergo two successive one-electron reductions by polarography in acetone[10] (Scheme 3.1).

Scheme 3.1

$$[M(SacSac)_2]^0 \Longleftrightarrow [M(SacSac)_2]^{1-} \Longleftrightarrow [M(SacSac)_2]^{2-}$$

The nature of this redox activity has become a topic of some controversy. Schrauzer's conclusions, by excluding ligand-based processes, would require successive M^{II}/M^{I} and M^{I}/M^{O} assignments for the whole series. As we have already stated, true metal-based reductions have been identified recently for the "odd"-membered 1,1-dithiocarbamate complexes (i)[5-8] and even for the nickel-1,2-dithiolenes themselves beyond the second ligand-based reduction[11-13].

Figure 3.1 Schematic π-molecular orbital energy level diagram

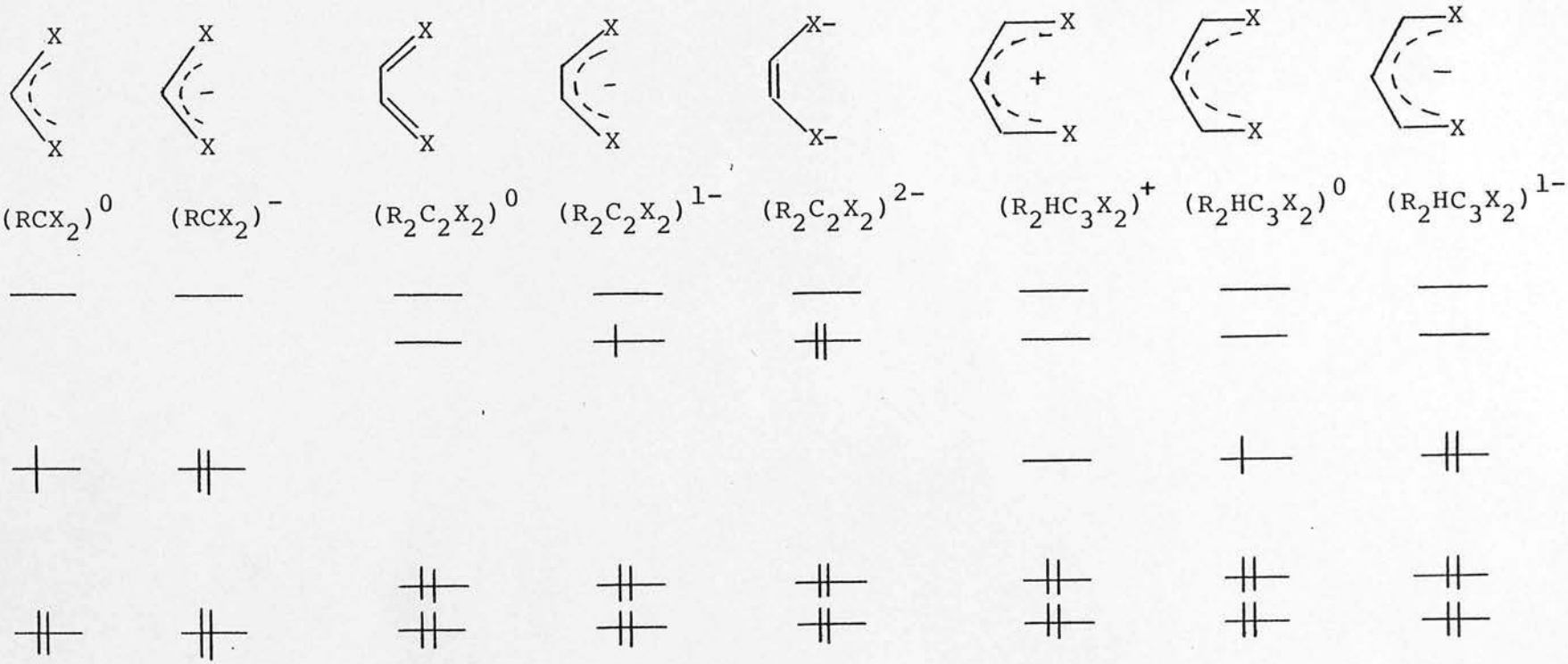

Notwithstanding similar formal assignments for the d^8 1,3-dithioacetylacetonates, Bond et al described the acceptor orbitals as substantially delocalised over the whole molecule[10]. Martin et al found an orderly variation in E^o with changing substituent within the nickel series, suggestive of ligand participation [14] and Geiger et al noted a corresponding shift in the parent compound (R = R' = H)[15]. The substituent effect, although informative, requires calibration for proper assessment as, for example, the unquestionably metal-based reductions of $[Ru(O_2C_3RHR')_3]$ show a qualitatively similar trend[16].

In this chapter we present comparative a.c. and d.c. voltammetric studies on the electro-reduction of the nickel, palladium and platinum complexes $[M(S_2C_3RHR')_2]$ (iii; R,R' = ^tBu, CH_3, Ph, CF_3) in non-aqueous media. Consistent electrode potential/inductive parameter correlations emerge for the successive one-electron transfer steps, and these trends are assessed in relation to the behaviour of variously substituted metal-1,2-dithiolenes (ii) and (non-metallated) dithiolylium ions (iv), $[S_2C_3RHR']^+$. Similar comparisons are made with the 1,3-monothio—complexes, $[M(SOC_3RHR')_2]$, and with the planar $[M(O_2C_3RHR')_2]$ systems. The latter are found to parallel their dithio congeners much more closely than might be expected from cursory observation of their generally irreversible electrochemical behaviour.

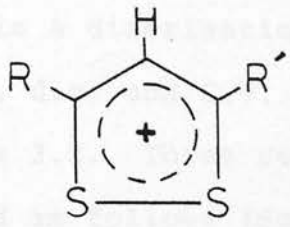

(iv)

The wealth of new data collected for the $[M(S_2C_3RHR')_2]$ complexes, together with the comparisons of related systems, suggests that the redox-active orbital of the 1,3-dithio complexes is of largely, if not entirely, ligand character. This belief is substantiated by a recent molecular orbital calculation which shows that the parent 1,3-dithio-nickel complex $[Ni(S_2C_3H_3)_2]$ has approximately the same percentage metal character in its lowest unoccupied orbital as the corresponding 1,2-dithio-nickel system (ii)[17].

Results and Discussion

3.2 Voltammetry of $[M(SacSac)_2]$ complexes (iii: R,R' = CH_3)

The original polarographic studies demonstrated that the complexes showed two successive one-electron reductions, although there was substantial evidence that the electro-generated monoanion $[M(SacSac)_2]^{1-}$ was prone to rearrangement to form a new species, which was itself capable of reduction[10]. A subsequent study for M = Ni and Pt using cyclic voltammetry firmly established this behaviour[15]. In this laboratory we have now re-examined

in detail the complete triad of complexes, and shown that the rearrangement is a dimerisation (Chapter 4). Complementary a.c., d.c. and C.V. data for $[Pd(SacSac)_2]$ are shown in Figure 3.2. Three reduction waves are apparent and may be assigned as follows (Scheme 3.2).

Scheme 3.2

$$[M(SacSac)_2]^0 \overset{a}{\Longleftrightarrow} [M(SacSac)_2]^{1-} \overset{b}{\Longleftrightarrow} [M(SacSac)_2]^{2-}$$

$$\text{"dimerisation"} \quad k \downarrow$$

$$[M(SacSac)_2]_2^{2-} \overset{c}{\Longleftrightarrow} [M(SacSac)_2]_2^{4-}$$

Our study confirms that the rate of rearrangement follows the order

$$Ni << Pd < Pt$$

The palladium complex is thus extremely useful, as the rate of rearrangement of the monoanion is intermediate between that of nickel and platinum, and leads to competing electrochemical behaviour. A more extensive discussion of the nature of the rearrangement of the monoanion together with a detailed examination of the kinetics of the system are to be found in Chapter 4.

Oxidation of the $[M(SacSac)_2]$ complexes cleaves the chelate ligand to yield the resonance-stabilized dithiolylium ion (iv) (Scheme 3.3).

Figure 3.2 Complementary a.c., d.c. and C.V. data for $[Pd(SacSac)_2]$

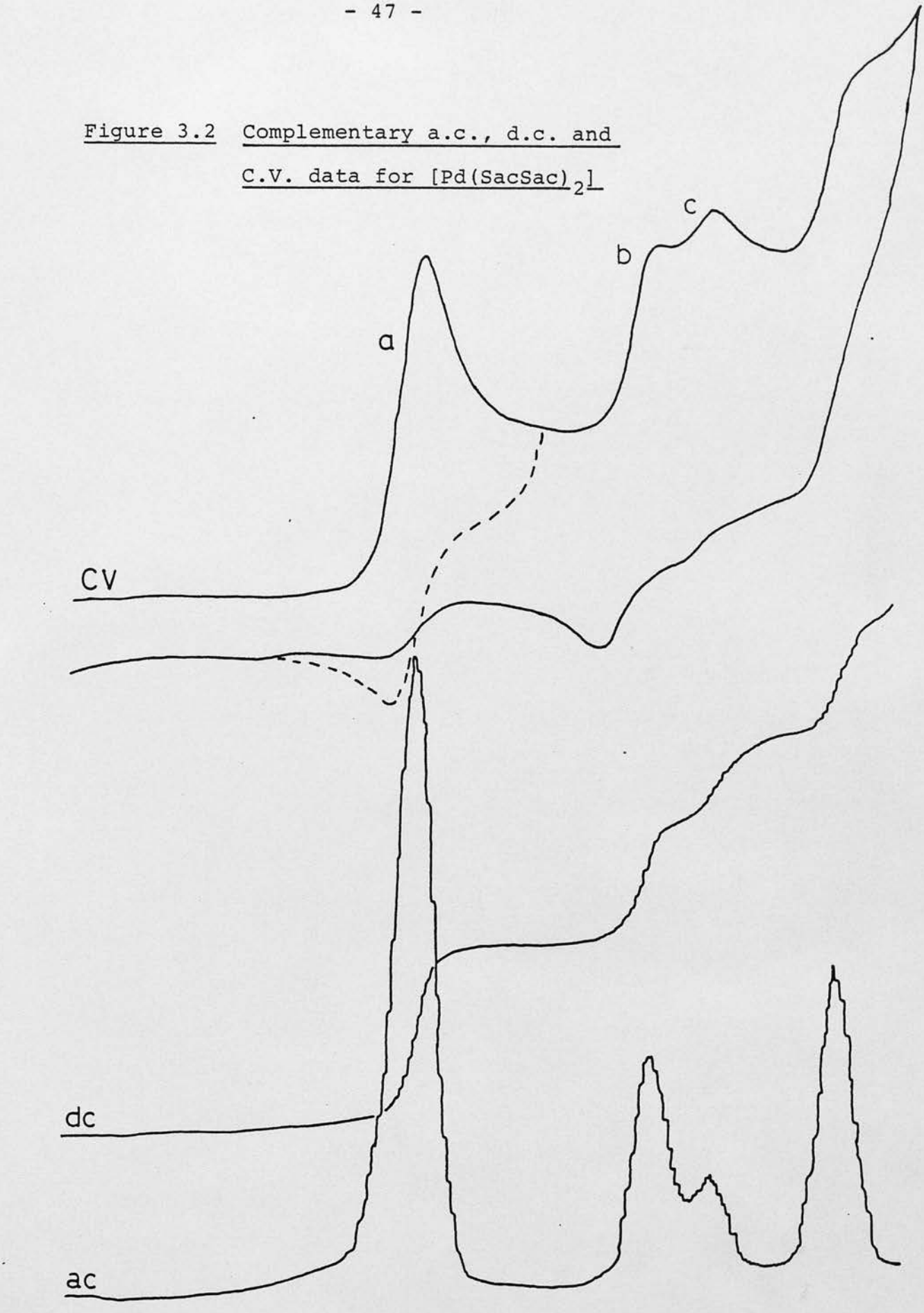

Scheme 3.3

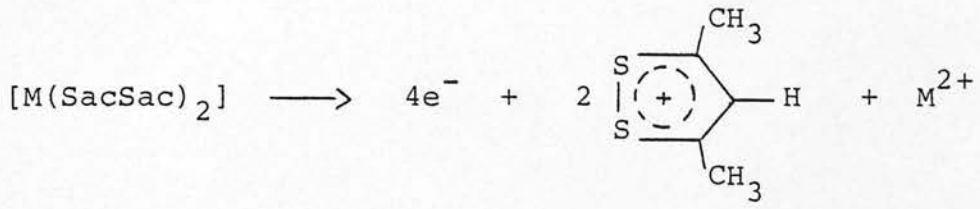

The chemically irreversible nature of this 4-electron oxidation of $[Ni(SacSac)_2]$ at a Pt electrode is shown most clearly by cyclic voltammetry (Figure 3.3).

3.3 The Substituted Complexes

Several novel, substituted complexes of palladium and platinum have been prepared with the bulkier groups ^tBu, Ph, or CF_3 replacing one or both methyl groups on each ligand. The complexes all show two one-electron reductions, satisfying the standard criteria for rapid electron transfer. In each case, the monoanion rearrangement described above is found to be largely, or entirely, suppressed. Thus the palladium complexes have two fully reversible reduction waves only (Figure 3.4). The platinum complexes show evidence of rearrangement, but only as a minor pathway (<10%). It appears that the tendency of the monoanion to react is controlled by steric factors, since the rate of rearrangement is effectively suppressed by groups with both electron-withdrawing (Ph, CF_3) and electron-donating (^tBu) effects relative to CH_3. It is found that the parent complex $[Pt(S_2C_3H_3)_2]^{1-}$ rearranges even more rapidly than $[Pt(SacSac)_2]^{1-}$ itself[15].

Figure 3.3 Cyclic voltammogram of $[Ni(SacSac)_2]$ in CH_2Cl_2 showing oxidation to $[S_2C_3CH_3HCH_3]^+$ and its subsequent reduction

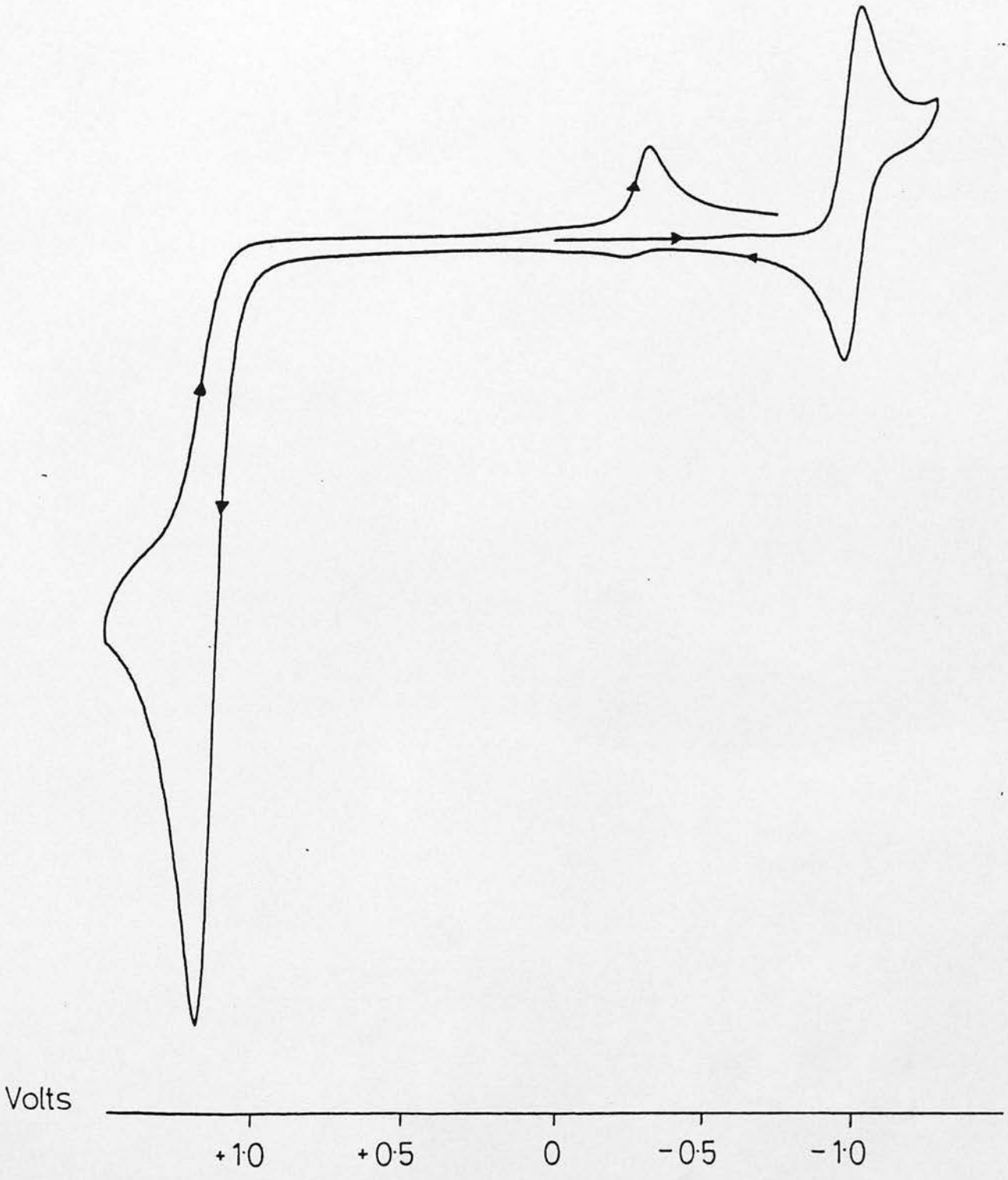

Figure 3.4 Electrochemical behaviour of $[Pd(S_2C_3CF_3HCH_3)_2]$

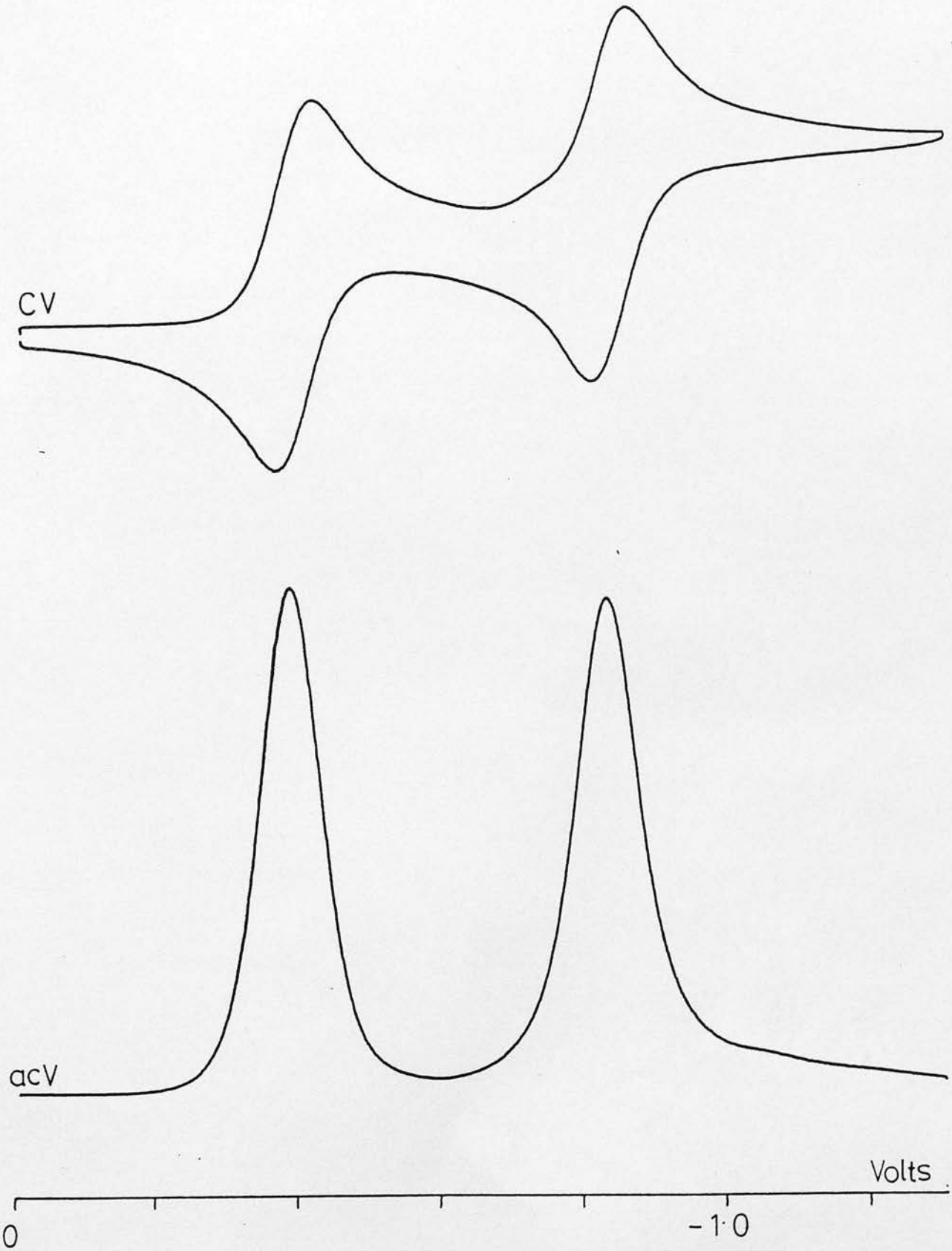

The substituted complexes show a marked gradation in their characteristic electrode potentials. The range of data collected here (Table 3.1) for a wide variety of substituted ligands on three metal centres allows systematic analysis of the influence of substituent group. Superimposed in Figure 3.5 are the E^{o}_{red} (1) and E^{o}_{red} (2) for all the $[M(S_2C_3RHR')_2]$ complexes available to this study, plotted against the one-ligand sum of the Taft inductive parameters $(\sigma_R^* + \sigma_{R'}^*)$[18], i.e. considering the polar effects of the substituent group only.

The linearity observed for both 1st and 2nd reductions justifies our conclusion that the substituent influence is inductive in nature, in accord with an earlier analysis of the first reduction of a range of nickel complexes, using the meta-Hammett parameter[14]. Successive reduction potentials are virtually independent of the identity of the metal centre, but are determined by the substituents, maintaining an almost constant gap of 0.45 ± 0.05 Volts between successive reductions.

A more detailed examination of, for example, the $[Pd(S_2C_3RHR')_2]$ E^{o}_{red} (1) shows small but discernible deviations from the line of least-squares best fit. This behaviour is not random since this divergence is reflected in the $E^{o}_{red}(2)$ vs. $\Sigma\sigma^*$ profile and are also reproduced for nickel and platinum. These systematic deviations from the classical Taft plot probably indicate the limitations of applying the kinetically determined

Table 3.1

Electrode potentials for the complexes $[M(S_2C_3RHR')_2]$ (E^{o}_{red} (1) and E^{o}_{red} (2)/Volts vs Ag/AgCl)

R,R' =	Ni	Pd	Pt
^{t}Bu, ^{t}Bu	-1.07	-1.06	-
	-1.58[a]	-	-
CH_3, CH_3	-0.94	-0.96	-0.96
	-1.42	-1.44	-1.41
CH_3, Ph	-0.75	-0.72	-0.80
	-1.16	-1.13	-1.24
Ph, Ph	-0.61	-0.60	-
	-1.02	-1.01	-
CF_3, CH_3	-0.43	-0.38	-0.46
	-0.93	-0.90	-0.91
CF_3, Ph	-0.25	-0.24	-0.23
	-0.73	-0.73	-0.69
CF_3, CF_3	-	+0.17	-
	-	-0.38	-

[a] by a.c. voltammetry on platinum

Figure 3.5 Reduction potential vs Taft parameter for the $[M(S_2C_3RHR')_2]$ complexes

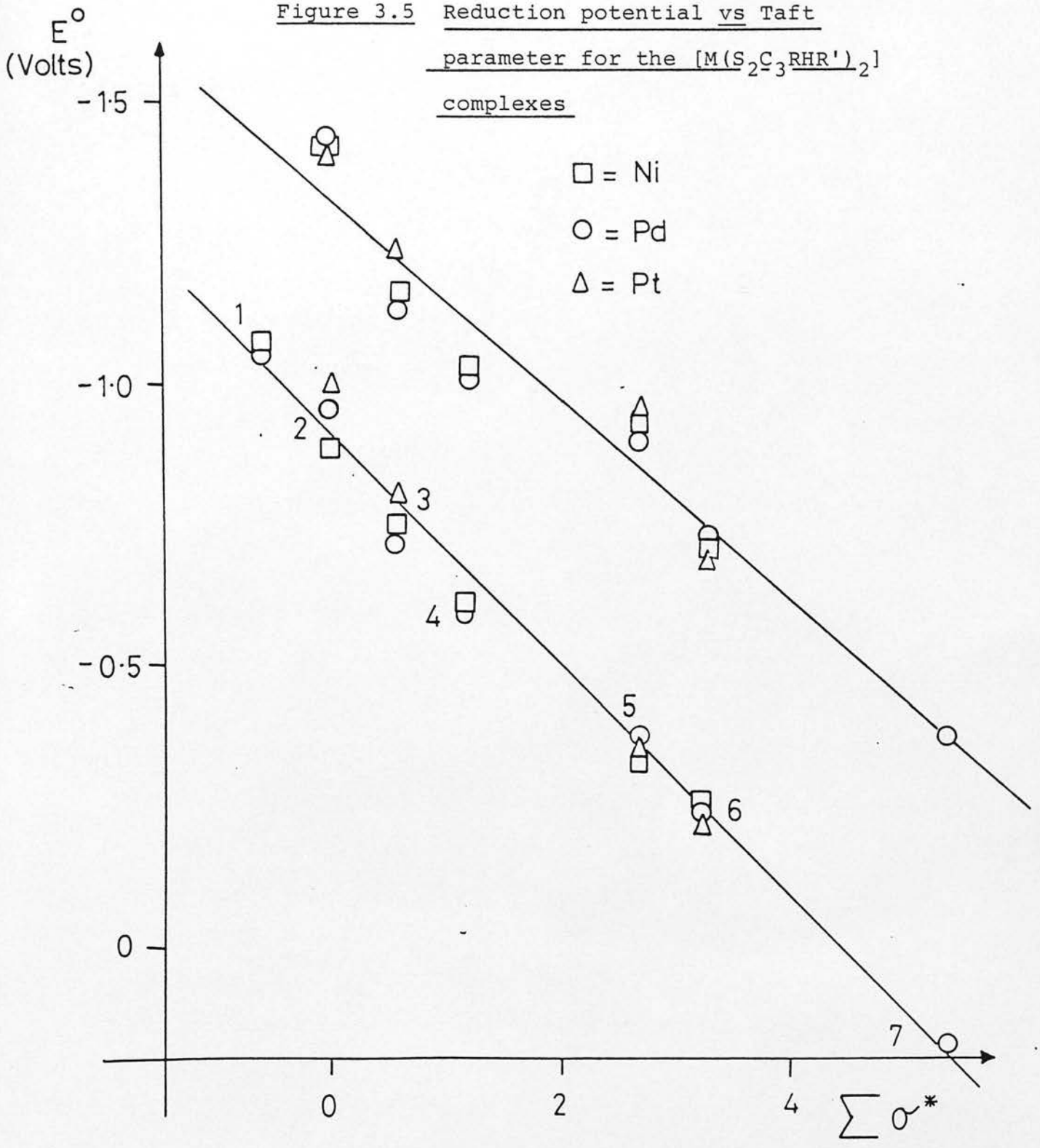

1 = $^{t}Bu/^{t}Bu$; 2 = CH_3/CH_3 ; 3 = CH_3/Ph ;

4 = Ph/Ph ; 5 = CH_3/CF_3 ; 6 = CF_3/Ph ;

7 = CF_3/CF_3

"linear free energy" parameter in such a remote context. This can be well illustrated by considering the correlation coefficients for the $E^{o}_{red}(1)$ vs. $\Sigma\sigma^{*}$ plot for $[M(S_2C_3RHR')_2]$ where M = Pd and Pt. Considering all data points collected for the palladium series, a correlation coefficient of 0.994 is found, whereas for the more limited range of platinum complexes, a correlation coefficient of 0.988 is obtained. Consideration of a matched subset of data yields a correlation coefficient of 0.988 for the palladium compounds; i.e. the deviations from linearity are dependent on the substituent bias in the set of data considered.

For this reason, we find it justified and desirable to define a new scale of electrochemically-derived induction parameters, designated σ^{e}. This scale has been established using the first reduction potentials for the $[Pd(S_2C_3RHR)_2]$ family, which provides the widest range of symmetrically substituted derivatives. The new values are obtained by horizontally "smoothing" the measured values onto a line parallel to the $E^{o}_{red}(1)$ vs. $\Sigma\sigma^{*}$ line of least squares best fit previously determined and located so that the inductive parameter for R = Me remains arbitrarily defined as zero, so as to maintain a correlation of unaltered physical significance. The appropriate, $2\sigma^{e}_{R}$, for each $[Pd(S_2C_3RHR')_2]$ complex is then simply read off at the experimentally measured potential. The modified and classical Taft parameters are listed in Table 3.2.

Table 3.2 Substituent Inductive Parameters

R =	Taft (σ^*_R)	Modified[a] (σ^e_R)
t_{Bu}	-0.30	-0.25
CH_3	0	0
Ph	+0.6	+0.90
CF_3	+2.70	+2.80

[a] see text

The validity of this new scale is confirmed by the fact that the originally excluded asymmetrically substituted complexes also fit well onto the modified scale, and by the observation that analogous plots of $(\sigma^e_R + \sigma^e_{R'})$ vs. E^o_{red} (2) for palladium and both E^o_{red} (1) and E^o_{red} (2) for nickel and platinum show significantly improved correlation coefficients. Consequently, slight, but significant trends in gradient become apparent. The least squares analyses for all six redox couples, based on the modified σ^e parameters are listed in Table 3.3.

For comparative purposes, the gradient, or substituent sensitivity, can be conveniently expressed in mV per σ^e unit as we observe an electrode potential shift of approximately 100 mV per unit numerical change in an individual substituent σ^e value. Thus we can define the useful relationship

$$\delta E^o \text{ (in mV)} = 200 \; \Sigma \, \sigma^e$$

where δE^o is the shift in $E^o_{red}(1)$ between $[Pd(SacSac)_2]$ and any other $[Pd(S_2C_3RHR')_2]$ complex. Approximately the same relationship extends to the nickel and platinum systems as well. Several significant points now emerge from the data which should be stressed. Firstly, for a given metal ion, the gradients for $E^o_{red}(1)$ and E^o_{red} (2) are close to parallel, illustrating that the redox-active orbital is of similar character for both first and second electron transfers. This would be inconsistent with metal-based followed by ligand-based stepwise reductions, for example. Secondly, the

Table 3.3

Linear E^{o}/Inductive Parameter Correlations in $[M(X_2C_3RHR')_2]$

$E^{o} = k(\sigma^{e}_{R} + \sigma^{e}_{R'})$

(least squares fitted gradients, 1000 k/V, with correlation coefficients in parentheses)

MX_4 =	NiS_4	PdS_4	PtS_4	PdO_4	NiS_2O_2
E^{o}_{red} (1): k =	190 (1.00)	198 (1.00)	206 (1.00)	208 (0.96)	166 (0.99)
E^{o}_{red} (2): k =	172 (0.98)	176 (0.99)	186 (0.99)	-	-

magnitude of the substituent influence on the electrode potentials is consistent with substantial ligand participation in charge acceptance, and is relatively immune to change in the central metal ion.

Comparison with the metal-1,2-dithiolenes, with their ligand-based redox activity, is inevitable. The series of nickel complexes, $[Ni(S_2C_2RR')_2]$, where R,R' = CH_3, Ph or CF_3 [3,4], gives an E^o_{red} (1) gradient, on the σ^e scale, which is negligibly different from the corresponding range of $[Ni(S_2C_3RHR')_2]$ complexes, (i.e. 186 mV versus 190 mV per σ^e unit).

Furthermore, comparisons can be made with the one-electron reduction potentials of the related metal-free dithiolylium ions (iv) related to the corresponding 1,2-dithiolyl radicals. An early analysis was limited to R = ^tBu, CH_3, or Ph [19]. In this study we have extended this series to include R = CF_3 (Table 3.4). As we have previously stated, the oxidation of $[M(SacSac)_2]$ results in the breakdown of the complex to yield the 1,2-dithiolylium ion. This behaviour is also true for the substituted complexes, each giving rise to the analogous substituted 1,2-dithiolylium ion, which is then detected by its reduction (Figure 3.6). The presence of the strongly electron-withdrawing CF_3 group will tend to destabilize the $[S_2C_3RHR']^+$ ion by exaggerating the positive charge on the hetero-nuclear ring. Indeed, such species have not been isolated, but are likely to be highly unstable and difficult

Table 3.4 Electrode potentials for the electrochemically derived 1,2-dithiolylium ions

R, R' =	$(E^{o}/V$ vs. Ag/AgCl$)^{(a)}$ $[S_2C_3RHR']^{+/0}$	$[M(S_2C_3RHR')_2] \xrightarrow{-4e^-} 2[S_2C_3RHR']^{+} + M^{2+}$
^{t}Bu, ^{t}Bu	-0.46	+1.12
CH_3, CH_3	-0.35	+1.18
CH_3, Ph	-0.09	+1.23
Ph, Ph	0.00	+1.37
CF_3, CH_3	+0.19	+1.51
CF_3, Ph	+0.30	+1.69

(a) Calculated as the potential at 85% of the forward peak current.

Figure 3.6 Electrochemical production of $[S_2C_3CF_3HCH_3]^+$ by the irreversible oxidation of $[Ni(S_2C_3CF_3HCH_3)_2]$ and its subsequent reduction

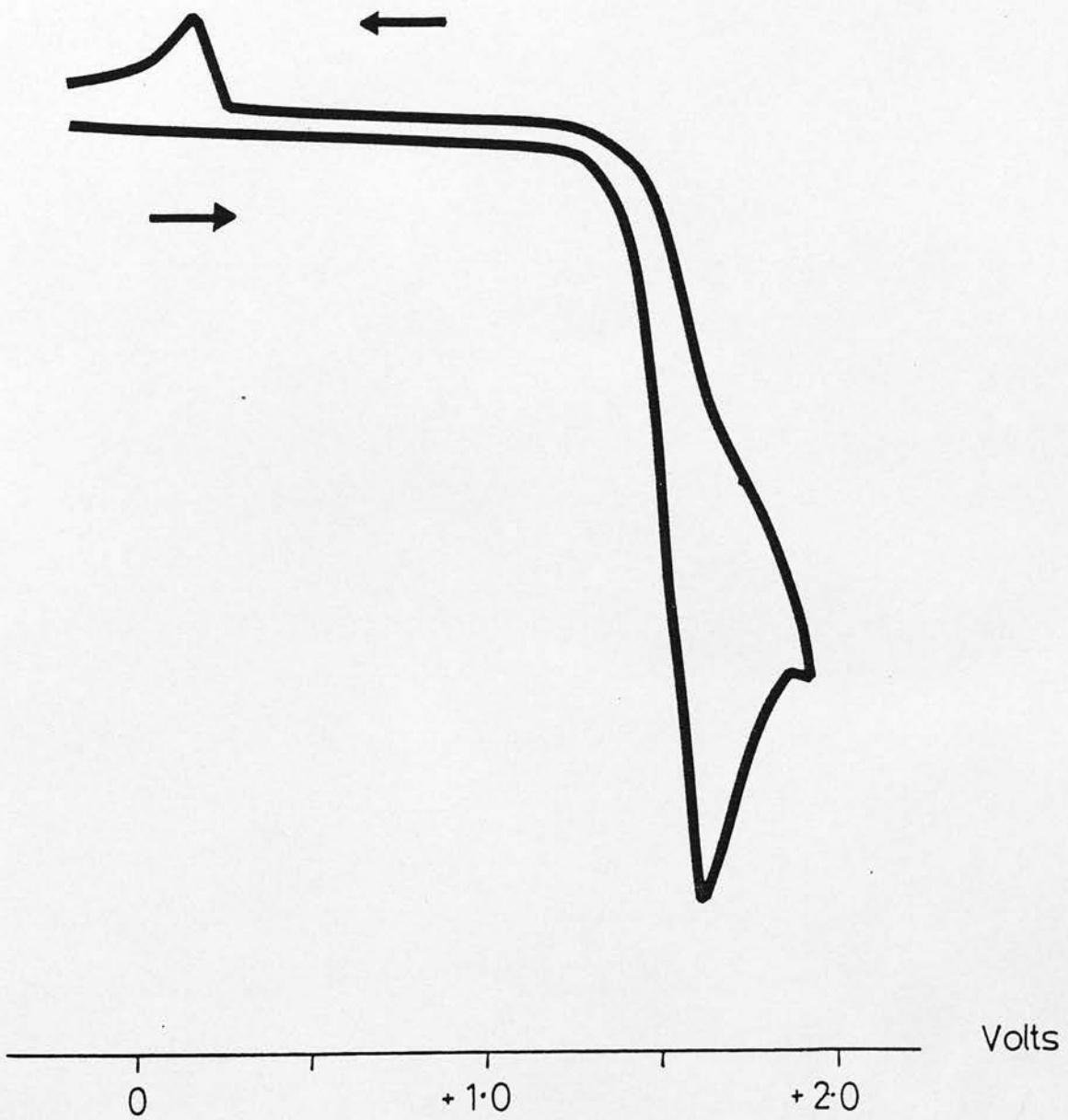

to prepare *via* chemical methods. However, by the electrochemical oxidation of the $[M(S_2C_3RHR')_2]$ complex, we can produce the dithiolylium ion and determine its electrode response, *in situ*. We have taken advantage of this as shown in Table 3.4. Note, that the bulk electrochemical preparation of the 1,2-dithiolylium ion was not attempted, consequently only very small quantities of $[S_2C_3RHR']^+$ and the neutral radical $[S_2C_3RHR']^{\cdot}$ are produced. The detailed electrochemical analysis of the $[S_2C_3RHR']^{\cdot}$ radical is not therefore possible as it will rapidly diffuse into the bulk solution.

We have now demonstrated that the reduction of the 1,2-dithiolylium ion shows the same degree of sensitivity to substituent group as the metal-1,3-dithio series, for example, comparing $[S_2C_3RHR']^+$ with $[Pd(S_2C_3RHR')_2]$ gives gradients of 180 mV and 198 mV per σ^e unit respectively. The close parallel between the substituent sensitivity can be well represented graphically (Figure 3.7). The slight differences observed in sensitivity is no greater than that between the isostructural nickel, palladium and platinum systems (Table 3.3). It should also be noted that the correlation coefficients (in the order 0.99) for these structurally distinct species vindicate the use of the modified parameters in a wider context.

We believe that the present data clearly establish the dominant ligand character in the redox-active orbital, since we encounter close to the maximum expected substituent influence and almost negligible metal ion participation.

Figure 3.7 Substituent sensitivity for delocalised organosulphur systems

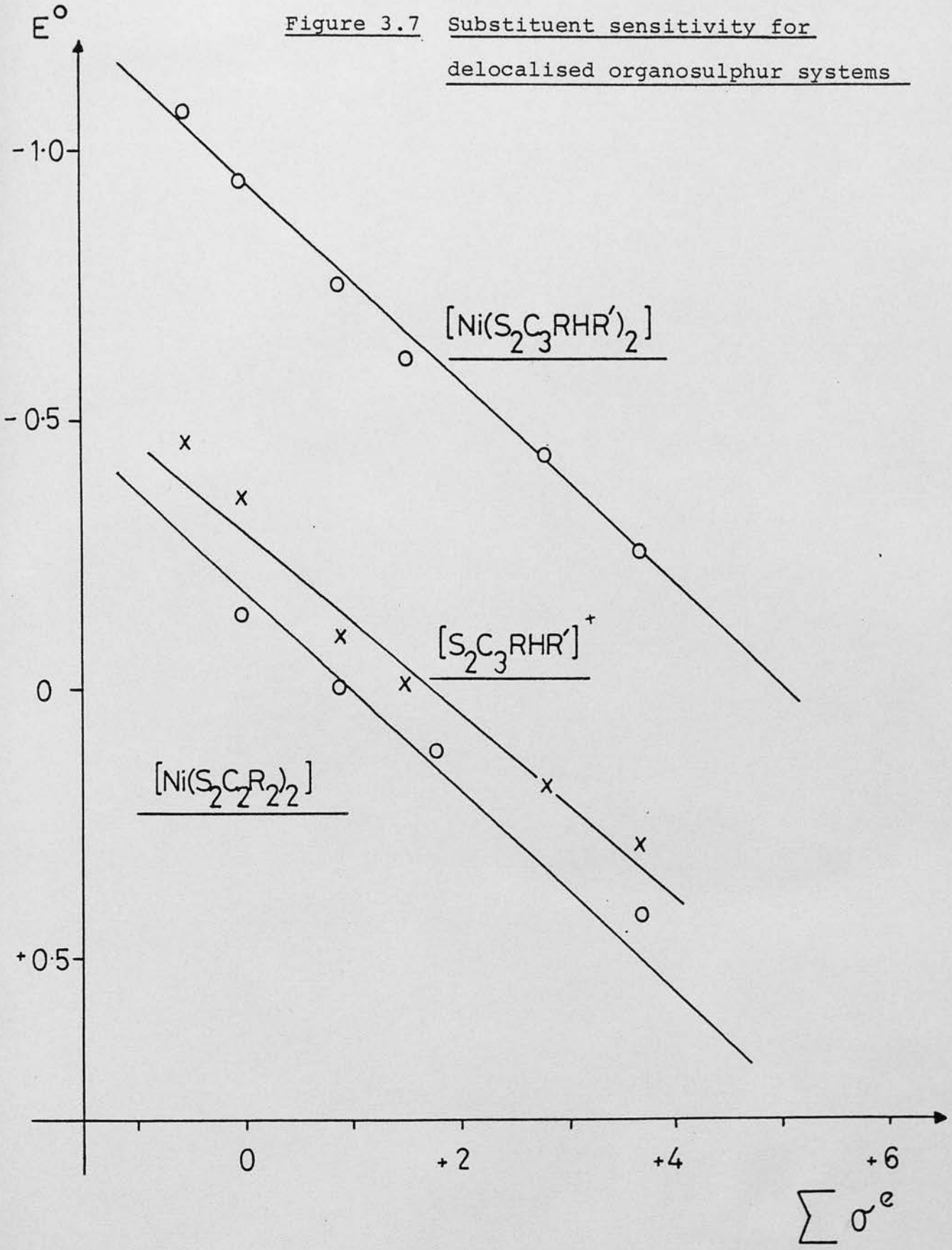

Vlcek reported that, for a ligand-mediated redox-couple, changing the substituent on the metal complex should result in the same shift in E° potential as the free ligand[20]. Clearly in our case, comparison with the unco-ordinated ligand is impossible, due to its tendency to dimerise, which is why comparison with the 1,2-dithio-complexes and, more importantly, the dithiolylium ion is so essential.

The behaviour of the 1,3-dithio system raises questions regarding Schrauzer's "odd-even" criterion for predicting redox character. It now seems apparent, that the correct inference from the topological distinction between the resonance-stabilized 1,2-dithio and 1,3-dithio chelates is that the acceptor orbital in the latter lies to higher energy (by approximately 0.8 eV), leading to more cathodic, reversible reduction potentials, rather than the absence of ligand-based electron transfer activity.

This ligand-mediated redox character is bourne out by molecular orbital calculations. Although original work attributed largely metal character to the lowest unoccupied orbital[21], a recent and more elaborate analysis suggests that the redox-active orbital has virtually no metal character[17].

3.4 Comparison with the oxo system

The monomeric nickel-1,3-dithio systems (NiS_4) differ strikingly from the corresponding β-diketonates (NiO_4) which generally adopt oligomeric, octahedral structures. The palladium and platinum bis-1,3-diketonates, however, provide

a true isostructural sequence of resonance-stabilized chelates, allowing comparison of donor atom effect over a range of substituted complexes.

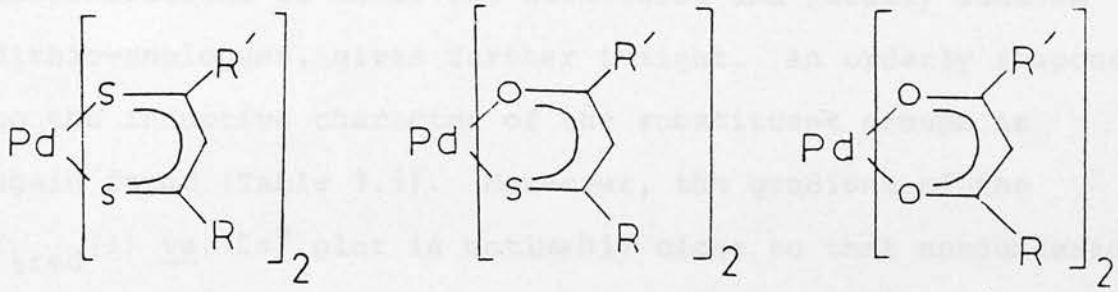

A study of $[Ni(X_2C_3{}^tBuH{}^tBu)_2]$ (X = S, O), where the steric bulk of the ^{t}butyl group yields a planar NiO_4 complex, showed that on changing the donor atom from sulphur to oxygen we observe a shift in redox couples to more negative potentials, and for the NiO_4 complex, the electron transfer is sluggish and irreversible[22]. The faster rate of electron transfer of the sulphur-containing ligands was thought to imply donor atom involvement in the charge transfer process. This was found to be consistent with the evidence that the redox process was dependent on electrode material, i.e. the electron transfer occurs via a bridging mechanism.

To date, we are unaware of a comparative investigation on the planar palladium and platinum bis-1,3-diketonates. We have extended our study to include complementary a.c. and cyclic voltammetric data on a useful set of substituted palladium complexes, $[Pd(O_2C_3RHR')_2]$ (R,R' = CH_3, Ph or CF_3)

in non-aqueous media. Analysis confirms that these complexes generally undergo a sluggish one-electron reduction. Comparison of a series of complexes, together with considerations of their iso-structural and ideally behaved dithio-analogues, gives further insight. An orderly response to the inductive character of the substituent groups is again found (Table 3.5). Moreover, the gradient of the $E_{\frac{1}{2}red}(1)$ *vs.* $\Sigma\sigma^e$ plot is noticeably close to that encountered for the corresponding $[M(S_2C_3RHR')_2]$ series of reductions (Figure 3.8), suggesting that distribution of charge in the two systems is similar. As previously, the oxo systems are systematically found to be more difficult to reduce than their dithio-analogues by approximately 0.45 Volts. Thus the introduction of the "harder" more electronegative heteroatom, leads to destabilization of the anti-bonding (acceptor) molecular orbitals[23].

A limited set of data collected for the reversible first reduction of the monothio chelates in the $[Ni(SOC_3RHR')_2]$ series, shows that, not surprisingly, the $E^o_{red}(1)$ potential lies between those of the corresponding MS_4 and MO_4 complexes (Table 3.5). Note that the $E^o_{red}(1)$ *vs.* $\Sigma\sigma^e$ plot is again closely linear, even for the asymmetrically substituted complexes, although there is a discernible departure from the gradients found for the MS_4 and MO_4 systems. However, the lower symmetry of the $[M(SOC_3RHR')_2]$ series restricts any simple interpretation of these data. A detailed analysis of a wider range of complexes is required, together with the behaviour of $E^o_{red}(2)$ before any conclusions are possible.

Table 3.5

Electrode potentials for diketonato and monothiodiketonato complexes

($E_{red}(1)$/V *vs.* Ag/AgCl)

R,R' =	$[Pd(O_2C_3RHR')_2]$[(a)]	$[Ni(SOC_3RHR')_2]$
^tBu, ^tBu	-	-1.21
CH_3, CH_3	-1.37	-1.11
CH_3, Ph	-1.27	-
Ph, Ph	-1.14	-0.89
CF_3, CH_3	-0.80	-
CF_3, Ph	-0.65	-0.49

(a) $E_{\frac{1}{2}red}(1)$ calculated as the potential at 85% of the cathodic peak current

Figure 3.8 Reduction potential/substituent effect correlations for $[Pd(X_2C_3RHR')_2]$ systems (X = O, S)

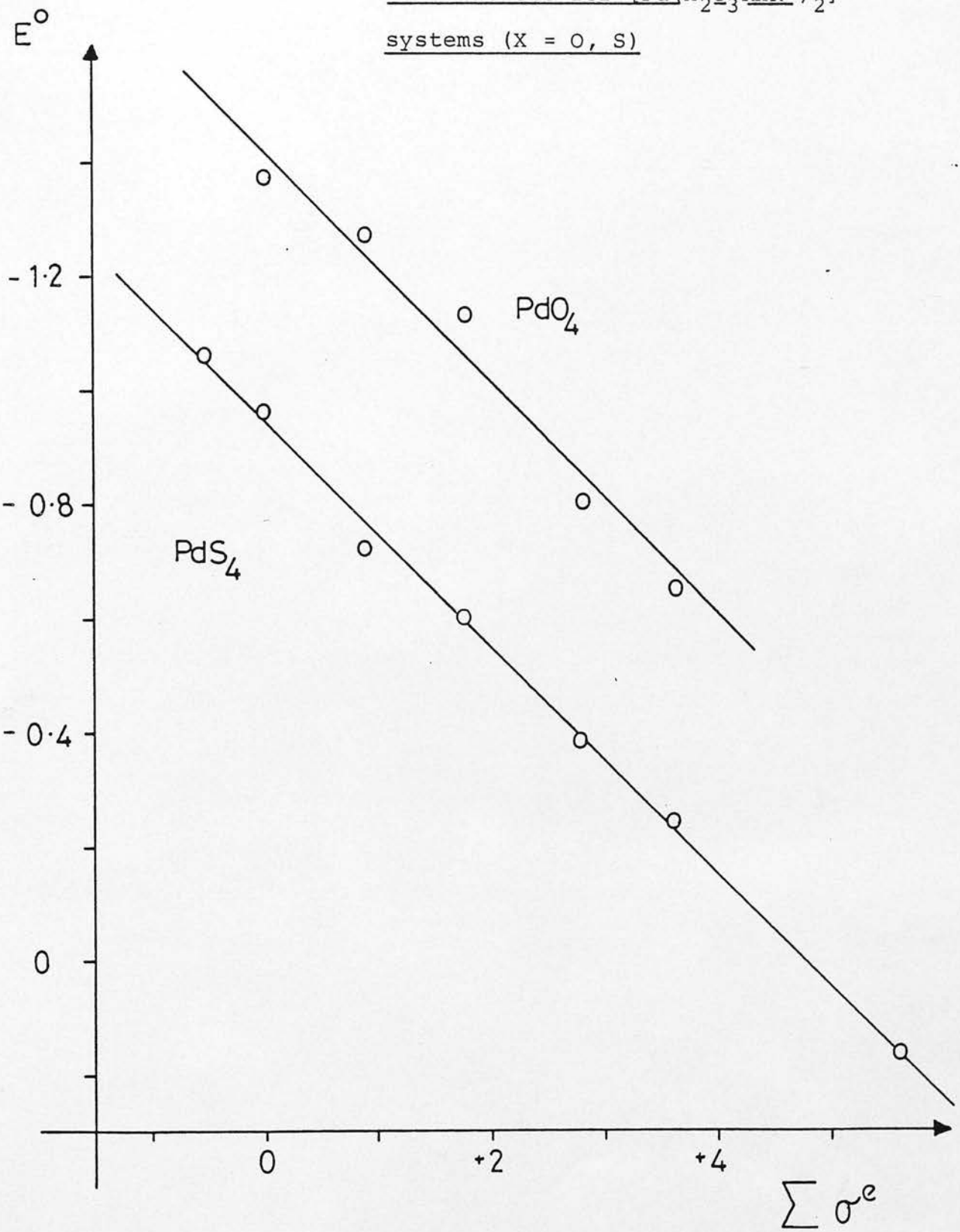

3.5 Experimental

(i) Materials

All complexes described were prepared as detailed in Chapter 2.

For electrochemistry, CH_2Cl_2 was stored over KOH pellets, then distilled from P_2O_5 immediately prior to use. Other electrochemical solvents were Analar grade and used without further purification. The Bu_4NBF_4 supporting electrolyte was prepared from Bu_4NOH and HBF_4 in water, recrystallized from a 1:1 ratio Analar methanol:water, then dried at 90°C in vacuo.

(ii) Instrumentation

Voltammetric studies in CH_2Cl_2/0.25 M Bu_4NBF_4 employed a P.A.R. 170 Electrochemistry System (potentiostat and programmer), interfaced with a Metrohm E505 cell stand and three-electrode cell configuration. A non-aqueous $Ag/AgCl/Cl^-/CH_2Cl_2$ reference electrode (against which ferrocene was oxidised at +0.62 Volts), separated by a further fritted salt-bridge, and a platinum counter-electrode were used in a 10 ml jacketted glass cell. The polarographic dropping mercury electrode (d.m.e.) functioned at electronically controlled drop times (t_d normally = 0.5 s). Other a.c. and cyclic voltammograms employed platinum wire or micro-disk working electrodes, whereas d.c. voltammograms

and diffusion current measurements were obtained with a Tacussel EDI rotating platinum electrode (r.p.e.) in the range 1,000 to 6,000 r.p.m. Routine scan rates were 100 mV/sec in C.V. and 10 mV/sec in other modes.

Cell solutions, normally ≈ 1.0×10^{-3} molar in complex, were degassed with CH_2Cl_2-saturated argon and cell temperatures in the range 225 to 295 Kelvin were maintained by a Haake F3Q circulating bath. The internal temperature of the cell was monitored using a Comark 5000 digital thermometer.

Routinely, the electrochemistry was studied in CH_2Cl_2, due to the higher solubility of the complexes in this medium, however, other solvents were at times also employed (e.g. acetone, dimethylformamide or acetonitrile). This involved the same basic set-up as described above, but 0.1 M Bu_4NBF_4 was found to be sufficient in these cases.

(iii) Voltammetric Analysis

Each compound's electrode response has been studied in detail; however, to prevent repetition of data, a representative analysis for a typical complex is presented below.

In CH_2Cl_2, at both d.m.e. and r.p.e., $[Pd(S_2C_3CF_3HCH_3)_2]$ shows two cathodic waves of equal height (Figure 3.9) and logarithmic analysis confirms d.c. Nernstian behaviour appropriate to stepwise one-electron reductions; i.e. plot of $\log(i_d - i)/i$ vs. E linear with slope = 59 mV.

Figure 3.9 D.c. voltammogram of $[Pd(S_2C_3CF_3HCH_3)_2]$ using r.p.e., showing two reduction waves of equal height

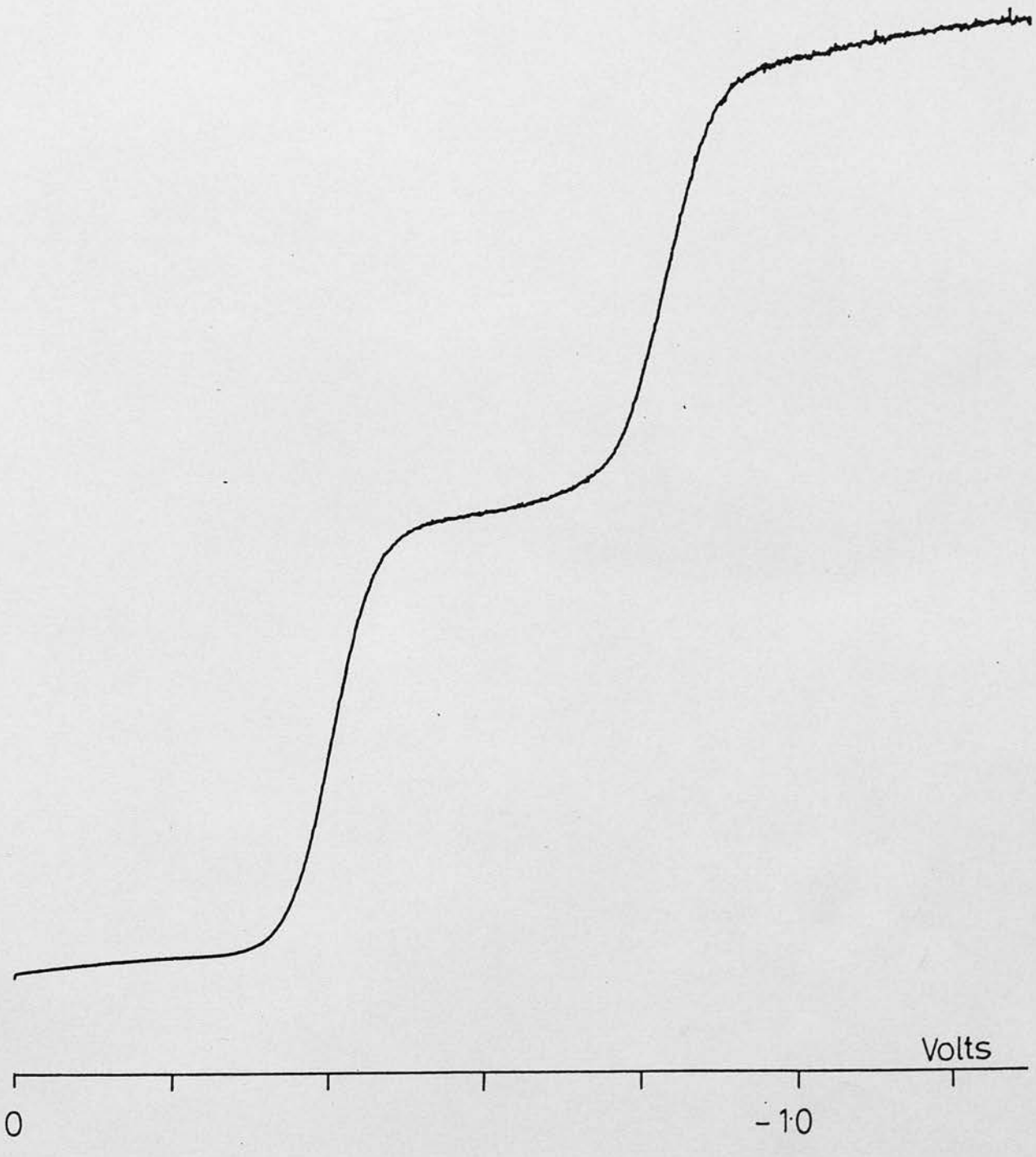

A.c. waves are symmetric, with half-height widths of 90 ± 5 mV and a linear i_p *vs.* $\omega^{\frac{1}{2}}$ plot (through the origin), in the frequency range ω = 20 to 1,000 Hz with phase angle $\phi = 45^{\circ}$ (Figure 3.10). Similarly a linear plot of $E_{d.c.}$ *vs.* $\log[(I_p/I)^{\frac{1}{2}} - (I_p-I/I)^{\frac{1}{2}}]$ was obtained, with a slope of 121 mV at 293 K.

Cyclic voltammograms in the scan-rate range ν = 50 to 2000 mV/sec have ΔE_p = 60 ± 5 mV, I_p (reverse)/I_p (forward) ratios of unity and linear I_p *vs.* $\nu^{\frac{1}{2}}$ dependence, through the origin.

$E_{\frac{1}{2}}$ (d.c.V. and C.V.) and E_p (a.c.V.) values are negligibly altered by concentration or other experimental parameters in the range 225 to 295 K.

The $[M(SacSac)_2]$ systems, in particular, show deviations from ideality attributed to the chemical reaction following charge transfer.

A change of solvent to, for example, acetone or acetonitrile, yields only minimal changes in the electrochemical behaviour of the system. Changing the solvent, however, to dimethylformamide, d.m.f., can result in the degradation of the complex. This is dependent on the chelated ligand used; for example, R,R' = CH_3, CF_3 degrades quickly, over a period of a few minutes, whereas R,R' = CF_3, Ph shows no such mannerism. The identity of the metal centre in this context is not relevant. Pre-cooling the d.m.f. medium to 243 K, before addition of the complex, sufficiently slows the decomposition

Figure 3.10 Frequency dependence (a.c. measurement, first and second reductions) for $[Pd(S_2C_3CF_3HCH_3)_{-2}]_-$

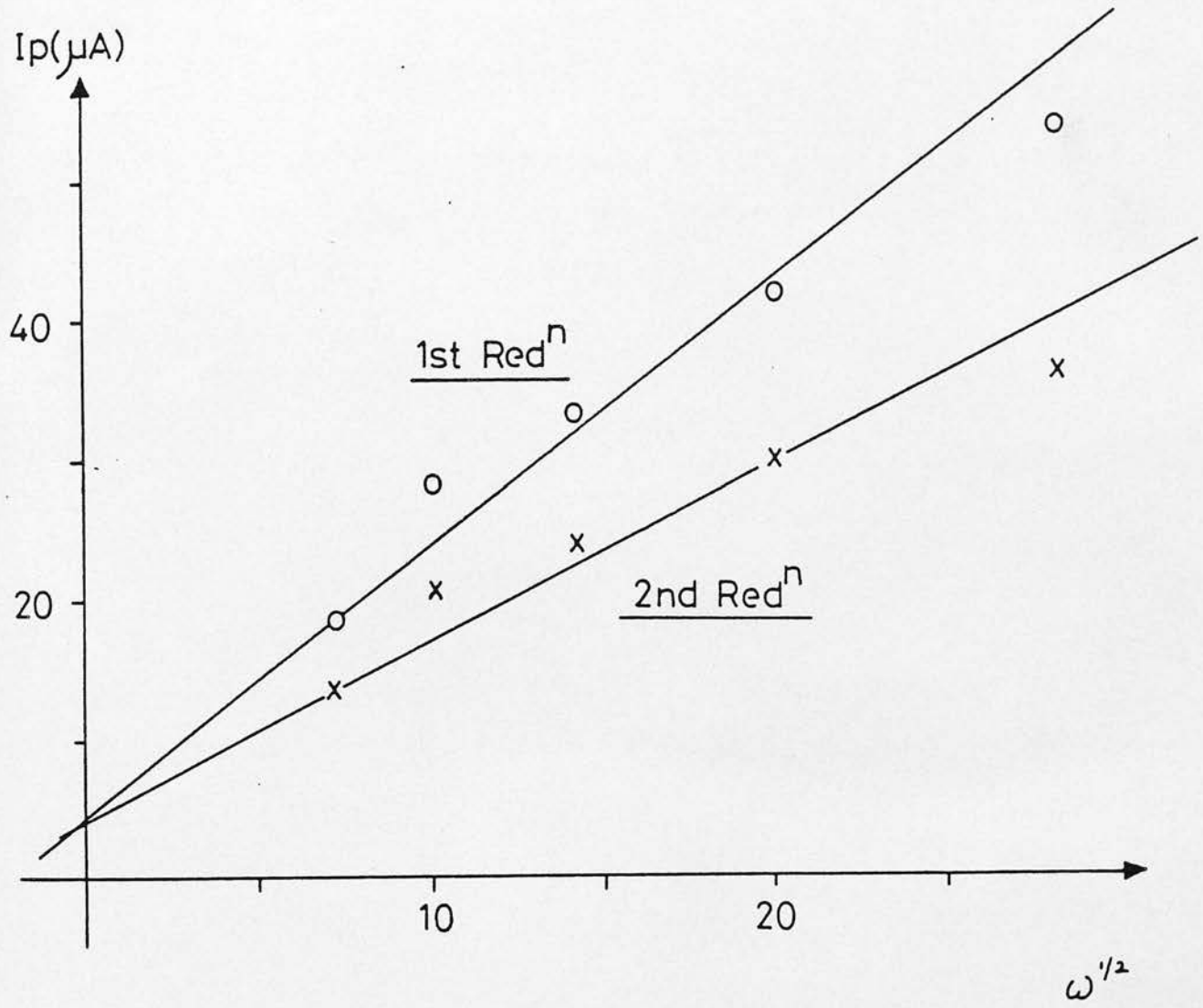

to show the "classical" behaviour found in other solvents. Warming to room temperature yields irreversible degradation of the complex.

An extensive study of transition metal tris-bipyridyl complexes has shown that highly co-ordinating solvents, such as d.m.f. and dimethyl sulphoxide , d.m.s.o., can co-ordinate to the metal centre with the release of free 2,2'-bipyridine[24]. However, the solvolysis of the tris-"bipy" complexes can be suppressed by the addition of excess free "bipy" ligand to the solution. Similar explanation may be in order here, but no indications as to why only certain complexes are affected have been ascertained.

It should also be noted that the use of inert electrolytes containing alkali metal ions should be avoided as this results in the loss of return wave, in the C.V. mode, even at 223 K. An early polarographic investigation of a series of nickel complexes $[Ni(S_2C_3RHR')_2]$ where R,R' = CH_3, Ph, CF_3 [25] showed irregularities in comparison with later data, but the exclusive use of either $NaClO_4$ or LiCl as a supporting electrolyte, or d.m.f. as solvent, suggests that these results must be treated with extreme caution.

Diffusion currents are directly proportional to concentration in the range 1×10^{-5} to 5×10^{-3} M, with a measured diffusion coefficient $D(293\ K) = 6.8 \times 10^{-6}\ cm^2 s^{-1}$ at the r.p.e. This value is determined using the relationship

$$I_D = 0.62\ nFA\ cD^{2/3}\ \nu^{-1/6}\ \omega^{\frac{1}{2}}$$

where the terms are defined as

I_D = diffusion current (mA)
n = number of electrons transferred per mole
F = 96,500 coulombs
A = electrode area (cm^2)
c = concentration of electroactive species (mol l^{-1})
D = diffusion coefficient of electroactive species ($cm^2\ s^{-1}$)
ν = cinematic viscosity ($cm^2\ s^{-1}$)
ω = angular speed of disc (= $2\pi N$ in Rad s^{-1})
N = revolutions per second

Experimentally, the diffusion current is measured over a range of rotation speeds, thus a plot of I_D vs. $\omega^{\frac{1}{2}}$ gives a linear relationship, the gradient of which allows easy determination of D. At the d.m.e. a value for $D = 6.16 \times 10^{-6}$ $cm^2\ s^{-1}$ was found. Similar D values (within 5%) for the nickel and platinum analogues, and for $[Pd(SOC_3CF_3HCH_3)_2]$ are obtained.

References

1. J. Willemse, J.A. Cras, J.J. Steggerda and C.P. Keijzers, Structure and Bonding, 1976, 28, 83, and references therein.

2. D. Coucouvanis, Prog. Inorg. Chem., 1970, 11, 233, and references therein.

3. J.A. McCleverty, Prog. Inorg. Chem., 1968, 10, 49, and references therein.

4. D.C. Olson, V.P. Mayweg and G.N. Schrauzer, J.Am.Chem.Soc., 1966, 88, 4876.

5. R. Chant, A.R. Hendrickson, R.L. Martin and N.M. Rohde, Aust. J. Chem., 1973, 26, 2533.

6. A.R. Hendrickson, R.L. Martin and N.M. Rohde, Inorg.Chem., 1975, 14, 2980.

7. A. Nieuwpoort, Ph.D. Thesis, Nijmegen, Netherlands, 1975.

8. R.L. Martin, G.A. Bowmaker, P.D.W. Boyd, C.K. Campbell, J.M. Hope, Inorg. Chem., 1982, 21, 1152.

9. G.N. Schrauzer, Accounts Chem.Res., 1969, 2, 72.

10. A.M. Bond, G.A. Heath and R.L. Martin, Inorg.Chem., 1971, 10, 2026.

11. T.E. Mines and W.E. Geiger, Jr., Inorg. Chem., 1973, 12, 1189.

12. W.E. Geiger, Jr., T.E. Mines and F.C. Senftleber, Inorg.Chem., 1975, 14, 2141.

13. F.C. Senftleber and W.E. Geiger, Jr., J.Am.Chem.Soc., 1970, 92, 2297.

14. A.R. Hendrickson, J.M. Hope and R.L. Martin, Inorg. Chem., 1976, 15, 1118.

15. W.L. Bowden, J.D.L. Holloway and W.E. Geiger, Jr., Inorg.Chem., 1978, 17, 256.

16. R.H. Holm and A.S. Patterson, Inorg.Chem., 1972, 11, 2285.

17. U.T. Mueller-Westerhoff, Z.S. Herman, R.F. Kirchner, G.H. Loew, A. Nazzal and M.C. Zerner, Inorg.Chem., 1982, 21, 46.

18. R.W. Taft, Steric Effects in Organic Chemistry, 1956, Wiley, New York.

19. K. Bechgaard, V.D. Parker and C.Th. Pedersen, J.Am.Chem.Soc., 1973, 95, 4373.

20. A.A. Vlcek, Prog. Inorg. Chem., 1963, 5, 211.

21. O. Süman and J. Fresco, J.Am.Chem.Soc., 1970, 92, 2652.

22. A.F. Masters, Ph.D. Thesis, Australian National University, 1975.

23. I. Fleming, Frontier Orbitals and Organic Chemical Reactions, 1976, Wiley, New York, Ch. 2.

24. L.J. Yellowlees, Ph.D. Thesis, University of Edinburgh, 1982.

25. A. Furuhashi, S. Kawai, Y. Hayakawa and A. Ouchi, Bull. Chem. Soc. Japan, 1970, 43, 553.

CHAPTER 4

The Monoanion Rearrangement:- A Kinetic Study

4.1 Introduction

Reactions which are induced at an electrode surface should not be necessarily considered in the same manner as homogeneous chemical reactions. Whereas this proviso applies to reactions occurring during the time interval when the molecular species is very close to the electrode, there are many chemical reactions which occur as a result of the charge-transfer process, but are purely homogeneous reactions, having no reaction parameters specific to charge transfer. Indeed, rather than the charge-transfer process altering the course of the chemical reaction, the result of such "coupled" chemical reactions is to alter the flux of the electroactive species. Thus the nature of the chemical reaction and its kinetics may be examined by the effect on the flux of reactant for the charge-transfer process and the attendant change in electrode response.

There are two objectives in studying the kinetics of electrochemical reactions coupled with chemical reactions, (a) full characterisation of the electrochemical processes and, (b) evaluation of the kinetic parameters of the chemical reaction where this is of intrinsic interest.

A.c. polarography and cyclic voltammetry can be used to obtain useful kinetic information in these areas. Consider a reversible redox couple, the product of which undergoes reversible chemical reaction (Scheme 4.1).

Scheme 4.1

$$O + ne^- \Longleftrightarrow R$$

$$R \underset{k_b}{\overset{k_f}{\rightleftharpoons}} Z$$

In both techniques the current response will be significantly altered from that attending the simple reversible redox scheme. In the cyclic voltammetry experiment, for example, the magnitude of the current flow detected on the reverse potential scan is less than that observed in the absence of the chemical reaction. The detailed nature of the reaction influences the extent to which the response will differ from the unperturbed charge-transfer system. For example, a first-order following reaction of a given rate constant will produce a characteristically different electrode response from a second-order reaction, having a similar rate. Likewise, a second-order reaction involving only the product of the charge transfer step (i.e. a dimerisation) will exert a different influence from a reaction which is second-order in product, but involves other reactants as well. These differences lead to severe difficulties in the theoretical descriptions of these processes, but ultimately provide the means by which we obtain mechanistic information and hence analyse the kinetic processes in detail.

The manner in which the coupled chemical reaction manifests itself in the electrochemical reaction is also dependent on the nature of the charge-transfer step. If the charge-transfer process is irreversible, then a chemical reaction of the electrode product will have no effect on it. A quasi-reversible charge transfer will be influenced by a coupled chemical reaction, but theoretical analysis is especially complex.

Thus four possible scenarios for chemical reactions coupled to the charge-transfer process have been discussed[1].

(a) reversible chemical reaction following reversible charge transfer,

(b) irreversible chemical reaction following reversible charge transfer,

(c) chemical reaction preceding reversible charge transfer,

(d) chemical reaction preceding irreversible charge transfer.

Fortunately, for the present purpose, our discussion can be confined to chemical reactions following reversible charge transfer (a and b above) and to their analysis using cyclic voltammetry. The principal variables determining the experimental time scale are the potential scan range beyond the couple, $(E_\lambda - E_{\frac{1}{2}})$ and the scan rate (ν).

(a) Reversible chemical reactions following charge transfer

In such systems the equilibrium constant for homogeneous regeneration of R is defined as

$$K = k_b/k_f \qquad \text{(see Scheme 4.1)}$$

Both the position of equilibrium and the rate at which equilibrium is reached are important aspects of the overall chemical reaction, (which is assumed, for the moment, to be a first-order process).

A coupled following reaction is not expected to alter the magnitude of the forward (cathodic) current significantly, however large changes in the return (anodic) current are found. Thus the variation of anodic current or the ratio of anodic to cathodic current (ia/ic) as a function of the time-scale of the experiment becomes a primary parameter in both qualitative and quantitative observations.

If the rate constant for the forward chemical reaction is small and the equilibrium constant is large (i.e. equilibrium shifted toward the reactant), in the limit the system simplifies to the electrochemically reversible case. If the equilibrium constant is small, the system reduces to the case of an irreversible following reaction with the exception of a shift in potential response. Thus examples in which the rate of the chemical following reaction is significant and the equilibrium

constant not excessively small best typify this class, i.e. class (a).

For these cases, the dependence of anodic-to-cathodic current ratio on scan rate serves as a useful parameter for quantitative measurements. The magnitude of the anodic current, however, is also a function of the switching potential, E_λ (Figure 4.1).

Using computer-simulation techniques, a working curve of ia/ic as a function of $(a/l)^{\frac{1}{2}}/K$ (at any specified arbitrarily-selected switching potential), may be constructed[2], where the terms "a" and "l" are defined as

$$a = \frac{nF\nu}{R\,T} \qquad l, \text{ the "kinetic parameter"}, = k_f + k_b$$

For any particular chemical system, having its own characteristic K value, then it will be noted that on the working curve ia/ic increases towards unity as $(a/l)^{\frac{1}{2}}$ (and hence $\nu^{\frac{1}{2}}$) decreases, and that ia/ic decreases as $(a/l)^{\frac{1}{2}}$ (and hence $\nu^{\frac{1}{2}}$) increases. This behaviour allows differentiation of this case from all others, and makes the variation of ia/ic with scan rate a very useful diagnostic aid. Equally if we compare analogous systems under the same experimental conditions we find that larger K values are associated with ia/ic increasing towards unity, and smaller K values lead to decrease in ia/ic. Thus, qualitatively, larger K or slower experimental time-scale have the same effect on ia/ic, in accord with the form of the working curve.

Figure 4.1 Variation of anodic current with switching potential

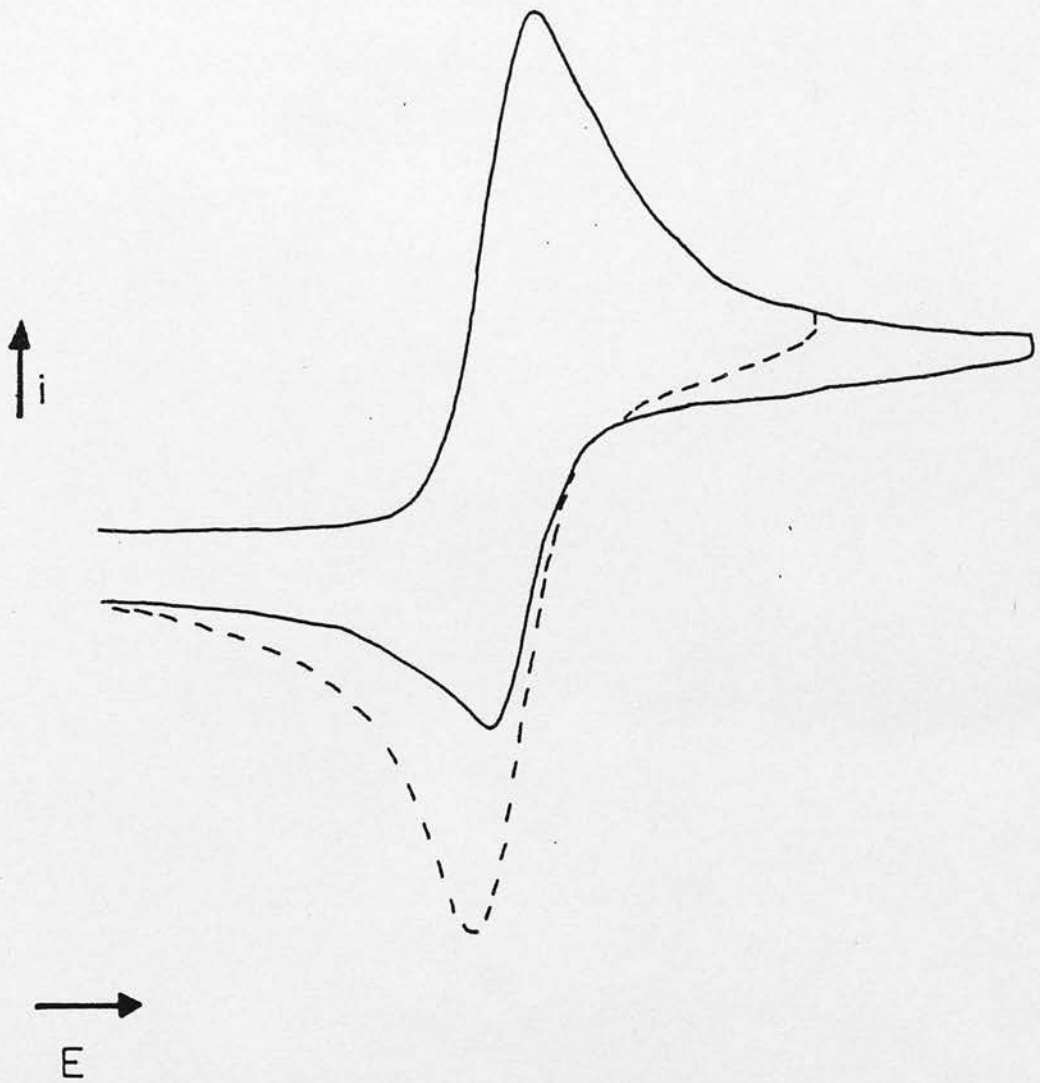

for an irreversible following reaction

The behaviour of the cathodic peak is more complex. If the rate of the chemical reaction is very slow, so that essentially no chemical reaction takes place during the experiment, then the response occurs at the reversible potential

$$E_p = E_{\frac{1}{2}} - (1.109)RT/nF$$

Where the rate of the chemical reaction is very fast, so that the system will be in equilibrium at all times, the current response has the appearance of a reversible system, but undergoes an anodic potential shift by $(RT/nF)\ln[(1 + K)/K]$.

Where a/l is small (i.e. $k_f + k_b$ large) and $(a/l)^{\frac{1}{2}}/K$ is also small, then the relationship

$$E_p = E_{\frac{1}{2}} - (RT/nF)[0.078 + \ln(a + l)^{\frac{1}{2}} - \ln(1 + K)]$$

has been shown to hold, corresponding to a cathodic potential shift of up to 60/n mV for a ten-fold increase in $(a/l)^{\frac{1}{2}}/K$.

It is possible to construct a working curve relating potential (rather than ia/ic) to the kinetic parameter[2].

(b) Irreversible first-order chemical reaction following charge transfer

The situation can be represented as in Scheme 4.2 i.e. first-order reaction of the charge-transfer product.

Scheme 4.2

$$O + ne^- \Longleftrightarrow R$$

$$R \xrightarrow{k_f} Z$$

This can be interpreted as merely a limiting case of the conditions described above. Indeed, experimental conditions are often adjusted so that reaction at equilibrium can be simplified to this less complicated case. This reaction is the most amenable to quantitative study.

As previously, the "following reaction" produces only minor variation in the magnitude of the cathodic peak current in comparison to the reversible charge transfer with no following reaction. However, the magnitude of the anodic response, i.e. the "return wave", is greatly affected by the chemical reaction unless it is very slow, i.e. except at very low values of rate constant relative to scan rate (low values of k_f/a). Very large values of rate constant yield an anodic response which is essentially that of the irreversible charge transfer i.e. no detectable return wave, in which case little information concerning the fast chemical reaction can be gleaned. At intermediate values of k_f/a, however, the magnitude of the anodic response provides an excellent basis for kinetic measurements of the following reaction.

In Nicholson and Shain's analysis, a large number of theoretical cyclic voltammograms were calculated, varying both k_f/a and switching potential[2]. The switching potential is a relevant variable since at a given scan rate it determines the time which elapses between the onset of electrolysis (forward passage through $E_{\frac{1}{2}}$) and the surmounting of the anodic (reverse) peak on the return scan. Solution of the mathematics shows that this time lapse, in the irreversible case, does influence the flux of "R" at the electrode on the return scan. This is accommodated by introducing a quantity, τ, which represents the scan-time in seconds from $E_{\frac{1}{2}}$ to E_λ. Conveniently, for a constant value of the product $k_f\tau$, the ia/ic ratio was found to be constant. Thus a working curve could be constructed as a function of $k_f\tau$, from which the rate constant for the chemical reaction, k_f, can be determined by inspection from the measured ia/ic values, since τ will be a specified experimental parameter at every point. To make use of this relationship, $E_{\frac{1}{2}}$ must be accurately known (so as to determine τ).

For qualitative purposes, the anodic response as a function of scan rate is extremely useful. As the scan rate is increased, the ia/ic ratio increases towards

unity. Other mechanisms in which the anodic current is measured behave differently from this (c.f. class a above), therefore the variation of ia/ic with scan rate is a valuable diagnostic probe.

The variation of forward-peak potential with kinetic parameter is also useful. At higher values of k_f/a the relationship

$$E_p = E_{\frac{1}{2}} - (RT/nF)[0.078 - \ln(k_f/a)^{\frac{1}{2}}]$$

has been found to hold, embodying a shift of 30/n mV anodically for a ten-fold increase in k_f/a. This relationship can also provide quantitative characterisation of k_f if a sufficiently large range of scan rates can be employed.

(c) Irreversible dimerisation reaction following charge transfer

Few higher-order following reactions have been examined, however, a dimerisation of the charge transfer product has been studied[3,4] (Scheme 4.3).

Scheme 4.3

$$O + ne^- \rightleftharpoons R$$

$$2R \xrightarrow{k_f} Z$$

A number of theoretical cyclic voltammograms were calculated, varying both k_f/a and switching potential. In each case the ratio ia/ic was determined. In a manner analogous to the irreversible case b just considered, the ia/ic ratio can be now expressed as a function of $k_f \tau C$ (where C is the initial [or analytical] concentration of O). Again the rate constant, k_f, can be evaluated from an appropriate working curve (see Section 4.3 for a detailed description). The dependence of ia/ic on concentration, when carefully analysed, provides a convenient clear-cut method for distinguishing between first and higher-order reactions. The variation of $E_{\frac{1}{2}}$ with scan rate may allow differentiaion between first and second order processes as well[5] (but less emphatically).

(d) Kinetic analysis using other techniques

Although we have discussed in detail the kinetic characterisation of chemical reactions subsequent to the charge-transfer process using parameters derived from cyclic voltammetry, other techniques may also be employed, for example, a.c. and d.c. polarography, cyclic a.c. voltammetry and ring-disk methods.

A number of elaborate theoretical studies using a.c. polarography as a kinetic investigation mode have been undertaken[6-8]. Methods of analysis include, (a) peak potential shifts as the frequency of the

a.c. current, ω, or drop-time, t_d, is varied, (b) a.c. current variation as ω or t_d is increased, and, most importantly for quantitative purposes, (c) properties of the phase angle, i.e. the phase relationship between the applied potential and the resulting current, cot ϕ, as a function of frequency.

Cyclic a.c. voltammetry[9,10], an extension of the linear sweep technique, has the advantage over conventional C.V. that as well as retaining the high diagnostic value of C.V., it also shows the additional phase-angle data which should permit detailed quantitative analysis. The study of chemical reactions following charge transfer is well suited to this investigation mode. The ratio I_{P_r}/I_{P_f} is a sensitive indication of the chemical stability of the charge transfer product. However, the a.c. ratio is much easier to measure precisely than ia/ic (C.V.) and thus lends itself readily to analysis of homogeneous rate constants.

A number of theoretical investigations for coupled chemical reactions using rotating disk electrodes have been undertaken, despite the complexities involved, for both preceding and following chemical reactions. In the former case, parameters can be determined from the variation of the limiting current, i_d, with rotation rate, ω.[11,12]

In the latter, the limiting cathodic current is not affected by the following reaction, but a positive potential shift as a function of ω is observed[13,14]. The rotating ring-disk electrode (R.R.D.E.) is particularly suited for the study of such systems, where the potential of the ring and disk can be independently controlled[15-17]. The potential of the ring is set so that the product of charge transfer is reoxidised, and the deviation of the measured collection efficiency from the value found in the absence of the complicating chemical reaction, as a function of ω, allows determination of k_f. Theoretical treatments are also available for second-order reactions[18,19].

The study of chemical reactions coupled to charge transfer using d.c. polarography is similar in principal to the rotating disk electrode. For a simple, reversible charge transfer, the limiting current is determined by the rate of diffusion of the electroactive species. However, when there is also the complication of chemical reaction, the limiting current is frequently determined by the rate of that reaction[20,21]. A simple test of diffusion control is to monitor the limiting current as a function of the height of the head of mercury above the column, h, as i_d is proportional to $\sqrt{h}$. The unemphatic nature of the deviations from "Nernstian" behaviour in the available time domain mean that d.c. polarography is now the least attractive method for kinetic analysis.

Results and Discussion

4.2 Qualitative study of the $[M(SacSac)_2]^{1-}$ rearrangement reaction

As briefly mentioned in Chapter 3, the original d.c. polarographic study of $[M(SacSac)_2]$ (M = Ni, Pd, Pt) showed two successive one-electron reductions, but with a marked tendency for the monoanion to undergo rearrangement to yield a species which was itself redox-active[22]. A more recent study of the nickel and platinum complexes using cyclic voltammetry confirmed this behaviour, but was hampered by lack of the palladium complex[23].

We have now undertaken a study of the complete triad of complexes, employing complementary d.c., a.c. and cyclic voltammetric investigation modes.

The results of d.c. polarography, or d.c. linear voltammetry, on a rotating disk electrode, are generally consistent with results obtained previously.

The a.c. mode, not used hitherto, employing either d.m.e. or Pt working electrodes, generally confirms the results from the d.c. studies, which suggested a following reaction of the $[M(SacSac)_2]^{1-}$ species. For the palladium complex three peaks are clearly in evidence (see Figure 3.2) whereas $[Pt(SacSac)_2]$ shows only two a.c. peaks, though with a distinct shoulder on the second reduction at less negative potentials, which is either

absent or not resolved in the d.c. mode. Analysis of the data confirms the Nernstian behaviour of the first electron transfer.

Cyclic voltammetry at a stationary platinum electrode illustrates the nature of the following reaction most clearly (Figure 4.2), confirming the order of reaction

$$Ni << Pd < Pt$$

Thus the electrode behaviour of $[Pt(SacSac)_2]$ is dominated by the rearrangement pathway, giving rise to the relatively simple d.c. polarogram. The chemical instability of the monoanion is equally demonstrated on a stationary hanging drop mercury electrode, using a variety of solvents and over a range of electrolyte concentrations.

The electrode processes, labelled "a, b and c" in Figure 4.2, have been assigned as illustrated in Scheme 4.4.

Scheme 4.4

$$[M(SacSac)_2]^{0} \underset{e^-}{\overset{a}{\rightleftharpoons}} [M(SacSac)_2]^{1-} \underset{e^-}{\overset{b}{\rightleftharpoons}} [M(SacSac)_2]^{2-}$$

$$\downarrow \text{rearrangement}$$

$$[X]^{1-} \underset{e^-}{\overset{c}{\rightleftharpoons}} [X]^{2-}$$

where X = the rearrangement product of the monoanion.

Figure 4.2 Cyclic voltammetry of $[M(SacSac)_2]$

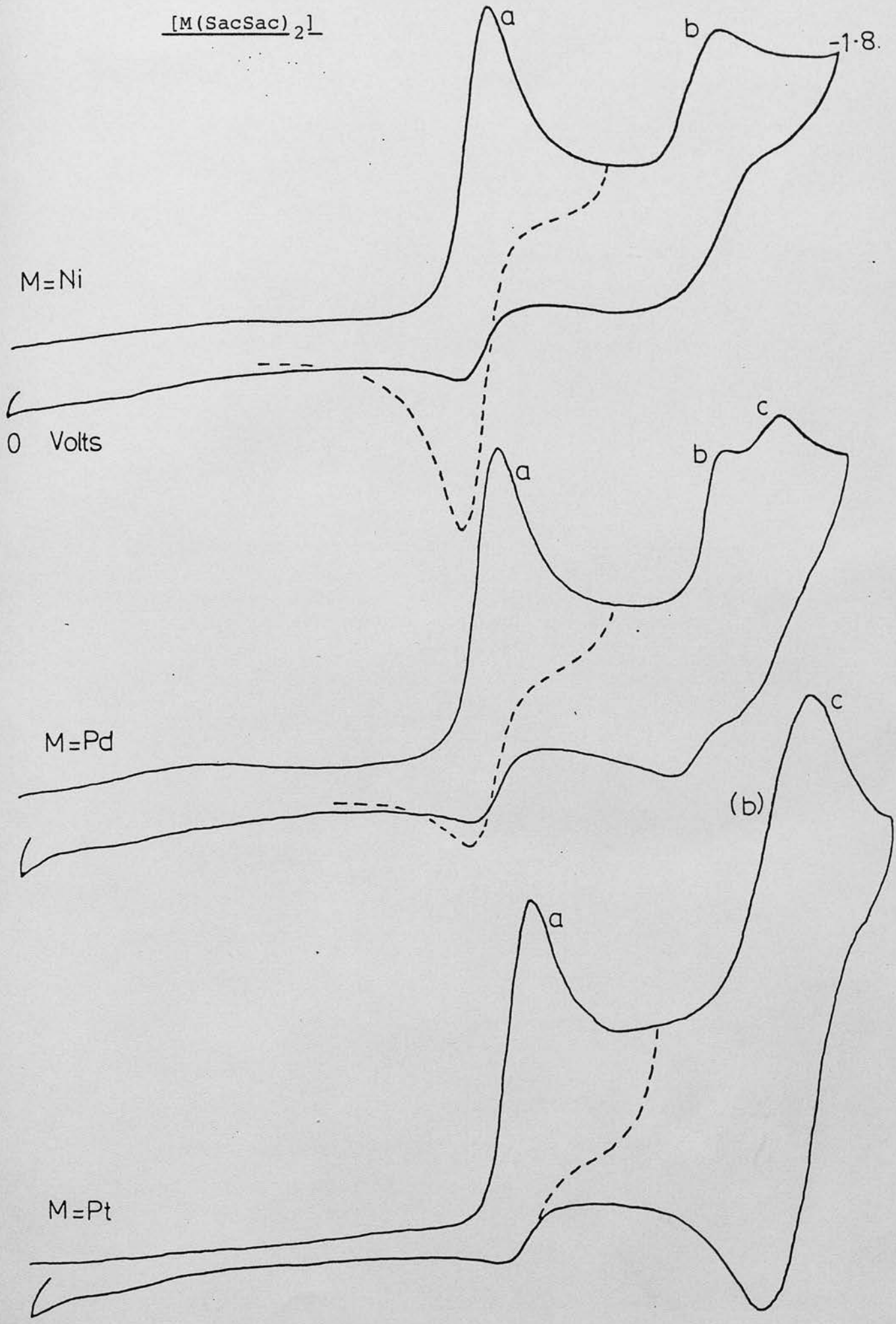

This description has been comprehensively established using ultra-fast scanning techniques of up to 100 Volts per second in the C.V. mode, yielding ia/ic ratios approaching unity for waves "a" and "b" as the scan rate is increased.

As the return wave "a" develops, we observe concurrent collapse of wave "c" and growth of "b". This behaviour can also be obtained by cooling the system to 225 Kelvin; i.e. lowering the temperature helps to stabilize the monoanion sufficiently on an electrochemical time-scale for reversible C.V. characteristics to be observed. (Figure 4.3 shows the temperature dependence for $[Pd(SacSac)_2]$). The a.c. voltammetry shows changes corresponding with those observed in the C.V. so that at 225 Kelvin $[Pd(SacSac)_2]$ exhibits only two peaks of equal height, both analysing for reversible charge transfer.

A suggestion that the monoanion may react with hydrolytic protons present in solution prompted a semi-quantitative cyclic voltammetric investigation of $[Pt(SacSac)_2]$ in methyl naphthalene at 423 Kelvin. Under these conditions the electrolytic medium is expected to be strictly anhydrous, but the efficient characteristically irreversible process found previously is again observed. Indeed, even at low concentrations no indications of a return wave is distinguishable; i.e. the reaction rearrangement rate has increased with rise in temperature.

Figure 4.3 C.V. of $[Pd(SacSac)_2]$ showing temperature dependence

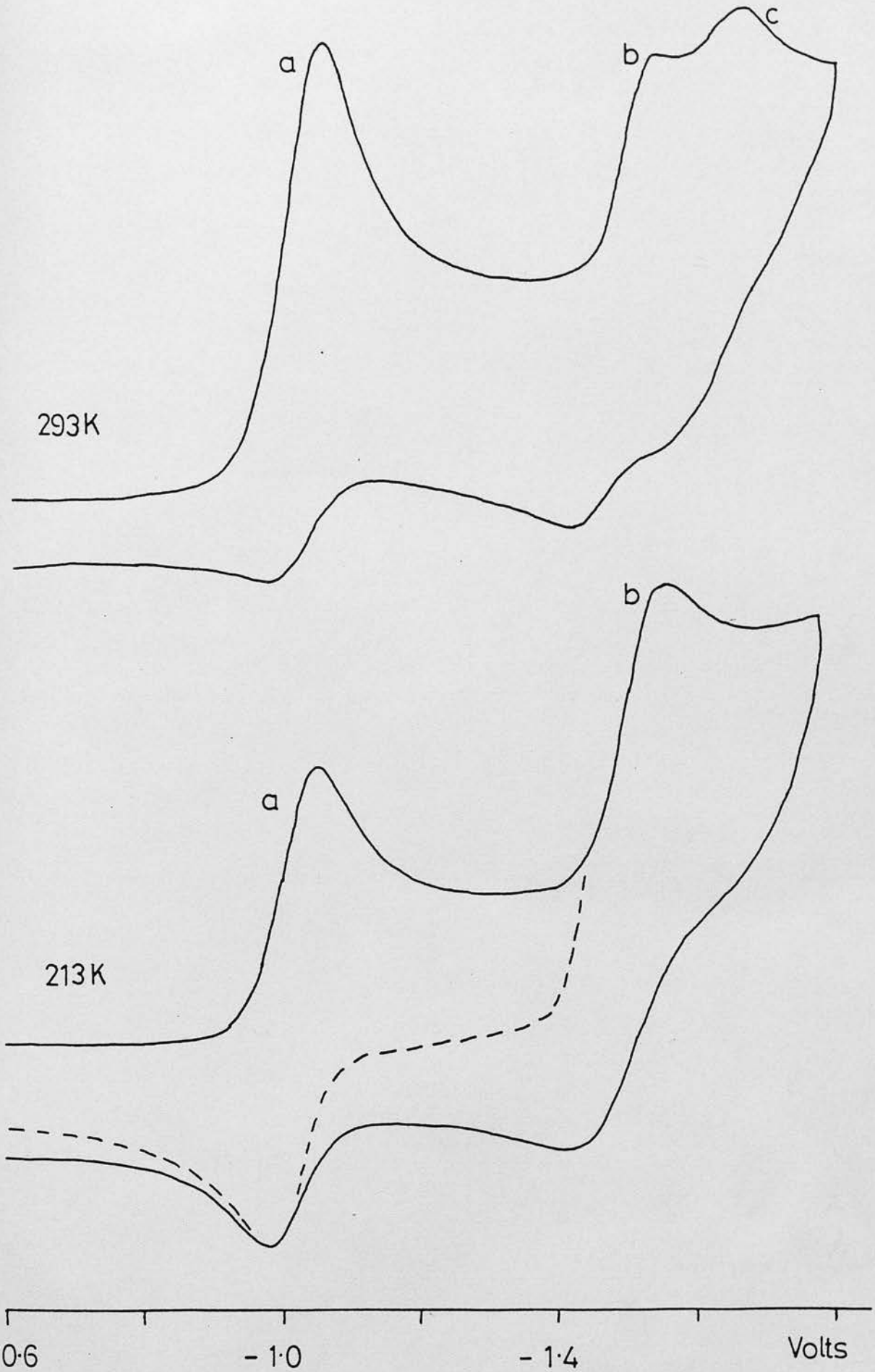

These qualitative observations permit us to classify the rearrangement of the monoanion as of the general type "b" discussed earlier, i.e. reversible charge transfer followed by irreversible chemical reaction.

Unfortunately, the structure of the product of the monoanion rearrangement is unknown. Geiger et al noted that ia/ic was sensitive to concentration suggesting higher order kinetics, but no quantitative measurements were attempted[23]. A dimeric structure was regarded as plausible, and as was pointed out, dimerisations of certain other planar dithiolate complexes are well known[24-27]; $[Pd(S_4C_4H_4)_2]$ and its platinum analogue are dimeric in the crystal[27] and weaker interactions between monomeric metal dithiolene monanions are also well established[28-30]. Geiger recorded the U.V./visible spectrum of the electrosynthesised product, which he reported was red in colour. A spectrum similar in character to the $[M(SacSac)_2]$ starting material was recorded and felt to be consistent with non-disruptive dimerisation. However, these results must now be treated with caution.

Nevertheless, a dimerisation reaction is still the most probable fate of the monoanion. Our detailed kinetic studies establish that second-order kinetics hold for the triad of $[M(SacSac)_2]$ complexes over widely varied

conditions of scan-rate, concentration and temperature (Section 4.3). Analysis of the temperature-dependence of the data yields a small positive value for the enthalpy of activation, $\Delta H^{\neq}$, suggesting a substantial degree of bond formation in the transition state (Section 4.4).

Our own efforts to monitor the U.V./visible spectrum during the course of the electrolysis has met with some success. A substantial amount of work has been undertaken in this laboratory towards the development of a system which allows the spectroscopic characterisation of electrogenerated species *in situ*[31]. This is possible using an optically transparent thin-layer electrode (O.T.T.L.E.), which involves the generation of the electron-transfer product at a mini-grid electrode in the beam of a spectrophotometer.

Our preliminary studies have been devoted to the dimerisation of the $[Pt(SacSac)_2]^{1-}$ monoanion. Unfortunately, no discrete bands are present in the final spectrum of the electrogenerated dimeric species (Figure 4.4). However, close examination of the visible region in our O.T.T.L.E. experiment reveals two distinct isosbestic points as the peak collapses (Figure 4.5). This shows that the one-to-one reaction is involved rather than any ill-defined decomposition or complicated sequence of reactions. This is further substantiated by the mole for mole regeneration of the $[Pt(SacSac)_2]^{o}$ on application of a positive potential to the system,

Figure 4.4 Electronic spectra of [Pt(SacSac)$_2$] and its electrogenerated dimer

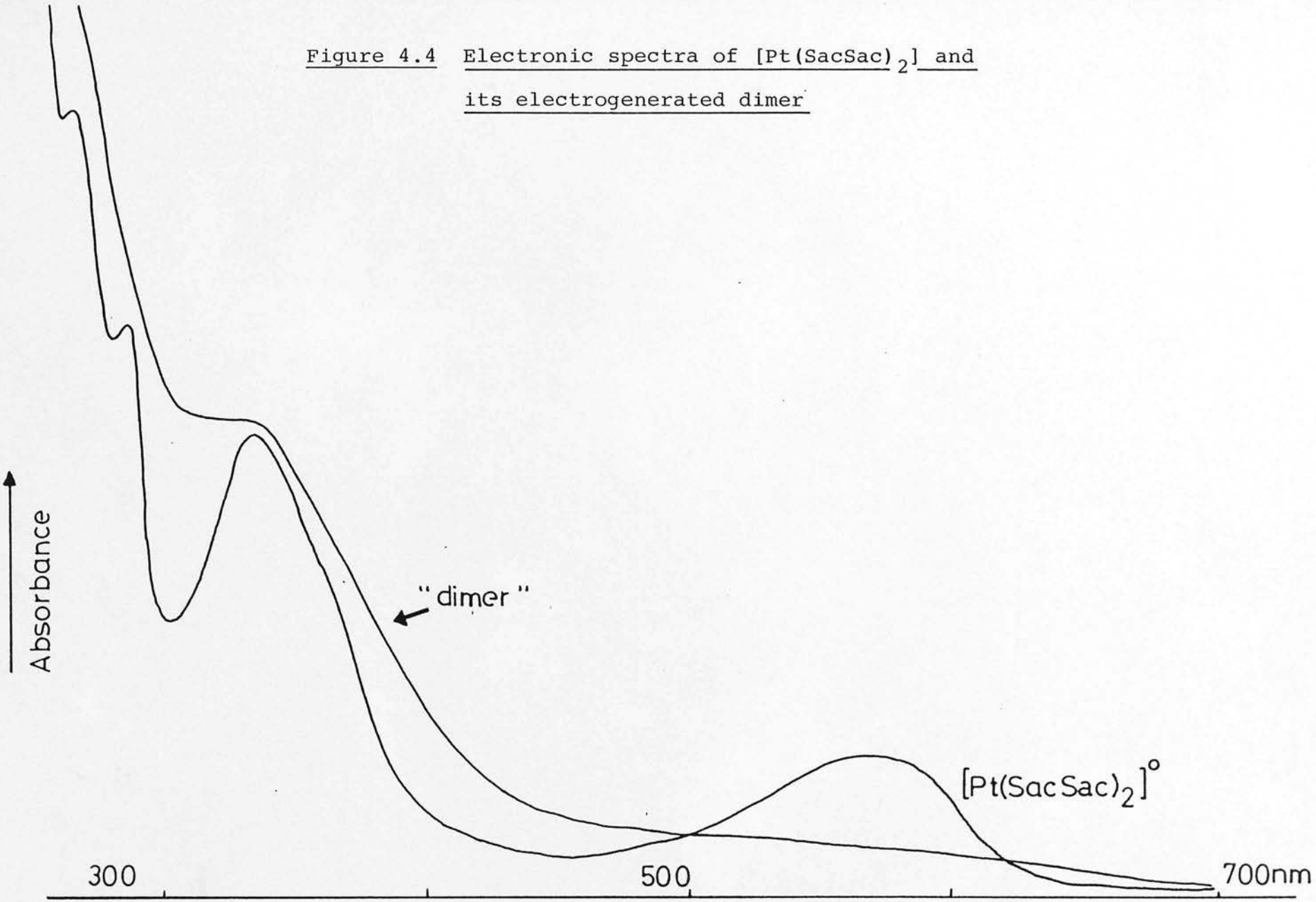

Figure 4.5 O.T.T.L.E. generated spectra of $[Pt(SacSac)_2]^{1-}$ dimerisation in the visible region, showing isosb estic points

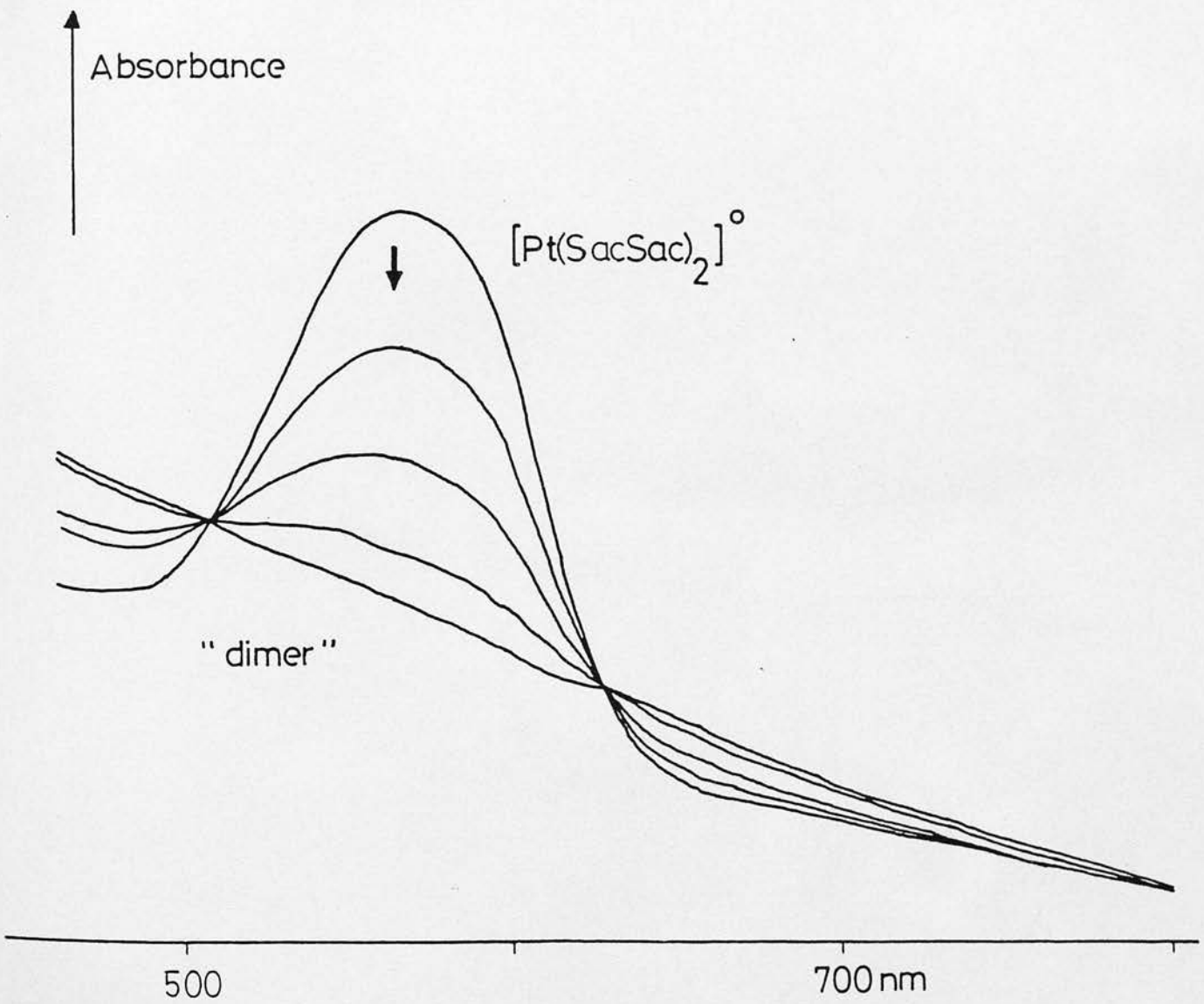

accompanied by recovery of its distinctive spectrum. The essentially featureless spectrum of the dimer does, however, suggest a substantial disruption of the resonance-stabilization present in the neutral species, perhaps indicative of a saturated species, much in the same manner as SacSacH itself rapidly dimerises to form a saturated adamantane-type structure (Chapter 2).

The positive potential required to regenerate the neutral species from the dimer (approximately 1.5 Volts anodic of the $[Pt(SacSac)_2]^{o/1-}$ couple) is also indicative of a major reorganisation in electron distribution during the rearrangement reaction. Our observations are at odds with Geiger's reported spectrum of the dimer[23]. Indeed, it would be expected that the potential to regenerate the neutral species from the dimer which Geiger envisaged would not be so greatly removed from that required to form the $[Pt(SacSac)_2]^{1-}$ species originally.

The same spectroscopic behaviour is obtained when the experiment is repeated at 253 Kelvin. In no case was any evidence obtained for an intermediate spectrum which could be attributed to unreacted $[Pt(SacSac)_2]^{1-}$ monoanion. Further progress may depend on the substituted derivatives, where the rate of dimerisation is slow on an electrochemical time-scale. By further cooling of the system, we may be able to generate the spectrum of the monoanion, and then observe its gradual dimerisation, thus allowing the full characterisation of all species participating in dimer formation.

Care must be taken in these experiments to use freshly prepared $[Pt(SacSac)_2]$ solutions, as the complex gradually decomposes in the presence of dissolved oxygen, so that the intense purple colour characteristic of $[Pt(SacSac)_2]$ is replaced initially by a red colour, which finally yields a yellow-brown solution. The spectrum of the reddish material is closely similar to that reported by Geiger et al as being the spectrum of the dimer. (The dimeric product produced in the O.T.T.L.E. experiment is itself very pale pink in colour). If the oxidised material is inadvertently formed, then regeneration of the $[Pt(SacSac)_2]^{o}$ spectrum is impossible.

A number of attempts to prepare the dimer in bulk by the heterogeneous, chemical reduction of $[Pt(SacSac)_2]^{o}$ (using sodium, sodium amalgam or magnesium) were unsuccessful, with no apparent reaction. Preparation by electrochemical means should prove to be more profitable. The positive potential required to regenerate $[Pt(SacSac)_2]^{o}$ from the dimer may indicate that the dimer will be less prone to decomposition than previously thought.

Thus at this stage, the best corroborating evidence for dimerisation as the fate of the monoanion is the kinetic analysis, which we will now discuss in detail.

4.3 Kinetic and activation parameter analysis for monoanion rearrangements

(a) Kinetic Analysis

The proposed dimerisation reaction of $[M(SacSac)_2]^{1-}$ might occur via two possible intimate mechanisms; either the direct coupling of two monoanions [1] or by the reaction of monoanion with substrate molecule initially, to form $[M(SacSac)_2]_2^{1-}$. Since an overall one-electron reduction is observed, it is required in the second mechanism that the reduction potential of the monoanion dimer be less than the substrate itself [2].

$$2[M(SacSac)_2]^{o} + 2e^{-} \rightleftharpoons 2[M(SacSac)_2]^{1-} \xrightarrow{k_f} [M(SacSac)_2]_2^{2-} \quad ..[1]$$

$$[M(SacSac)_2]^{o} + e^{-} \overset{E_1^o}{\rightleftharpoons} [M(SacSac)_2]^{1-} + [M(SacSac)_2]^{o}$$

$$\Big| \; k_f \; \Big\downarrow$$

$$[M(SacSac)_2]_2^{2-} \overset{E_2^o}{\rightleftharpoons} e^{-} + [M(SacSac)_2]_2^{1-} \quad ...[2]$$

where $E_2^o < E_1^o$

Either scenario leads to an overall second-order rate equation. The kinetic analysis of such systems is ideally suited to a cyclic voltammetric investigation mode, where the rate constant, k_f, can be determined from the behaviour of the ratio I_p(reverse) : I_p(forward) (ia/ic).

The method applied to extract kinetic information was essentially that developed by Nicholson et al for a dimerisation reaction.[3] It seems appropriate to expand on the method of analysis at this point.

In the model employed, the characteristics of a current-potential curve depended on two variables, a kinetic parameter ($\psi = k_f C/a$) and the geometry of the electrode ($\emptyset$).

In an effort to correlate ia/ic to the rate constant, k_f, theoretical calculations for a number of C.V.s for several values of ψ, with $\emptyset$ equal to zero, i.e. planar, and three values of switching potential were considered. In each instance, the ratio ia/ic was evaluated. For each value of switching potential, the ratios ia/ic were plotted against the quantity $\log(\psi a\tau)$ [$= \log(k_f C\tau)$] where $a = \frac{nF\nu}{RT}$ and τ is the time from $E_{\frac{1}{2}}$ to E_λ, i.e. $(E_\lambda - E_{\frac{1}{2}})/\nu$. (Figure 4.6 shows the plot for $a\tau = 4$).

Variation of the $a\tau$ quantity produces similar plots except for small shifts along the $\log(k_f C\tau)$ axis, proportional to $a\tau$. It was thus possible to incorporate effects of switching potential in a new variable, ω, which was defined as

$$\log\omega = \log(k_f C\tau) + 0.034(a\tau - 4).$$

Figure 4.6 Variation of ia/ic with kinetic parameter for a dimerisation reaction (with Ø = zero and aτ = 4)

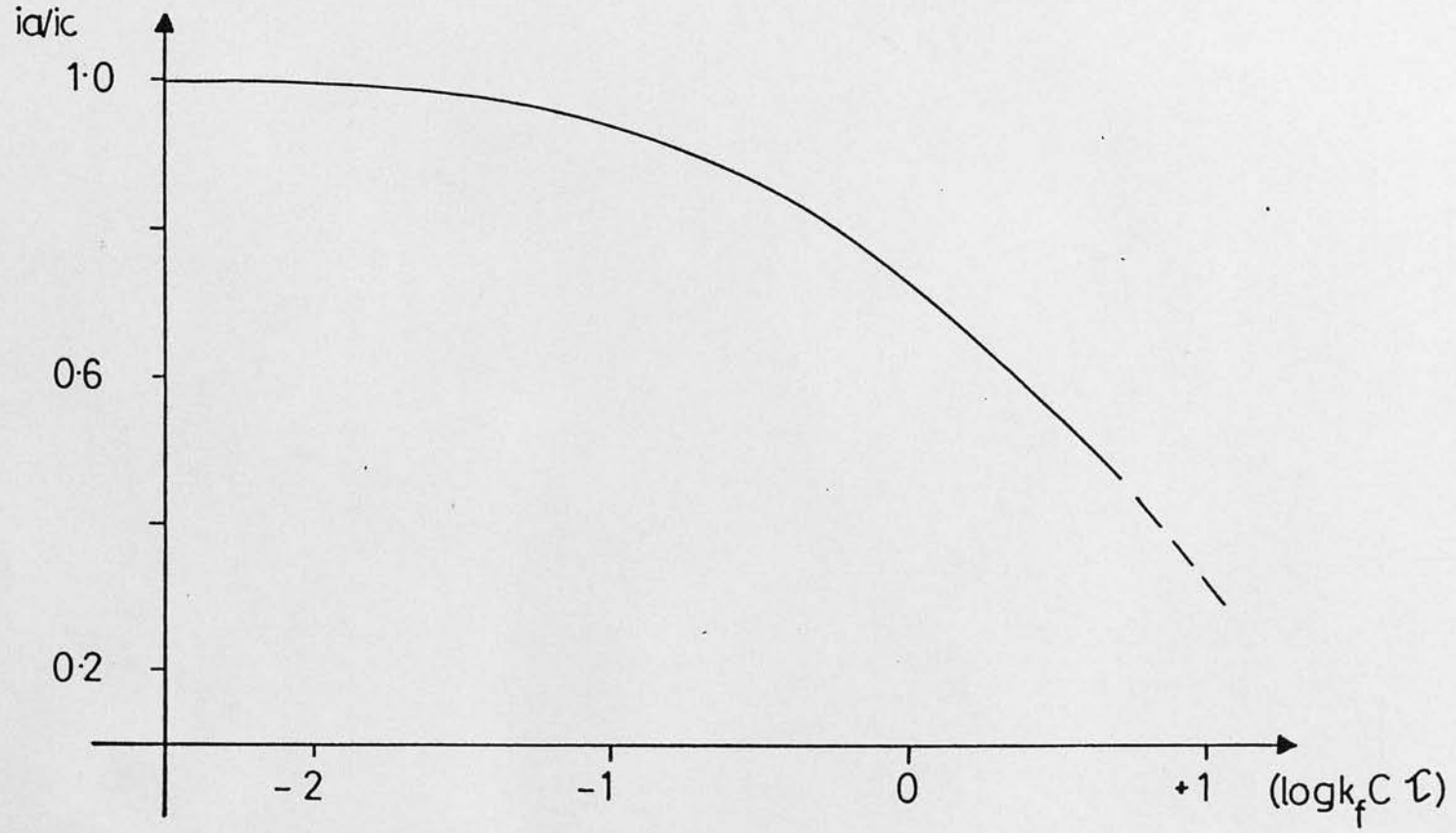

Tabulated values of ia/ic as a function of ω are available. Therefore, provided the geometry of the electrode is known, it is possible to construct a working curve from which ω can be determined graphically from experimental values of ia/ic.

Thus our procedure has been to construct from these data a plot of ω vs. τ, at fixed C, which gives a slope of $k_f C \exp[0.078(a\tau - 4)]$, and consequently k_f can be calculated. Similarly, a plot of ω vs. C, at fixed τ can be employed, giving a gradient of $k_f \tau \exp[0.078(a\tau - 4)]$.

Experimentally, the rate constant can in principle be established from one cyclic voltammogram, however, we insisted on estimating each k_f value by least-squares analysis of ia/ic data as above. A sample calculation for a typical set of data collected for the $[Pt(SacSac)_2]$ complex is detailed below.

By varying the concentration and keeping τ constant, i.e. constant ν and E_λ, with a temperature of 293 Kelvin, the data collected in Table 4.1 were established. From the relationship

$$\log\omega = \log(k_f C\tau) + 0.034(a\tau - 4)$$

a plot of ω vs. C should give a linear relationship with slope = $k_f \tau \exp[0.078(a\tau - 4)]$.

Experimentally, using a least-squares analysis, a gradient of 3,776 (±150) is found for the ω/C plot.

Table 4.1 Rate constant determination of $[Pt(SacSac)_2]^{1-}$ dimerisation: Variation of concentration; keeping τ constant at 1.12 seconds [where $(E_\lambda - E_{\frac{1}{2}}) = 224$ mV and $\nu = 200$ mV per second] temperature = 293 Kelvin

concentration ($mol^1 dm^{-3}$)	ia/ic ratio	ω
5.34×10^{-5}	1.00	0
1.07×10^{-4}	0.790	0.58
2.14×10^{-4}	0.648	1.06
4.27×10^{-4}	0.567	2.63
8.54×10^{-4}	0.537	3.35
1.07×10^{-3}	0.498	4.07

for ω vs C

gradient = 3,776 (±150) mol^{-1} dm^3

Therefore, making use of the above

$$k_{f(293K)} = \frac{3776}{1.14 \times 1.46} = \underline{\underline{2270\ (\pm 90)\ mol^{-1}\ dm^3\ sec^{-1}}}$$

(τ = 1.12 sec; C = 6×10^{-5} - 1×10^{-3} M)

Equally, by independent measurements, varying the scan rate but keeping C constant, the data collected in Table 4.2 are found. A plot of ω vs. τ again yields a linear relationship with gradient ($k_f C \exp[0.078(a\tau - 4)]$)= 0.360 (±0.0072) (via least-squares analysis).

Therefore

$$k_{f(293K)} = \frac{0.360}{1.07 \times 10^{-4} \times 1.46} = \underline{\underline{2,300(\pm 47)\ mol^{-1}\ dm^3\ sec^{-1}}}$$

($C = 1.07 \times 10^{-4}$ M; τ = 0.5 - 5.5 sec)

By further consideration of the latter measurements, we can demonstrate the high degree of consistency found for these systems, using this mode of analysis. Table 4.3 shows the rate constants obtained if each voltammogram is employed singly to determine k_f. Note no trend or bias with τ is found.

Repeating this method of analysis over a wide range of concentrations and scan rates for the triad of $[M(SacSac)_2]$ complexes has allowed calculation of k_f over a variety of experimental variables. Table 4.4 shows some typical results obtained for $[Pt(SacSac)_2]$.

Table 4.2 Rate constant determination of $[Pt(SacSac)_2]^{1-}$ dimerisation: Variation of scan rate; keeping C_o constant at 1.07×10^{-4} $mol\ dm^{-3}$ temperature = 293 Kelvin

scan rate (mV/sec)	τ (seconds)	ia/ic ratio	ω
50	4.48	0.622	1.795
100	2.24	0.711	0.995
200	1.12	0.790	0.580
500	0.48	0.838	0.345

for ω vs τ

gradient = 0.360 (±0.0072) sec^{-1}

Table 4.3 Rate constant determination using a single cyclic voltammogram for $[Pt(SacSac)_2]$

Concentration = 1.07×10^{-4} mol dm^{-3}

temperature = 293 Kelvin

τ (seconds)	ia/ic	ω	k_f (mol^{-1} dm^3 sec^{-1})
4.48	0.622	1.795	2,296
2.24	0.711	0.995	2,324
1.12	0.790	0.580	2,272
0.448	0.838	0.345	2,343

Table 4.4 Calculated rate constants for the $[Pt(SacSac)_2]$ complex

by variation of concentration, keeping τ constant

[conc] = 5.34×10^{-5} to 1.07×10^{-3} $mol^{1} dm^{-3}$

τ (seconds)	k_f (mol^{-1} dm^3 sec^{-1})
4.48	2,150
2.24	2,215
1.12	2,270

by variation of scan rate, keeping concentration constant

(ν = 50 to 500 mV per second)

concentration ($mol^{1} dm^{-3}$)	k_f (mol^{-1} dm^3 sec^{-1})
1.07×10^{-4}	2,300
2.14×10^{-4}	2,195
4.27×10^{-4}	1,975

N.B. - temperature in all instances = 293 Kelvin

The effective constancy of the rate constant, k_f, under all conditions bears out the success of the analysis used.

The results obtained for all three complexes are summarized in Table 4.5. This confirms our qualitative observations that the rate of dimerisation follows the order

$$Ni << Pd < Pt$$

The most sensitive method of establishing which intimate dimerisation mechanism operates is by the shift in potential with changing concentration or scan rate[32] (if a sufficient range is available). For mechanism [1] the shift in potential from the reversible system with no following reaction is given by

$$E_p = E_{\frac{1}{2}} - 1.038(RT/F) + (RT/3F)\ln(RT/F)k_f C\nu^{-1}$$

whereas for mechanism [2], the potential shift is

$$E_p = E_{\frac{1}{2}} - 0.456(RT/F) + (RT/2F)\ln(RT/F)k_f C\nu^{-1}$$

Thus a plot of E_p vs. log C results in a straight line of slope 19.7 mV (at 298 K) for mechanism [1] and 29.6 mV for mechanism [2]. Attempts at applying this criterion to the $[Pt(SacSac)_2]$ complex have been met with partial success. As the concentration is increased, an anodic shift in potential is observed. A plot of E_p vs. log C yields a straight line of gradient 14.5 mV, suggesting mechanism [1] as the favoured dimerisation route.

Table 4.5 Rate constants for the dimerisation of $[M(SacSac)_2]^{1-}$ at 293 Kelvin

M =	k_f ($mol^{-1}\ dm^3\ sec^{-1}$)
nickel	65
palladium	1,300
platinum	2,120

N.B. averaged values of k_f

The effect of methyl replacement by other substituent groups is illustrated quantitatively by the kinetic parameters of the $[Pt(S_2C_3CF_3HPh)_2]$ complex. Using the same method of analysis as above, a rate constant of

$$k_{f(293K)} = \underline{\underline{5.6\ mol^{-1}\ dm^3\ sec^{-1}}}$$

Cyclic a.c. voltammetric studies for $[Pd(SacSac)_2]$ and $[Pt(SacSac)_2]$ show, qualitatively, the expected behaviour of the ratio I_p(return):I_p(forward), when the frequency of the a.c. current is 805 Hz, i.e. a decrease in ratio, representing increased quantity of dimer formed, with increasing concentration (Figure 4.7 shows typical cyclic a.c. V for $[Pt(SacSac)_2]$). The dependence of I_{p_r}/I_{p_f} on frequency of the a.c. current prevented the use of this technique as a mode of kinetic analysis for these systems, and further work is necessary to correlate cyclic a.c.V. with rate constant determination.

Figure 4.7 Typical cyclic a.c. voltammogram for the one-electron reduction of $[Pt(SacSac)_2]$

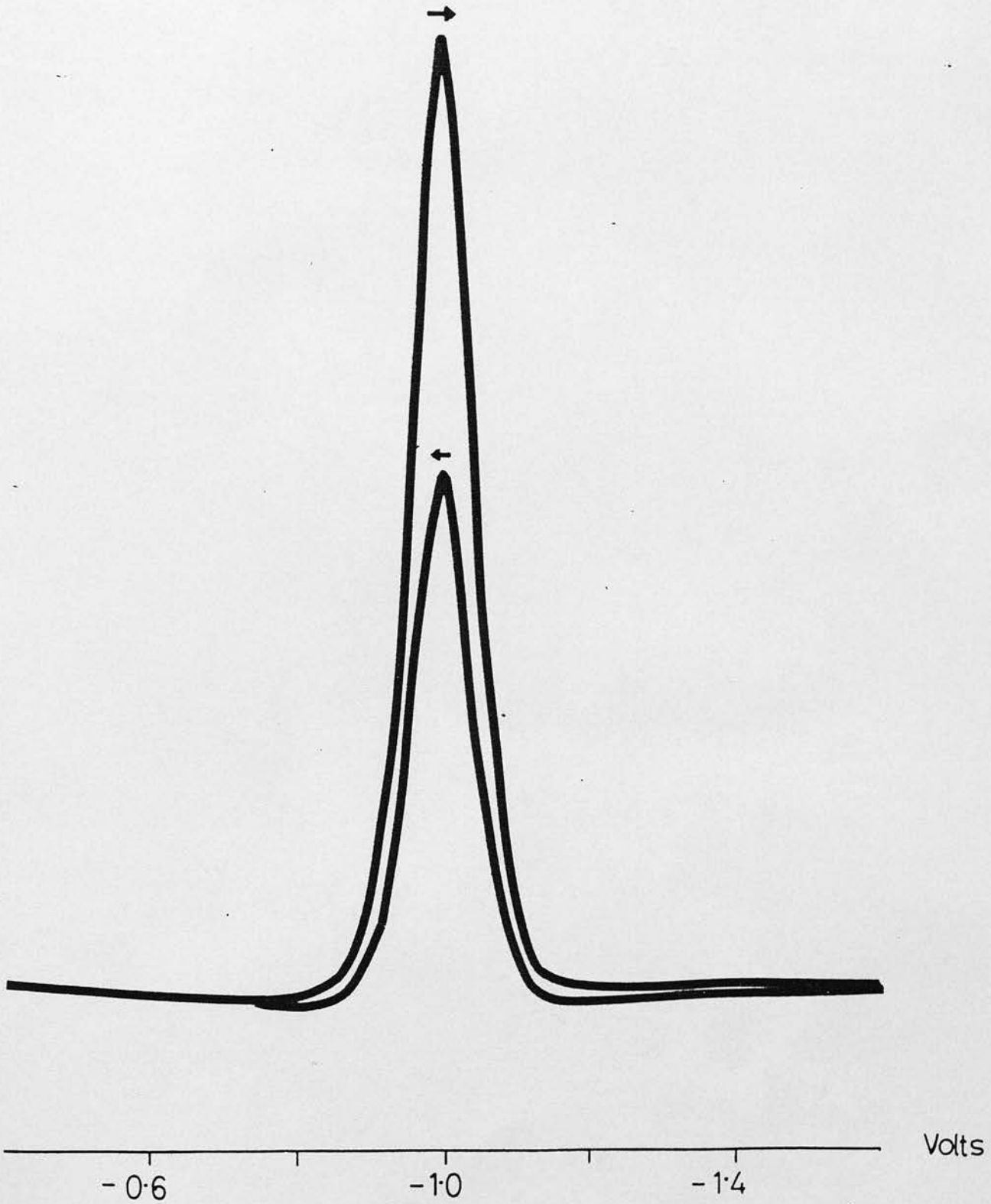

(b) Variation of temperature - Determination of activation energies

We have already made the qualitative observation that the rate of dimerisation is effectively slowed by cooling the electrolyte solution, so that reversible C.V. characteristics are found. The dimerisation is thus ideally suited to analysis of activation energies.

The observed variation of kinetic parameters with temperature can be used to calculate the enthalpy and entropy of activation, by making use of the Eyring equation, derived from the absolute rate theory.

$$k_f = \frac{kT}{h} e^{-\Delta G^{\neq}/RT}$$

from which we obtain

$$\log_e k_f - \log_e \frac{kT}{h} = -\frac{\Delta H^{\neq}}{R}\left(\frac{1}{T}\right) + \frac{\Delta S^{\neq}}{R}$$

Thus a plot of $R\log_e\left[k_f \cdot \frac{h}{kT}\right]$ vs. $\frac{1}{T}$ (Kelvin)

should have gradient = $-\Delta H^{\neq}$ and intercept = $\Delta S^{\neq}$

Accordingly, $[Pd(SacSac)_2]$ and $[Pt(SacSac)_2]$ were subjected to such analysis in the range 303 to 223 and 303 to 253 Kelvin respectively, to yield the activation energies listed in Table 4.6, together with the values obtained for a typical inorganic, chemically induced, bimolecular redox reaction[33]. This serves to illustrate that the thermodynamic parameters obtained for our systems are perfectly reasonable.

Table 4.6 Comparison of Activation Energies for bimolecular reactions

Reagents[a]	k_f/mol^{-1} dm^3 sec^{-1}	$\Delta G^{\neq}$/kJ mol^{-1}	$\Delta H^{\neq}$/kJ mol^{-1}	$\Delta S^{\neq}$/J^{1} K^{-1} mol^{-1}
$[Pd(SacSac)_2]^{1-}$	1,300 (293 K)	54.2	14.02	-137
$[Pt(SacSac)_2]^{1-}$	2,120 (293 K)	53.03	6.15	-160
$[Ru(NH_3)_5Br]^{2+}/V^{2+}$	3,000 (298 K)	50.1	12.6	-126

[a] $2[M(SacSac)_2]^{1-} \xrightarrow{k_f} [M(SacSac)_2]_2^{2-}$

$[Ru(NH_3)_5Br]^{2+} + V^{2+} \xrightarrow{k_f} [Ru(NH_3)_5Br]^{+} + V^{3+}$

4.4 Implications of the kinetic analysis

The most important aspect of the kinetic data mentioned so far is the remarkable consistency obtained, whether through variable concentration or scan rate determination. This bears out the success of the analysis used and is strong evidence for the proposed dimerisation.

The analysis also confirms quantitatively that $[Pt(SacSac)_2]^{1-}$ is easily the most prone to rearrangement and that substitution of methyl by more bulky groups results in the vast improvement of monoanion kinetic inertia. Indeed, $[Pt(S_2C_3CF_3HPh)_2]$, with a rate constant of $k_f = 5.6\ mol^{-1}\ dm^3\ sec^{-1}$ shows a rate of dimerisation even slower than that of $[Ni(SacSac)_2]$.

Attempts to identify the mechanism by variation of E_p with concentration led to a rather inconclusive result, which we strongly suspect has its origins in systematic effects of residual uncompensated cell resistance (IR drop) over the extreme range of cell currents entailed in this kind of experiment. Efforts to compare this are still in hand. The result did, however, suggest that mechanism [1] *i.e.* direct monoanion-monoanion coupling, was the favoured dimerisation route.

A number of organic dimerisation reactions have been studied using cyclic voltammetry; for instance diethyl fumarate (D.E.F.) undergoes a reversible one-electron reduction to form a radical anion followed by a coupling reaction of rate constant of about $34\ mol^{-1}\ dm^3\ sec^{-1}$ [34-36] (Scheme 4.5).

Scheme 4.5

$$D.E.F. + e^- \Longleftrightarrow DEF.^-$$

$$2D.E.F.^- \xrightarrow{k_f} (DEF)_2^{2-}$$

Likewise, a wide range of aryl-α,β-unsaturated ketones have been subjected to kinetic analysis, to reveal a dimerisation reaction following charge transfer with rate constants typically of $k_f = 1.4 \times 10^5$ $mol^{-1}dm^3sec^{-1}$.

The dimerisation rate constants obtained for our systems are well within this range, even the $[Pt(SacSac)_2]^{1-}$ reaction being approximately two orders of magnitude slower than that of the α,β-unsaturated ketones. Thus the experimental values obtained in this study appear reasonable in comparison with rates of dimerisation generally encountered in unrelated compounds.

More particular and significant comment depends on analysing the associated activation parameters, derived by kinetic measurements over a temperature range.

During the recording of these data an initially puzzling observation was made concerning the behaviour of the $[Pt(SacSac)_2]$ complex. The $R \log_e[k_f \frac{h}{kT}]$ vs. $\frac{1}{T(K)}$ plot shows two distinct sections, each with linear distribution (Figure 4.8). This would suggest that the process with the higher enthalpy of activation was dominant at low temperatures! In an attempt to explain this apparent anomaly, the diffusion-limited current for the first reduction of $[Pt(SacSac)_2]$ was measured using a rotating platinum electrode from

Figure 4.8 The determination of activation parameters for the $[Pt(SacSac)_2]^{1-}$ dimerisation reaction

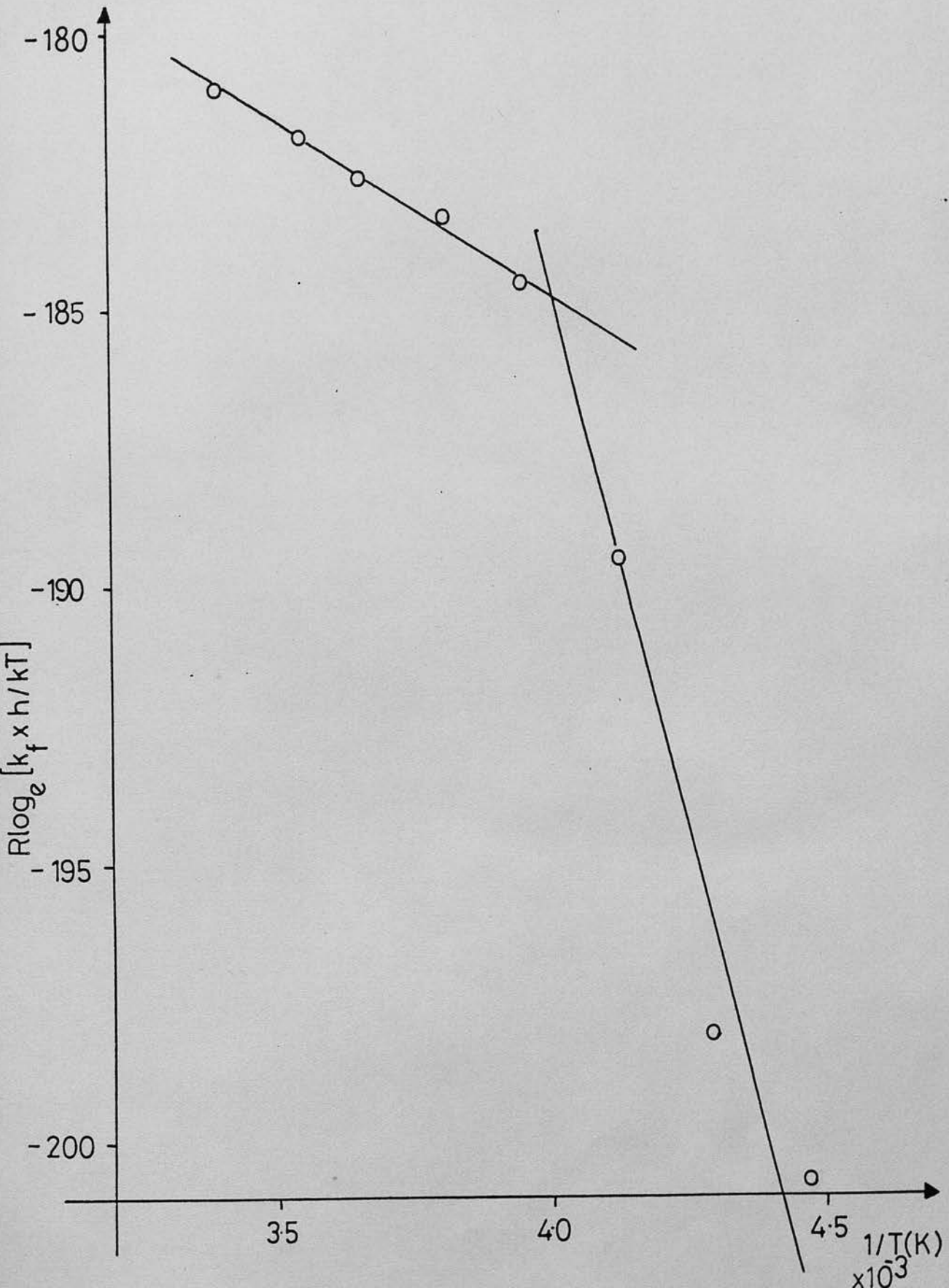

303 to 223 Kelvin and then compared with the behaviour of a similar concentration of ferrocene over the applicable temperature range. Whereas ferrocene shows a steady fall-off in current with decreasing temperature, the $[Pt(SacSac)_2]$ complex initially exhibits parallel behaviour then a very sudden decrease at ≈245 Kelvin (Figure 4.9), the same temperature at which the anomalous thermodynamic behaviour is found. This would seem to indicate that at lower temperatures $[Pt(SacSac)_2]$ begins to precipitate from solution, so that the nominal concentration is higher than the genuine concentration, leading to a smaller calculated k_f value. Therefore analysis must be restricted to the higher temperature portion of data.

In order to determine if the quantitative difference in rate constants observed between the palladium and platinum systems is dictated by the calculated $\Delta H^{\neq}$ terms (Table 4.6) we can consider the effect of changing $\Delta H^{\neq}$ at a fixed temperature.

$$\ln k_1 = \frac{-\Delta H_1^{\neq}}{RT} \qquad \ln k_2 = \frac{-\Delta H_2^{\neq}}{RT}$$

$$\ln \frac{k_1}{k_2} = \frac{\Delta H_2^{\neq} - \Delta H_1^{\neq}}{RT}$$

therefore $RT \ln \frac{k_1}{k_2} = \Delta H_2^{\neq} - \Delta H_1^{\neq}$ "$\delta\Delta H^{\neq}$"

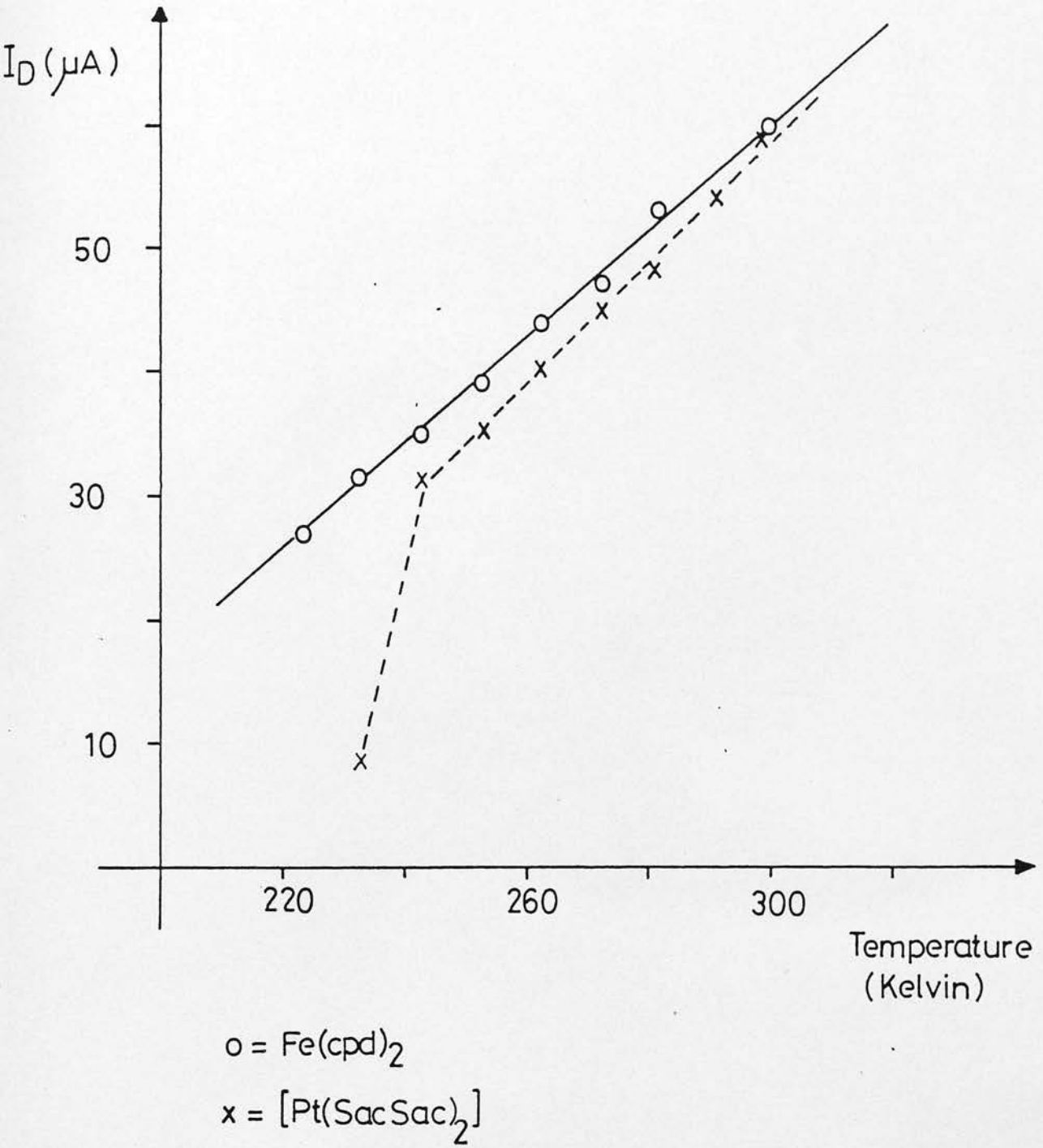

Figure 4.9 Variation of the diffusion-limited current with changing temperature

therefore at 293 Kelvin "$\delta\Delta H^{\neq}$" = 2.44 ln $\frac{k_1}{k_2}$

if observed rate changes by $\frac{2120}{1300}$ = 1.63 as in $\frac{Pt}{Pd}$

"$\delta\Delta H^{\neq}$" = 2.44 x 0.49 = $\underline{1.20\ kJ\ mol^{-1}}$

The change in $\Delta H^{\neq}$ found experimentally between $[Pd(SacSac)_2]$ and $[Pt(SacSac)_2]$ of 7.85 kJ mol^{-1} would therefore be expected to produce a far greater difference in observed rate constants than is found. However, $[Pt(SacSac)_2]$ has a more unfavourable $\Delta S^{\neq}$ term by $\simeq$40 J mol^{-1}, which will counteract the smaller $\Delta H^{\neq}$ term, leading to a smaller rate constant than predicted purely from $\Delta H^{\neq}$ considerations.

None-the-less, the data for the two $[M(SacSac)_2]$ complexes do follow the same general pattern, with $\Delta H^{\neq}$ small and positive ($\simeq$ + 10 kJ mol^{-1}) and $\Delta S^{\neq}$ large and negative ($\simeq$ -150 $J^{1}\ K^{-1} mol^{-1}$).

The highly negative $\Delta S^{\neq}$ term is strongly indicative of a significant degree of ordering required in the transition state, which is in line with a bimolecular reaction. The small, positive $\Delta H^{\neq}$ would suggest a large degree of bond formation in the transition state. (To reach the transition state the reactants require a positive input of energy, this can in turn be counteracted by the release of energy associated with bond formation, so that the overall $\Delta H^{\neq}$ will be small and positive).

Square planar Pt(II) complexes are generally found to be relatively inert species, so that one might expect $[Pt(SacSac)_2]^{1-}$ to be the slowest to react. However, in the present case, the small positive $\Delta H^{\neq}$ term, suggesting a high degree of bond formation, may lead to stabilization of the transition state by just those qualities which normally stabilize ground state platinum complexes against reaction.

The structure of the dimeric product must play an important role in rate determination. Two possible structures, by analogy with the dimeric dithiolene complexes[24-27], are <u>via</u> the formation of a direct metal-metal bond (i)[25] or a bond between the metal of one unit and the sulphur atom of another unit (ii). In the dithiolene systems, the latter is the more common.

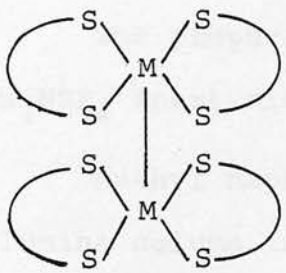

(i)

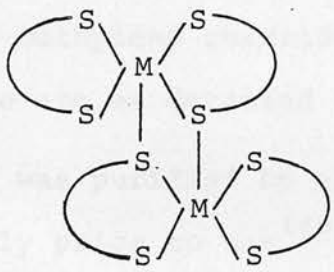

(ii)

We believe that the one-electron reduction of $[M(SacSac)_2]$ entails a largely ligand-based process (see Chapter 3). This would seem to suggest structure (ii) as being the more likely of the two. The driving force of the reaction could be the formation of metal-sulphur bonds. A hard metal centre plus soft donor

atom will not result in as stable a complex as a soft metal plus soft ligand, i.e. Ni-S not as favourable as Pt-S bond formation. This may be the reason for the relative ordering of the dimerisation reaction, viz. Ni << Pd < Pt.

At this stage, however, no confirmatory information is available as to the actual structure of the dimer. Until such evidence is obtained, no possible formulation of the dimer should be discounted. For example, the possibility of metal-carbon, as in $[(CH_3)_3Pt(O_2C_5H_7)]_2$ [38,39], or carbon-sulphur bonds, as in $(SacSacH)_2$, or even carbon-carbon bonds, should not be overlooked.

4.5 Experimental

(i) Materials

Complexes were prepared as described in Chapter 2.

The preparation of methylene chloride solvent and Bu_4NBF_4 inert electrolyte are as detailed in Section 3.5.

Methyl naphthalene was purified by elution from an alumina column immediately prior to use [40].

(ii) Instrumentation

Voltammetric studies in 0.25 M Bu_4NBF_4/CH_2Cl_2 employed the same equipment and basic 3-electrode cell configuration as described in Section 3.5, plus a Telequipment D66A oscilloscope as display mode for scan rates > 500 mV/sec.

Cyclic voltammetry in 0.1 M Bu_4NBF_4/methyl naphthalene employed a P.A.R. 170 system (potentiostat and programmer). In this case platinum was used as both working and counter electrodes, together with a platinum quasi-reference electrode. The temperature was maintained at 423 Kelvin using a jacketted cell and Haake F3S circulating bath.

Kinetic analysis again made use of a P.A.R. 170 electrochemistry system and 3-electrode cell. Cyclic voltammograms employed a Pt micro-disk working electrode, while d.c. voltammograms were recorded using a Tacussel E.D.I. rotating Pt electrode. Routine scan rates were in the range 50 to 500 mV/sec in C.V. and 10 mV/sec in the d.c.V. modes. Cell solutions, ranging from approx. 5×10^{-5} to 5×10^{-3} molar in complex, were degassed with CH_2Cl_2-saturated argon. It was of extreme importance that cell solutions, and the argon bubbler, were thermostatically controlled. This was done using a 10 ml jacketted cell, employing a Haake F3Q circulating bath, the internal temperature of the cell being monitored by a Comark 5000 digital thermometer.

O.T.T.L.E. experiments, in 0.5 M Bu_4NBF_4/CH_2Cl_2, employed a Metrohm Polarecord E505 and a Pye Unicam SP8-400 spectrophotometer, using the techniques developed in this laboratory by D.K. Vattis and L.J. Yellowlees[31]. A non-aqueous $Ag/AgCl/Cl^-/CH_2Cl_2$ reference electrode (against which ferrocene was oxidised at 0.58 Volts) and a Pt counter electrode, separated from the working

compartment by a fritted salt-bridge, were employed. A platinum mini-grid working electrode was used. Cell solutions were thoroughly degassed with CH_2Cl_2-saturated argon prior to experimentation. During the complete experiment a positive pressure of nitrogen was maintained in the spectrometer compartment. Cooling was obtained by passing nitrogen gas through a heat exchanger immersed in liquid nitrogen, which was then directed onto both faces of the O.T.T.L.E. cell. The temperature close to the electrode was measured using a Ni-Cd thermocouple, connected to a Comark 5000 digital thermometer.

(iii) Kinetic Analysis

The method applied to extract kinetic information has been explained previously (Section 4.3). Before such analysis can proceed three important parameters must be accurately determined:

(a) The geometry of the working electrode. This is achieved by using a micro-platinum disk, where the surface of the electrode is flat, i.e. Ψ equals zero. Figure 4.10 illustrates the appropriate working curve for determination of ω from ia/ic ratios.

(b) Determination of $E_{\frac{1}{2}}$ for irreversible system

This can be established (within 3/n mV) as the potential at 85% of the cathodic peak current.

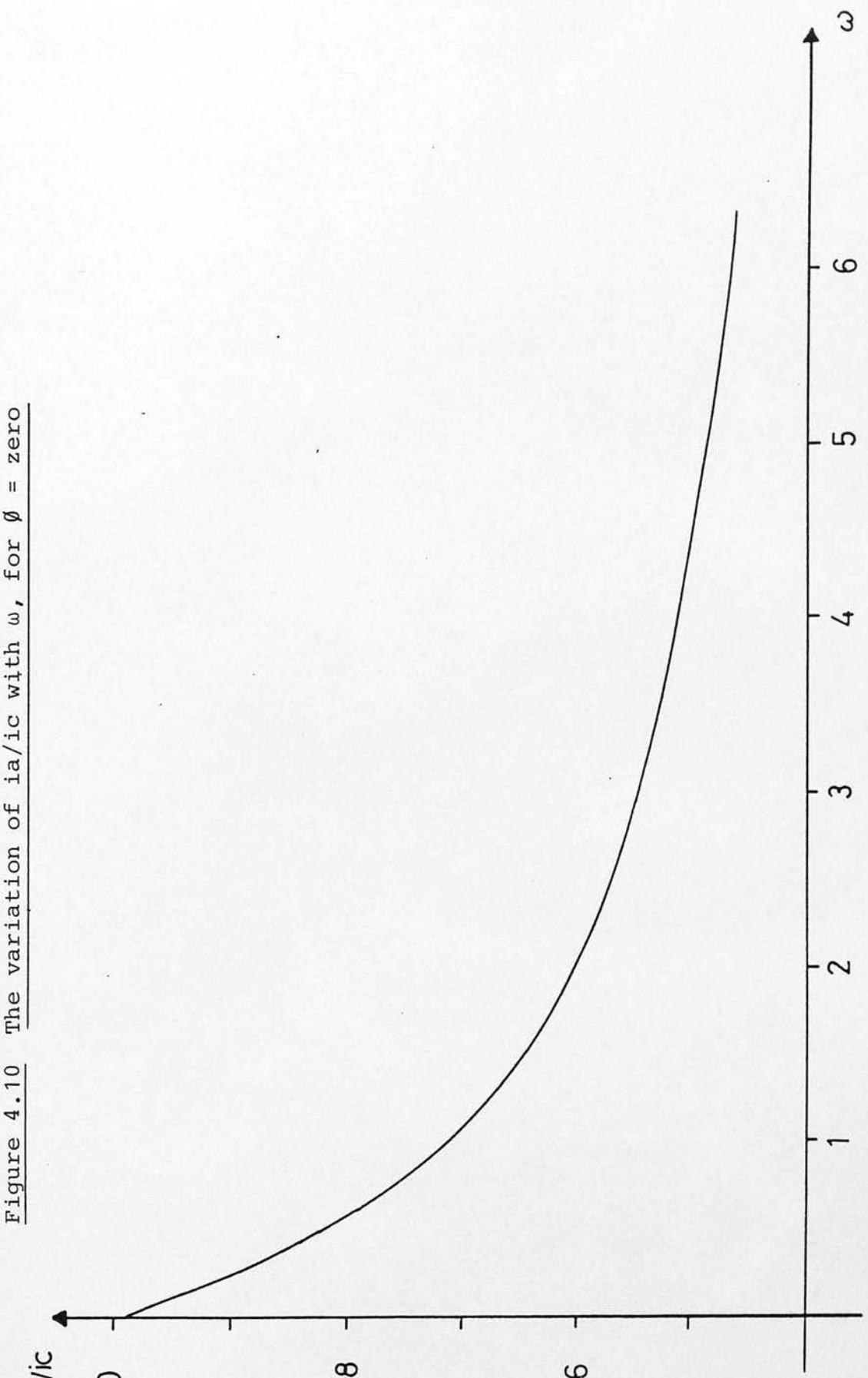

Figure 4.10 The variation of ia/ic with ω, for ϕ = zero

(c) Accurate calculation of ia/ic This can be done most effectively using the following relationships[41].

$$\frac{ia}{ic} = \frac{(ia)_o}{(ic)_o} + \frac{(0.485)\ (is)_o}{(ic)_o} + 0.086$$

where the terms $(ia)_o$, $(ic)_o$ and $(is)_o$ are the parameters defined in Figure 4.11.

Figure 4.11 Cyclic voltammogram defining the parameters $(ic)_o$, $(is)_o$ and $(ia)_o$ used to determine the ratio ia/ic

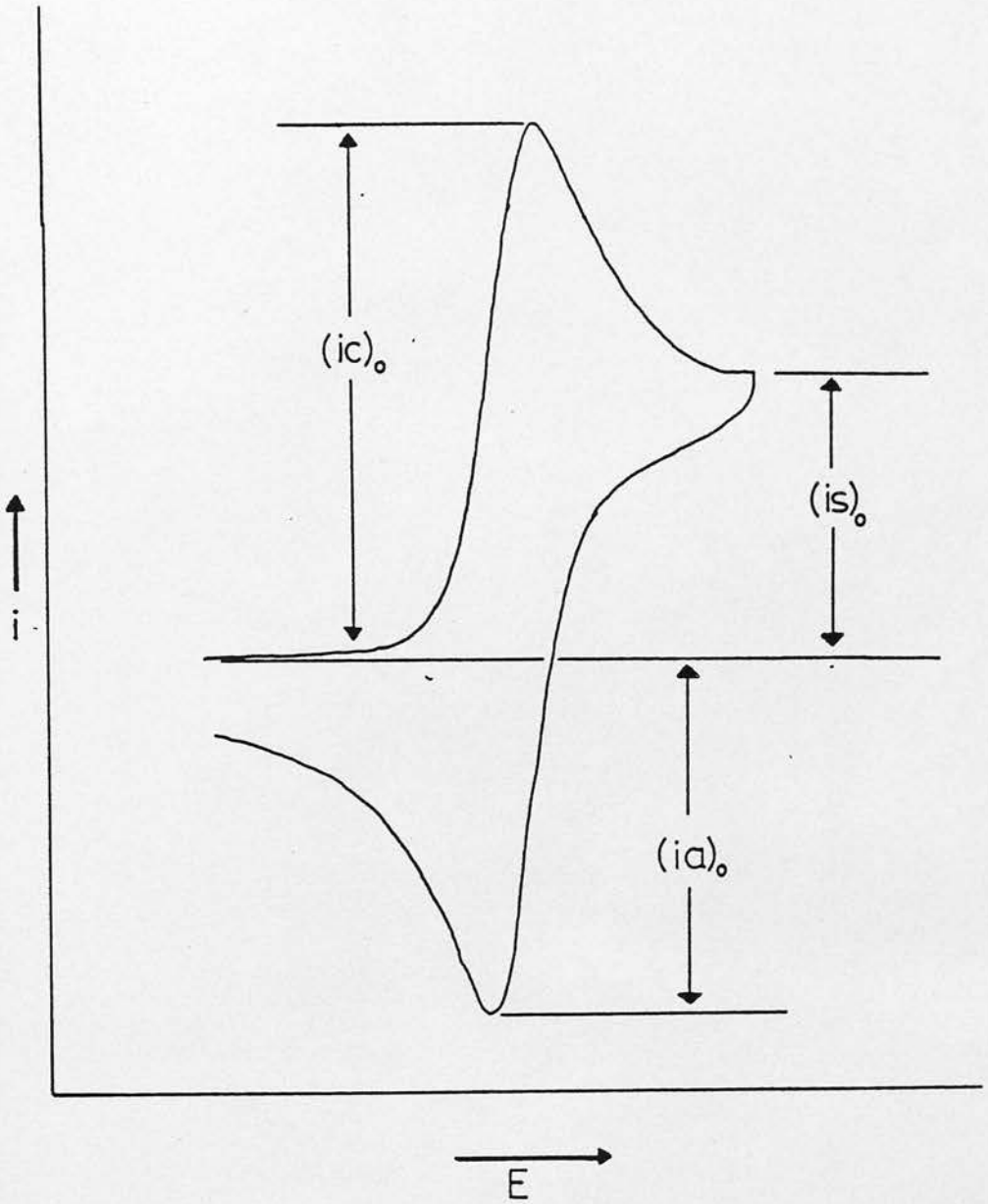

References (Chapter 4)

1. A. Weissberger and B.W. Rossiter, "Physical Methods of Chemistry. II A. Electrochemical Methods", Wiley, New York, 1971.

2. R.S. Nicholson and I. Shain, Anal.Chem., 1964, 36, 706.

3. M.L. Olmstead, R.G. Hamilton and R.S. Nicholson, Anal.Chem., 1969, 41, 260.

4. M. Mastragostino, L. Nadjo and J.M. Saveant, Electrochimica Acta, 1968, 13, 721.

5. J.M. Saveant and E. Vianello, Compt.Rend., 1963, 256, 2597.

6. T.G. McCord, H.L. Hung and D.E. Smith, J.Electroanal. Chem., 1969, 21, 5.

7. D.E. Smith, Anal.Chem., 1963, 35, 603.

8. T.G. McCord and D.E. Smith, Anal.Chem., 1969, 41, 116.

9. A.M. Bond, J.R. O'Halloran, I. Ruzic and D.E. Smith, Anal.Chem., 1976, 48, 872.

10. A.M. Bond, J.Electroanal.Chem., 1974, 50, 285.

11. W. Vielstich and D. Jahn, Z.Electrochem., 1958, 32, 2437.

12. H. Matsuda, J.Electroanal.Chem., 1972, 35, 77.

13. L.K.J. Tong, K. Liang and W.R. Ruby, J.Electroanal.Chem., 1967, 13, 245.

14. S.A. Kabakchi and V. Yu. Filinovski, Electrokhim., 1972, 8, 1428.

15. W.J. Albery and S. Bruckenstein, Trans.Faraday Soc., 1966, 62, 1946.

16. W.J. Albery, M.L. Hitchman and J. Ulstrup, Trans. Faraday Soc., 1968, 64, 2831.

17. W.J. Albery and M.L. Hitchman, "Ring-Disc Electrodes" Clarendon Press, Oxford, 1971.

18. K.B. Prater and A.J. Bard, J.Electrochem.Soc., 1970, 117, 335.

19. W.J. Albery and S. Bruckenstein, Trans.Faraday Soc., 1966, 62, 2584.

20. R. Guidelli, Electroanal.Chem., 1971, 5, 149.

21. P. Zuman, Prog.Phys.Org.Chem., 1967, 5, 81.

22. A.M. Bond, G.A. Heath and R.L. Martin, Inorg.Chem., 1971, 10, 2026.

23. W.L. Bowden, J.D.L. Holloway and W.E. Geiger, Jr., Inorg.Chem., 1978, 17, 256.

24. M.J. Baker-Hawkes, Z. Dori, R. Eisenberg and H.B. Gray, J.Am.Chem.Soc., 1968, 90, 4253.

25. W.C. Hamilton and I. Bernal, Inorg.Chem., 1968, 7, 2636.

26. J.H. Enemark and W.N. Lipscomb, Inorg.Chem., 1965, 4, 1729.

27. K.W. Browall, T. Bursh, L.V. Interrante and J.S. Kasper, Inorg.Chem., 1972, 11, 1800.

28. J.F. Weiher, L.R. Melby and R.E. Benson, J.Am.Chem.Soc., 1964, 86, 4329.

29. J.H. Enemark and J.A. Ibers, Inorg.Chem., 1968, 7, 2636.

30. J.D. Forrester, A. Zalkin and D.H. Templeton, Inorg.Chem., 1964, 3, 1507.

31. L.J. Yellowlees, Ph.D. Thesis, University of Edinburgh, 1982.

32. C.P. Andrieux, L. Nadjo and J.M. Saveant, J.Electroanal. Chem., 1973, 42, 223.

33. M.L. Tobe, "Inorganic Reaction Mechanisms", Nelson, Middlesex, 1977.

34. W.V. Childs, J.T. Maloy, C.P. Keszthelyi and A.J. Bard, J.Electrochem.Soc., 1971, 118, 874.

35. V.J. Puglisi and A.J. Bard, J.Electrochem.Soc., 1972, 119, 829, 833.

36. V.J. Puglisi and A.J. Bard, J.Electrochem.Soc., 1973, 120, 241.

37. J.P. Zimmer, J.A. Richards, J.C. Turner and D.H. Evans, Anal.Chem., 1971, 43, 1000.

38. R.N. Hargreaves and M.R. Truter, J.Chem.Soc., A, 1969, 2282.

39. D. Gibson, Coordination Chem.Rev., 1969, 4, 225.

40. R.C.S. McQueen, Ph.D. Thesis, Edinburgh University, 1983.

41. R.S. Nicholson and I. Shain, Anal.Chem., 1966, 38, 1406.

CHAPTER 5

Cobalt(II) bis(dithio-β-diketonates)

5.1 Introduction

Cobalt is an essential component in the biological activity of the co-enzymes related to vitamin B_{12} (organo-cobalamins), the basic structure of which is illustrated below (i). Vitamin B_{12} generally means cyano-cobalamin, which has a Co(III)-CN group. The best known co-enzyme also contains Co(III) and a 5-deoxyadenosyl group that replaces the CN.

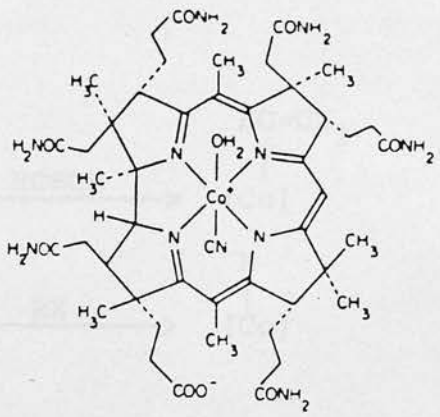

(i)

While it is known that the B_{12} co-enzymes act in conjunction with a number of enzymes, very little is known about their role in detail. However, the study of the non-enzymic behaviour of B_{12} co-enzymes has enabled the assembly of basic B_{12} chemistry, some of which undoubtedly plays an important role in its activities as a co-enzyme[1-3].

The cobalamins can be reduced in an alkaline or neutral solution to give Co(II) and Co(I) species, commonly referred to as B_{12r} and B_{12s} respectively. The latter is a powerful reducing agents, decomposing water to give hydrogen and B_{12r}. When cyano- or hydroxo-cobalamin is reduced, the ligand, CN^- or OH^-, is lost and the Co(I) complex is five-coordinate. In non-enzymic systems rapid reaction of B_{12s} occurs with alkyl halides, acetylenes, etc. as shown in Scheme 5.1, where [Co] represents the cobalamin group[4,5].

Scheme 5.1

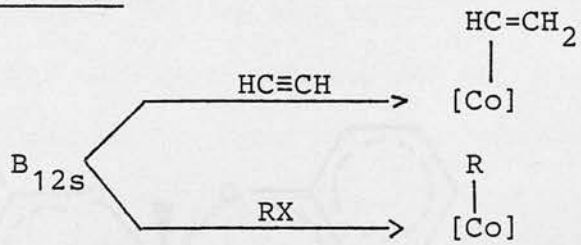

Likewise, 5-deoxyadenosyl cobalamin is known to function as a hydrogen-transfer agent, where the cleavage of the Co(III)-5-deoxyadenosyl bond is a necessary step in the reaction scheme[6]. Methyl cobalamin undergoes several known methyl-transfer reactions to various biological and inorganic substrates[7-10].

The formation and cleavage of cobalt-carbon bonds in these complexes is thus of intrinsic importance to their catalytic activity.

The biological importance of cobalt-carbon bonds has prompted study of a series of model complexes, in search of a chemical precedent for the B_{12} co-enzyme activity, to further elucidate the factors influencing the mechanisms of cobalamin reactions.

Model systems so far advanced generally consist of a rigid, planar ligand system, consisting of highly conjugated nitrogen and oxygen donor atoms, with the axial sites occupied by a Lewis base and by an anion, that may be a carbanion. Most of these complexes belong to the "Salen" (ii)[11,12] or "cobaloxime" (iii) series[13-16].

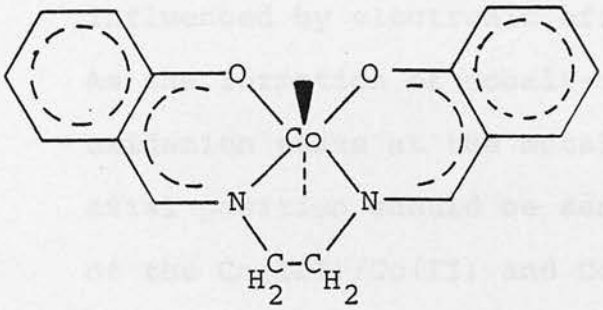

Cobalt(II)N,N'-ethylenebis-(salicylideneiminato)

(ii)

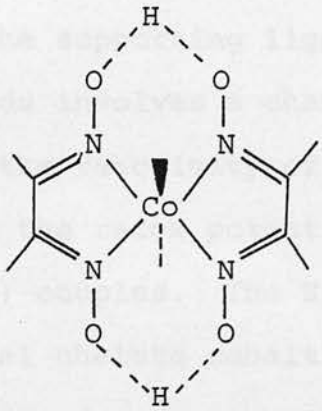

Cobalt(II) dimethylglyoximato

(iii)

Studies of the reaction of alkyl halides with a number of penta-coordinate cobalt(I), (II) and (III) complexes to give hexa-coordinate Co(III)-alkyl species has revealed various pathways of formation. Three routes have been distinguished:

$Co(III) + R^- \rightarrow Co(III)-R$	Carbanion transfer to Co(III) [17]
$Co(II) + R\cdot \rightarrow Co(III)-R$	Alkyl radical transfer to Co(II) [18-21]
$Co(I) + R^+ \rightarrow Co(III)-R$	Nucleophilic attack of Co(I) on R^+ [4,5]

All three categories have been recognised experimentally. For the model complexes, as for B_{12} itself, Co(III) is the oxidation state that stabilizes cobalt-alkyl bond formation.

Examination of the latter two reaction pathways shows that the mechanism of cobalt-carbon bond formation is dependent on the oxidation state of the cobalt ion, and thus on the electron density on the metal, which is inevitably influenced by electronic effects of the supporting ligands. As the formation of cobalt-carbon bonds involves a change in oxidation state at the metal centre, the reactivity of the axial position should be sensitive to the redox potentials of the Co(III)/Co(II) and Co(II)/Co(I) couples. The $E_{\frac{1}{2}}$ potentials for Schiff's base equatorial chelate cobalt complexes containing axial Lewis bases and organo-groups indeed shows a correlation between redox potentials of the cobalt couples and the nature of the ligand [15,22].

The formation of cobalt-carbon bonds can be explored electrochemically. The reduction of $[Co(II)\ Salen]^0$ to $[Co(I)\ Salen]^{1-}$ by controlled potential electrolysis, followed by excess addition of ethyl bromide results in the formation of a new electro-active species, postulated to be $[EtCo(III)Salen]^0$ [23,24]. The loss of $[Co(I)\ Salen]^{1-}$ and the generation of $[EtCo(III)Salen]^0$ can be easily monitored by changes in the cyclic voltammetry.

The applicability of the various model systems to the B_{12} co-enzymes is still a matter of discussion, but it is now thought that Costa's B_{12} model (iv)[25,26] is a closer electrochemical mimic than the more widely used cobaloxime model (iii)[27].

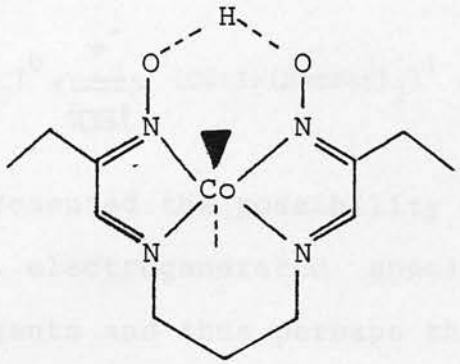

(iv)

The synthesis of cobalt(II)bis(dithioacetylacetonate), $[Co(SacSac)_2]$[28], and its subsequent characterisation by X-ray diffraction, showed a square planar cobalt(II) centre[29,30]. Although, in general, bis(dithioacetylacetonate) metal(II) complexes do not show axial coordination, $[Co(SacSac)_2]$ is known,
(a) to readily oxidise to $[Co(III)(SacSac)_3]$ in the presence of an additional source of $[SacSac]^-$,
(b) to form six-coordinate cationic cobalt(III) species, incorporating a bidentate nitrogenous base (for example, 1,10-phenanthroline and 2,2'-bipyridine gives complexes of the type $[Co(III)S_4N_2]^+$[31]) and
(c) to give five-coordinate square pyramidal cobalt nitrosyls, such as $[Co(III)(NO)(S_2C_5H_7)_2]$[32]. Thus when $[Co(SacSac)_2]$ is oxidised to Co(III), the coordination number tends to increase.

Electrochemical studies showed two reductions, the first reversible, assigned to a Co(II)/Co(I) couple, the second sluggish, and assigned to ligand reduction[33,34] (Scheme 5.2).

Scheme 5.2

$$[Co(II)(SacSac)_2]^0 \underset{\text{fast}}{\overset{e^-}{\rightleftharpoons}} [Co(I)(SacSac)_2]^{1-} \underset{\text{slow}}{\overset{e^-}{\rightleftharpoons}} [Co(I)(SacSac)^{1-}(SacSac)^{2-}]^{2-}$$

This presented the possibility of these highly nucleophilic, electrogenerated species reacting with alkylating agents and thus perhaps the use of $[Co(SacSac)_2]$ as a model for B_{12} activity. This would be despite the sterically unconstrained bis-dithioacetylacetonate arrangement being in stark contrast to the rigid tetradentate nitrogen and oxygen ligands discussed previously.

The use of electrochemistry as an investigation mode has three distinct advantages, (a) providing convenient access to the three oxidation states of the molecule i.e. $[Co(SacSac)_2]^0$, $[Co(SacSac)_2]^{1-}$ and $[Co(SacSac)_2]^{2-}$, (b) providing immediate graphic evidence of the reaction of the electro-active species with alkyl halide, RX, plus information on reaction rates, and (c) allowing study of transient species, which although stable on an electrochemical time-scale, could not be isolated.

Although $[Co(SacSac)_2]^0$ is stable in the presence of alkyl halide, the one-electron reduced species, $[Co(I)(SacSac)_2]^{1-}$, shows rapid reaction with equimolar

methyl iodide, to yield a redox-active species which is irreversibly reduced ≈0.4 Volts cathodic of the Co(II)/Co(I) couple[34]. This new redox-active species has been formulated as $[MeCo(III)(SacSac)_2]^0$, by analogy with Costa's work on the oxidative addition of RX to $[Co(I)Salen]^{1-}$ to form [RCo(III)Salen], which is likewise reduced at more negative potentials than the parent [Co(II)Salen] complex[23,24].

The irreversible nature of the reduction of the Co(I)/RX reaction product is also consistent with Co(III)-alkyl bond formation, the instability of Co(II)-alkyl bonds being well documented[35,36].

The reaction is best illustrated by cyclic voltammetry, where the Co(II)/Co(I) return-wave is completely eliminated in the presence of RX, irrespective of the switching potential beyond the Co(II)/Co(I) couple (Figure 5.1). The extension of the study to include a variety of organic halides provided details regarding the possible mechanism of reaction[34].

The observation that alkyl iodide was favoured above alkyl bromide suggested a substantial amount of bond breaking in the rate determining step. Similarly, the process occurred readily for small, primary alkyl iodides, but not for branched alkyl iodides, suggesting an S_{N_2} type mechanism, with short, linear alkyl groups presenting less steric hindrance in the five-coordinate transition state of a bimolecular process.

Figure 5.1 The use of C.V. to monitor the reaction of $[Co(SacSac)_2]^{1-}$ with MeI

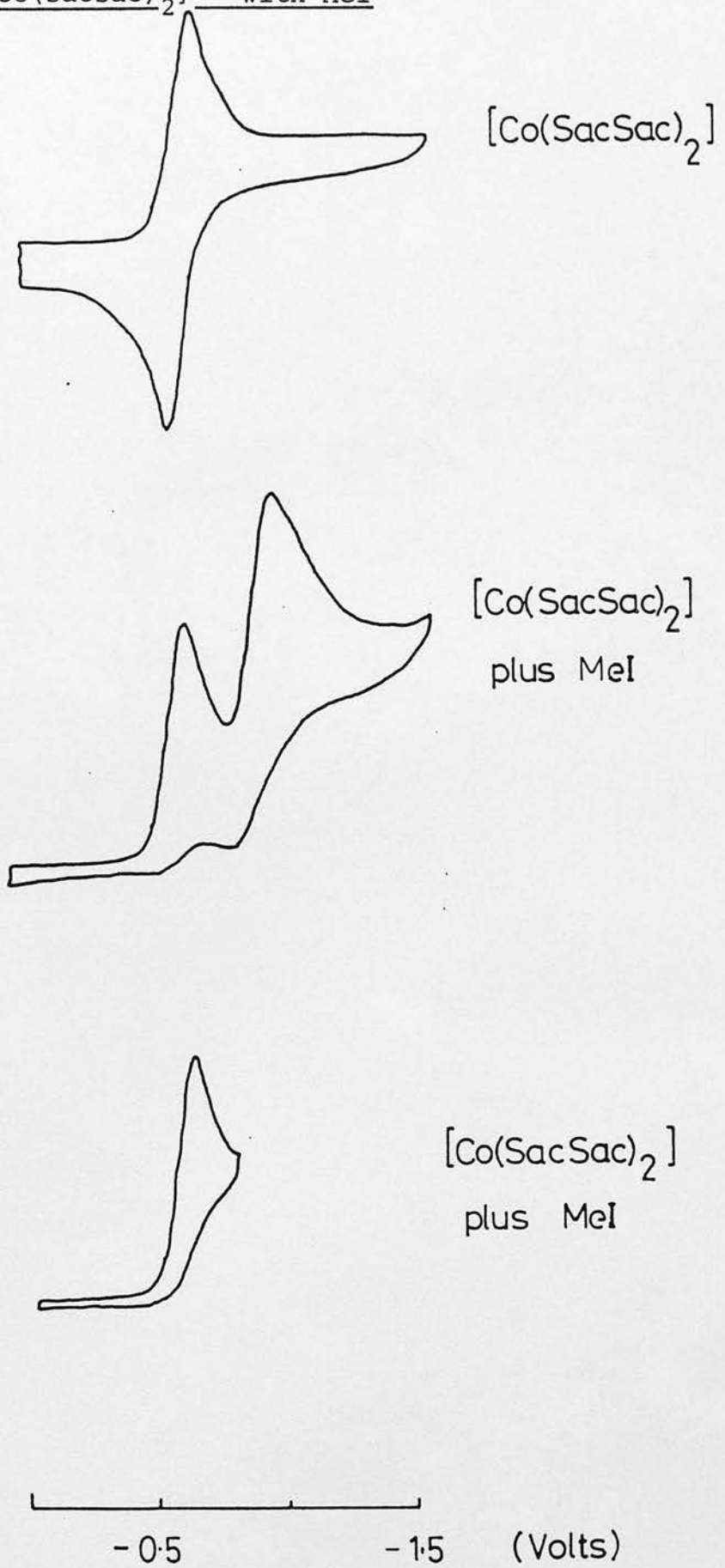

This reaction can be seen to be directly analogous to that of vitamin B_{12}, where B_{12s} (and "cobaloxime(I)") react with primary alkyl halides via a classical S_{N2} mechanism to give cobalt-alkyl complexes in quantitative yield[4,5]. No organo-cobalt complexes were isolated from reaction of B_{12s} (or "cobaloxime(I)") with secondary or tertiary alkyl halides.

Given the changes in cyclic voltammetric characteristics accompanying the reaction of $[Co(SacSac)_2]^{1-}$ with RI, kinetic analysis was possible for RI = EtI, ^{n}PrI and ^{n}BuI. This showed an overall second-order process, i.e. first order with respect to both $[Co(SacSac)_2]^{1-}$ and RI, but no particular trend in rate constant was apparent[34].

Attempts to date to isolate the $[Co(SacSac)_2]^{1-}$/RI reaction product have met with failure. This has prompted the study of substituted cobalt dithioacetylacetonate complexes, in the hope that, by replacing methyl substituents by electron-withdrawing groups, we might sufficiently stabilize the Co(I) species to allow bulk electrochemical generation of the radical anion, prior to reaction with equimolar RI, to yield a more robust cobalt-alkyl complex which would allow full characterisation of the cobalt-carbon bond.

Results and Discussion

5.2 The substituted Co(II)bis(dithio-β-diketonates)

The cobalt(II)bis(dithio-β-diketonate) complexes (v) were prepared by a method similar to that originally employed by Martin and Stewart in the synthesis of $[Co(SacSac)_2]$ itself (where $R,R' = CH_3$)[28].

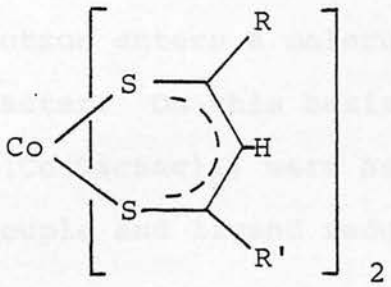

$R,R' = CH_3$, Ph; Ph, CF_3 or CF_3, CH_3

(v)

The substituted complexes, however, are much more soluble than $[Co(SacSac)_2]$ in the ethanolic-HCl reaction media, with the consequence that for successful synthesis, the concentration of Co^{2+} must be in the region of 0.01 moles per 5 ml of ethanol.

The complexes were identified by C:H analysis and infrared spectroscopy. As with $[Co(SacSac)_2]$ and $[Ni(SacSac)_2]$, the spectra of the substituted cobalt complexes are all very similar to their established d^8-analogues, thus the infrared spectrum is an extremely useful fingerprint for a successful synthesis. No attempt was made to make detailed assignments.

A detailed study of the electrode response of all the complexes was undertaken. As discussed previously, $[Co(SacSac)_2]$ has two reductions[33,34] (Scheme 5.2) at -0.71 and -1.70 Volts (vs. Ag/AgCl). The large difference ($\simeq$0.2 Volts) between the first one-electron reduction of $[Co(SacSac)_2]$ and $[Ni(SacSac)_2]$ (E^o = -0.94 V), suggests that in $[Co(SacSac)_2]^{1-}$ the additional electron enters a molecular orbital of very different character. On this basis, the successive reductions of $[Co(SacSac)_2]$ were assigned to a metal-based Co(II)/Co(I) couple and ligand reduction respectively.

From our observations concerning the sensitivity of E^o potentials to the inductive effect of the substituent groups for the two ligand-based reductions of the nickel, palladium and platinum complexes, (Chapter 3), we can make a number of predictions regarding the behaviour of $[Co(S_2C_3RHR')_2]$.

The first metal-based reduction might be expected to be fairly insensitive to changes in R, whereas the second (ligand-based) reduction should exhibit a similar degree of sensitivity to substituent as found in the $[Ni(S_2C_3RHR')_2]$ series. Furthermore, we may be able to see the second ligand reduction at extreme potentials, approximately 0.45 Volts cathodic of the first ligand-based process.

Experimentally, however, never more than two (generally reversible) reductions are observed. Indeed, and more surprisingly, comparison of the data collected for the cobalt complexes with the analogous nickel series

(Table 5.1) shows that both the first and second reduction potentials for the substituted cobalt complexes correspond closely to those found for the ligand-based reductions of $[Ni(S_2C_3RHR')_2]$ (with an expected difference of 0.45 Volts between first and second reduction for ligand-based processes).

This can be further illustrated by considering a plot of E^o_{red} *vs.* $\Sigma\sigma^e$ (where σ^e represents the substituent inductive parameter derived electrochemically - see Section 3.3). By considering the rather limited data available for the analogous cobalt and nickel complexes only, we obtain (by least squares analysis) the substituent sensitivities listed in Table 5.2. This similarity in E^o_{red} potential sensitivity (both first and second reductions) can also be represented graphically (Figure 5.2), where it appears that the behaviour of $[Co(SacSac)_2]$ differs importantly from that of its structural analogues.

From these observations it would appear that the substitution of methyl by phenyl, and/or CF_3 groups, results in a sufficient reorganisation of the molecular orbitals for ligand-based reductions to be favoured over metal-based ones. Indeed, a critical, relevant observation is that the substituted complexes show no reaction with methyl iodide. This is more readily understood if the reduction in these cases is ligand dominated so that a highly nucleophilic Co(I) metal centre is not generated. This is substantiated by the lack of reaction of any of the one-electron reduced d^8-complexes, $[M(S_2C_3RHR')_2]^{1-}$, with MeI, and by the

Table 5.1 Comparison of reduction potentials for the series $[M(S_2C_3RHR')_2]$ where M = nickel and cobalt

($E^{\circ}_{red}(1)$ and $E^{\circ}_{red}(2)$/Volts vs. Ag/AgCl

R,R′ =	Cobalt	Nickel
CH_3/CH_3	-0.71	-0.94
	-1.70	-1.42
CH_3/Ph	-0.76	-0.75
	-1.20	-1.16
CH_3/CF_3	-0.41	-0.43
	-0.94	-0.93
CF_3/Ph	-0.23	-0.25
	-0.68	-0.73

Table 5.2 Linear E^{o}/inductive parameter correlations in $[M(S_2C_3RHR')_2]$ (where M = nickel and cobalt)

$$E^{o} = k(\sigma^{e}_{R} + \sigma^{e}_{R'})$$

(least squares fitted gradients, 1000 k/V, with correlation coefficients in parenthesis)

		Cobalt	Nickel
$E^{o}_{red}(1)$:	k =	188 (1.00)	177 (1.00)
$E^{o}_{red}(2)$:	k =	178 (0.98)	148 (0.99)

Figure 5.2 Electrode potential/ substituent effect for the $[Co(S_2C_3RHR')_2]$ complexes

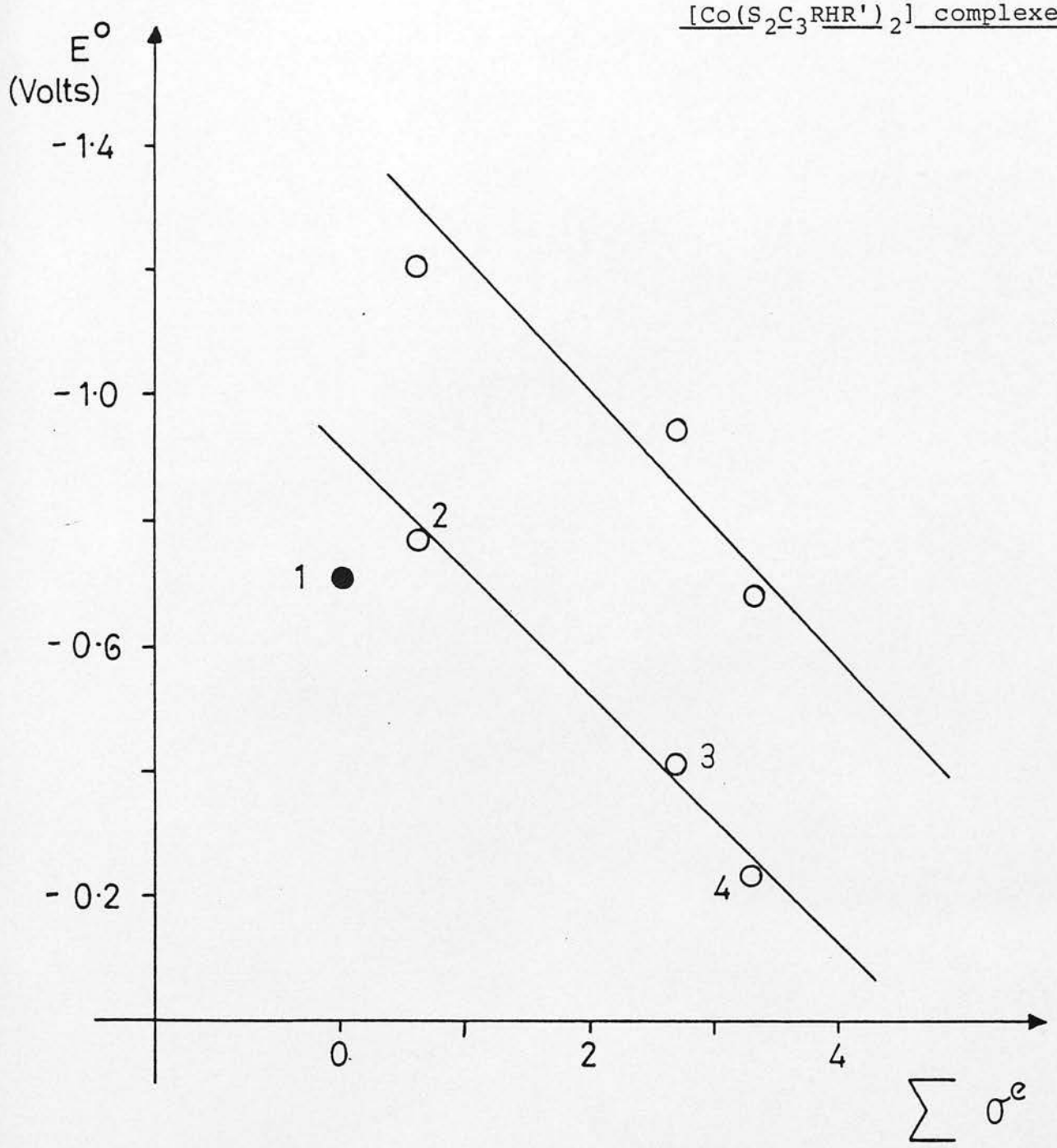

1 = CH_3/CH_3 ; 2 = CH_3/Ph ; 3 = CH_3/CF_3 ;

4 = CF_3/Ph

● not included in l.s. analysis

study of a range of square-planar Ni(II) Schiff's-base complexes, where reaction with MeI was only observed when a metal-based reduction was found, to give a reactive Ni(I) centre[37].

The rather unexpected behaviour of the substituted cobalt complexes obviously meant that we could not use an electron-withdrawing group to stabilize the Co(III)-alkyl species. A fairly limited range of complexes have been examined so far, and before drawing any definite conclusions as to why the electrochemical characteristics of the substituted complexes are so far removed from $[Co(SacSac)_2]$, the variety of complexes studied should be extended. Furthermore, a detailed examination of the U.V./visible and E.S.R. spectra might be helpful in detecting if orbital rearrangement upon substitution is in line with the electrochemical changes observed. It appears on qualitative examination that the U.V./visible spectra of the substituted cobalt(II) complexes are more similar in general character to the d^8-range of complexes than is $[Co(SacSac)_2]$ itself.

5.3 Complexities in the voltammetry of [Co(SacSac)$_2$] - Electrode adsorption phenomena (concentration dependence at the d.m.e.)

As discussed in the previous section (5.2), [Co(SacSac)$_2$] shows two successive reductions, attributed to the complex, at -0.71 and -1.70 Volts (vs Ag/AgCl), representing a fully reversible and a quasi-reversible one-electron reduction respectively. These potentials are obtained irrespective of whether a d.m.e. or a platinum wire working electrode are employed. However, a distinct adsorption wave at -0.90 Volts was observed on the d.m.e. which was completely absent on platinum[34]. (This is most clearly illustrated in the a.c. mode, Figure 5.3). This behaviour is found in both acetone and methylene chloride, hence, not a solvent effect. We have found, however, that the characteristic electrode response is dependent on [Co(SacSac)$_2$] concentration.

At high dilution, i.e. 10^{-5} molar in complex, only the adsorption wave is observed, while the first complex reduction wave at -0.71 Volts is completely absent on the d.m.e. (but is clearly evident on platinum). The adsorption wave increases in an approximately linear manner with concentration from 1×10^{-5} to 8×10^{-5} M, but then increases more slowly, until reaching a maximum at 8×10^{-4} M, (Figure 5.4). The first reduction attributed to complex at -0.71 Volts first becomes evident at 2×10^{-4} M in CH_2Cl_2 and 1.5×10^{-4} M in acetone (with concurrent development of the second reduction at -1.70 Volts), and then increases linearly with concentration.

Figure 5.3 Electrochemical behaviour of $[Co(SacSac)_2]$ in the a.c. mode, showing effect of changing working electrode

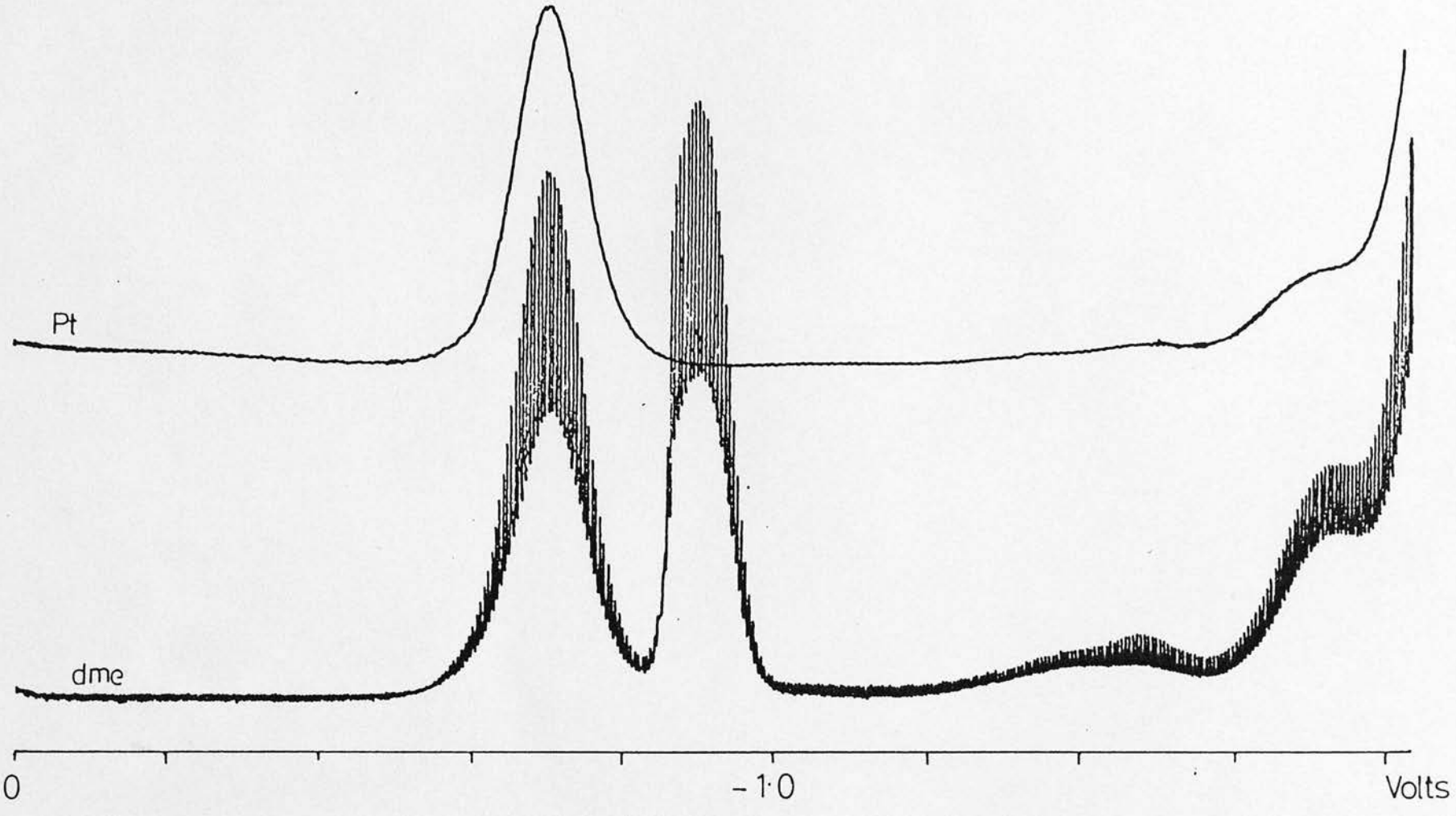

Figure 5.4 Variation of current response with changing concentration for the adsorption wave of $[Co(SacSac)_2]$ at d.m.e.

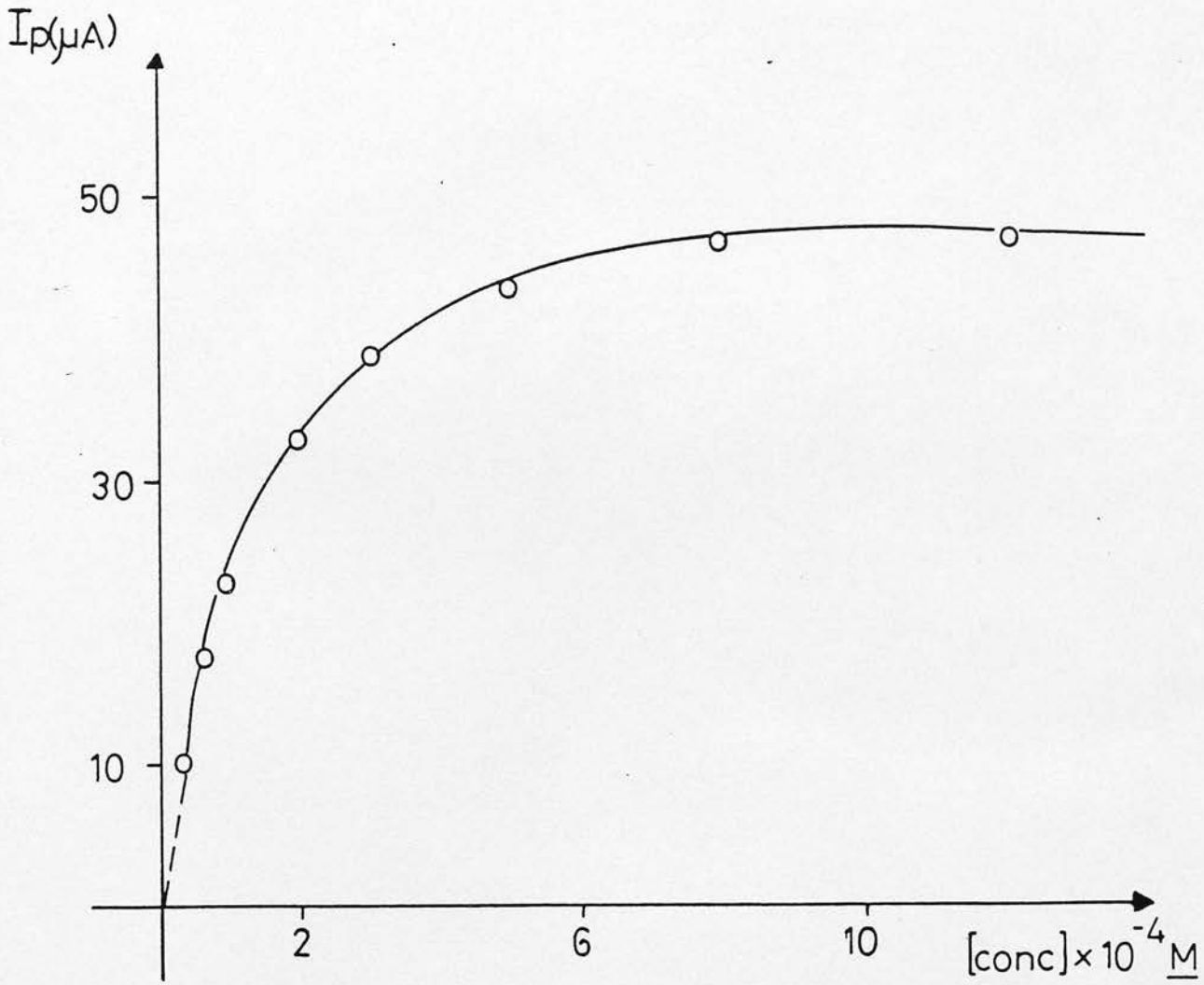

Thus, at "normal" electrochemical concentrations (1×10^{-3} M) the adsorption process appears to be a relatively minor operation, whereas at very dilute concentrations, this process is dominant and the true wave may be absent - an unusual and striking phenomenon.

Using a platinum wire working electrode, the two reduction waves attributable to complex reduction are clearly in evidence throughout the complete concentration range, with no indication of the adsorption process found for the d.m.e. The first reduction gives a linear dependence of I_p (a.c. measurement) with concentration. Thus, the characteristic electrochemical behaviour of $[Co(SacSac)_2]$ at a platinum electrode is independent of the concentration of the electroactive species.

As we expected, the adsorption phenomenon observed on mercury is temperature dependent. On lowering the cell temperature from 293 to 268 Kelvin, the first reduction of $[Co(SacSac)_2]$ at -0.71 Volts only becomes evident on the d.m.e. at 4×10^{-4} M (c.f. 2×10^{-4} M at 293 Kelvin), although even on cooling at 233 Kelvin, no adsorption process is observed on the platinum electrode.

High-temperature measurements employed methyl naphthalene at 423 Kelvin as an electrochemical solvent. At a concentration of 2.4×10^{-4} molar in $[Co(SacSac)_2]$, at which an adsoprtion wave would clearly be in evidence at room temperature, only single reduction on the d.m.e. was observed, at -0.70 Volts, with no indications of any adsorption phenomena.

Examination of $[Ni(SacSac)_2]$ over a similar concentration range, on both d.m.e. and Pt working electrodes, shows no such anomalous behaviour. Equally, careful study of $[Co(S_2C_3CF_3HCH_3)_2]$ at 2×10^{-5} and 2×10^{-4} molar in complex also shows no indications of any adsorption processes on the d.m.e.

It would seem apparent, therefore, that $[Co(SacSac)_2]$ specifically adsorbs onto the surface of the mercury electrode, to produce a complex which is reduced at more negative potentials than $[Co(SacSac)_2]$ itself. The extent of this reaction is limited by the mercury surface. Above certain concentrations ($> 2 \times 10^{-4}$ M) both reduction pathways are in evidence, but further increase in concentration produces growth only in the peak corresponding to reduction of $[Co(SacSac)_2]$ itself. By changing the temperature, i.e. changing the surface character of the mercury electrode, we alter the solution concentration necessary to achieve significant adsorption.

As $[Co(SacSac)_2]$ is the only planar dithio-β-diketonate which exhibits this adsorption process on mercury, it would be extremely interesting to establish (when a larger range of substituted cobalt complexes becomes available) if this behaviour is connected with the metal-based character of the first reduction of $[Co(SacSac)_2]$.

5.4 Reaction with dioxygen

If the a.c. background profile of non-degassed Bu_4NBF_4/CH_2Cl_2 is recorded, then a well-defined oxygen wave (O_2/O_2^-) is observed at -0.73 Volts (vs. Ag/AgCl) using a d.m.e. working electrode. This wave is also present when using a platinum working electrode, but is very much broader and consequently less well defined. By strenuous degassing with CH_2Cl_2-saturated argon, all traces of dissolved O_2 can be removed from the electrochemical medium.

Addition of $[Co(SacSac)_2]$ to the fully degassed medium shows the same electrochemical behaviour on both d.m.e. and platinum electrodes as recorded previously (see Section 5.3) i.e. the reduction of $[Co(SacSac)_2]$ at -0.71 Volts, with the adsorption wave (on d.m.e.) at -0.90 Volts, and the second, kinetically sluggish, ligand-based reduction of $[Co(SacSac)_2]$ at -1.70 Volts.

On deliberately admitting O_2 to the system, we observe a dramatic reduction in current response for the Co(II)/Co(I) couple, together with a shift to less negative potentials, -0.66 Volts. On mercury, the adsorption wave is still in evidence (although substantially reduced). The change in current response, and the shift in potential is observed irrespective of electrode material, but the platinum electrode shows the situation more clearly as there are no adsorption complications, or free O_2 peaks at similar potentials to the complex reduction. The behaviour of the

second complex reduction is less easily characterised, due to the sluggish nature of the charge transfer, but a decrease in current response is initially observed.

The reaction with O_2 is completely reversible, i.e. the characteristic electrode response of $[Co(SacSac)_2]$ can be regained to its original current intensity by degassing the solution, thus reaction of $[Co(SacSac)_2]$ with O_2 does not result in the irreversible degradation of the complex. This cycle can be reproduced repeatedly without loss of the original $[Co(SacSac)_2]$ species.

A number of transition metal chelates have been considered as models of biological oxygen carriers[38]. The cobalt(II) chelates are particularly suitable as reversible oxygen carriers (the analogous iron(II) chelates generally undergo irreversible oxidation), for example[39,40]

$$[Co(II)L(py)]^0 + O_2 \longrightarrow [Co(II)L(py)(O_2)]^0$$

where py = pyridine

L = quadridentate ligand obtained from salicyl-aldehyde and 1,2-disubstituted ethylenediamine.

Note, no change in oxidation state of the metal centre.

Thus, just as $[Co(SacSac)_2]^{1-}$ shows a reaction with RX directly analogous to the five-coordinate "Co(I) cobaloximes" (see Section 5.1), we also observe oxygenation reactions similar to the axially co-ordinated [CoL(py)] complexes.

The reaction of $[Co(S_2C_3CF_3HCH_3)_2]$ with dioxygen has also been studied. This significantly simplifies the electrochemistry as the complex reductions are well removed from the O_2/O_2^- couple (-0.41 and -0.94 Volts) and no adsorption phenomena are present. On the introduction of O_2 into the system (using a d.m.e. working electrode) we again observe a large decrease in current for the first reduction, together with an anodic shift to -0.33 Volts, with the concurrent disappearance of the second reduction and the development of a free dioxygen reduction. Again the process can be reversed by degassing. Corresponding changes are found when using a platinum working electrode.

This oxygenation reaction has great promise in the possible development of cobalt(II)dithio-β-diketonates as unusual dioxygen carriers. Further work, however, is obviously required, for example, the introduction of measured quantities of O_2 into the system, the isolation of the oxygenation product, measurement of equilibrium constants, effect of substituent groups (particularly those with a large degree of steric hindrance, e.g. ^{t}butyl) on the efficiency of oxygenation, in addition to the possibility of reaction with other small molecules, e.g. CO.

5.5 Experimental

(i) Materials

Preparations of complexes are as detailed below. Dry ethanol, HCl, and H_2S were prepared as described in Chapter 2. Cobaltous chloride (commercial grade) was dried *in vacuo* at 353 Kelvin. The appropriate β-diketonate ligand was obtained commercially and used without further purification.

Electrochemical solvents and Bu_4NBF_4 electrolyte were as described in Sections 3.5 and 4.5 (methyl naphthalene work).

Cobalt(II)bis(dithioacetylacetonate) $[Co(SacSac)_2]$

This was prepared using the method originally developed by Martin and Stewart[28]. Using nitrogen as a carrier gas, dry HCl followed by H_2S (30 minutes and 120 minutes) were bubbled through an ethanol solution of cobaltous chloride (5 g in 100 ml) to which acetylacetone (12 ml) has been added. The dark violet crystals were recovered by filtration, washed with ethanol and diethyl ether, then recrystallised from a 1:1 ratio of ethanol and methylene chloride. Yield 5.4 g (80%). Analysis: Found %C 37.4, %H 4.5, Calculated for $CoC_{10}H_{14}S_4$, %C 37.4, %H 4.4. Electronic spectrum (50,000 to 11,500 cm^{-1} in CH_2Cl_2): 17,860 cm^{-1} (log ε = 3.16), 21,830 cm^{-1} (3.11), 27,620 cm^{-1} (3.64), 29,590 cm^{-1} (3.74), 36,760 cm^{-1} (4.04), 40,000 cm^{-1} (3.86), 44,248 cm^{-1} (3.99).

Cobalt(II)bis(dithiotrifluoroacetylacetonate) $[Co(S_2C_3CF_3HCH_3)_2]$

Anhydrous cobaltous chloride (1.3 g) was suspended in ethanol (5 ml) containing excess 1,1,1-trifluoroacetylacetone (4.5 ml) cooled to 203 Kelvin and thoroughly degassed using nitrogen. Maintaining a slight positive pressure of N_2 throughout, HCl then H_2S were bubbled very rapidly through the solution, (15 and 30 minutes respectively). The reaction mixture was allowed to warm slowly to room temperature and then to stand for 24 hours under nitrogen. The dark blue crystalline material was isolated by filtration, then recrystallised from 1:1 ethanol and CH_2Cl_2, under nitrogen. Yield, recrystallised material, 0.5 g (11.5%). Analysis: Found %C 26.7, %H 2.1 Calculated for $CoC_{10}H_8F_6S_4$ %C 27.9, %H 1.9 Electronic spectrum (50,000 to 11,500 cm^{-1} in CH_2Cl_2): 16,835 cm^{-1} ($\log \varepsilon = 3.37$), 23,500 cm^{-1}(sh), 29,590 cm^{-1} (4.36) 36,765 cm^{-1} (4.71).

Cobalt(II)bis(dithio-1-benzoylacetonate) $[Co(S_2C_3PhHCH_3)_2]$

This was prepared and recrystallised by the same procedure as above, using 1-benzoylacetone (4 g) as ligand. Yield 0.3 g (6.8%), Analysis: Found %C 54.9, %H 4.1. Calculated for $CoC_{20}H_{18}S_4$ %C 54.7, %H 4.1. Electronic spectrum (50,000 to 11,000 cm^{-1} in CH_2Cl_2): 17,065 cm^{-1} ($\log \varepsilon = 3.28$), 22,730 cm^{-1} (3.64), 28,735 cm^{-1} (4.41), 33,670 cm^{-1} (4.40), 39,215 cm^{-1} (4.38).

Cobalt(II)bis(dithiobenzoyl-1,1,1-trifluoroacetonate

$[Co(S_2C_3CF_3HPh)_2]$

This was also prepared by the procedure detailed above, using benzoyl-1,1,1-trifluoroacetone (4.5g) as ligand. Yield 0.55 g (10%). Analysis: Found %C 43.2, %H 2.1 Calculated for $CoC_{20}H_{12}F_6S_4$, %C 43.4, %H 2.2. Electronic spectrum (50,000 to 11,500 cm^{-1} in CH_2Cl_2): 15,480 cm^{-1} (log ε = 3.16) 21,835 cm^{-1} (3.80), 27,780 cm^{-1} (4.49), 32,790 cm^{-1} (4.27), 37,880 cm^{-1} (4.37).

(ii) Instrumentation

Elemental analyses, infrared spectra (KBr disks) and U.V./visible spectra were obtained as described in Chapter 2.

Electrochemical studies employed the equipment and basic 3-electrode cell configuration described in Section 3.5.

(iii) Voltammetric Analysis

The substituted cobalt complexes in general show two, essentially reversible, one-electron reductions. To prevent repetition of data, a representative analysis for $[Co(S_2C_3CF_3HCH_3)_2]$ is described below.

In 0.25 M Bu_4NBF_4/CH_2Cl_2, at both d.m.e. and r.p.e. two cathodic waves of equal height are observed, both exhibiting d.c. Nernstian behaviour appropriate to stepwise one-electron reductions. A.c. peaks are

symmetrical, with half-height width of 90 ± 5 mV and a linear I_p *vs* $\omega^{\frac{1}{2}}$ (passing through the origin) in the frequency range ω = 20 to 1,000 Hz, with phase angle $\phi = 45^{o}$. Cyclic voltammograms in the scan-rate range ν = 50 to 500 mV/sec have E_p = 60 ± 5 mV, I_p(reverse)/I_p(forward) ratios of unity and linear I_p *vs* $\nu^{\frac{1}{2}}$ dependence through the origin.

Concentration studies of [Co(SacSac)$_2$] were conducted over a 1 x 10^{-5} to 1 x 10^{-3} molar concentration range in both methylene chloride and acetone. Voltammetric analysis of the reduction processes assigned to the complex showed the characteristic electrode response as described previously[34], indicative of a reversible first reduction followed by a kinetically sluggish second reduction. The intervening, anomalous reduction found when using a mercury working electrode shows behaviour typical of an adsorption process. A plot of I_p *vs* $\omega^{\frac{1}{2}}$ from a.c. measurements gives a random set of points with no obvious correlation. D.c. polarography yields a curved plot of i_d *vs* $h^{2/3}$, indicative that the anomalous process lacks diffusion control.

References (Chapter 5)

1. N.R. de Tacconi, D. Lexa and J.M. Savéant, J.Am.Chem.Soc., 1979, 101, 467 and references therein.
2. D. Lexa, J.M. Savéant and J. Zickler, J.Am.Chem.Soc., 1980, 102, 2654, 4851 and references therein.
3. T.M. Kenyhercz, T.P. De Angelis, B.J. Norris, W.R. Heineman and H.B. Mark, J.Am.Chem.Soc., 1976, 98, 2469 and references therein.
4. G.N. Schrauzer and E. Deutsch, J.Am.Chem.Soc., 1969, 91, 3341.
5. G.N. Schrauzer, E. Deutsch and R.J. Windgassen, J.Am.Chem.Soc., 1968, 90, 2441.
6. B.M. Babior, J.Biol.Chem., 1970, 245, 6125.
7. J.M. Wood, F.S. Kennedy and C.G. Rosen, Nature, 1968, 220, 173.
8. G. Mestroni, G. Zassinovich and A. Cumus, Trans.Met.Chem., 1976, 1, 32.
9. G. Costa, Coord.Chem.Reviews., 1972, 8, 63.
10. G. Agnes, S. Bendle, H.A.O. Hill, F.R. Williams and R.J.P. Williams, J.C.S. Chem.Comm., 1971, 850.
11. G. Costa and G. Mestroni, J.Organomet.Chem., 1968, 11, 325.
12. G. Costa, G. Mestroni and G. Pillizer, J.Organomet.Chem., 1968, 11, 333.
13. G.N. Schrauzer, L.P. Lee and J.W. Sibert, J.Am.Chem.Soc., 1970, 92, 2997, 7078.
14. G.N. Schrauzer, R.J. Holland, and J.A. Seck, J.Am.Chem.Soc., 1971, 93, 1505.

15. G. Costa, G. Mestroni, A. Puxeddu and E. Reisenhofer, J .Chem.Soc., A., 1970, 2870.

16. B.T. Holding, H.L. Holland, U. Horn and S. Sakrikar, Angew.Chem.Int.Edn., 1970, 9, 959.

17. G. Costa, G. Mestroni and C. Cocevar, Tet.Letters , 1971, 1869.

18. L.G. Marzilli, P.A. Marzilli and J. Halpern, J.Am.Chem.Soc., 1970, 92, 5752.

19. J. Halpern and J. Maher, J.Am.Chem.Soc., 1965, 87, 5361.

20. L.G. Marzilli, P.A. Marzilli and J. Halpern, J.Am.Chem.Soc., 1971, 93, 1374.

21. P.W. Schneider, P. Phelan and J. Halpern, J.Am.Chem.Soc., 1969, 91, 77.

22. G. Costa, A. Puxeddu, and E. Reisenhofer, J.C.S. Dalton, 1972, 1519.

23. D. Pletcher, Chem.Soc. Reviews, 1975, 4, 471.

24. G. Costa, A. Puxeddu and E. Reisenhofer, J.C.S. Dalton, 1973, 2034.

25. G. Costa, G. Mestroni and E. de Savorgnani, Inorg.Chim.Acta, 1969, 3, 323.

26. G. Costa, G. Mestroni and G. Tauzher, J.Chem.Soc. Dalton, 1972, 450.

27. R.G. Finke, B.L. Smith and M.W. Droege, J.Organomet.Chem., 1980, 202, C25 and references therein.

28. R.L. Martin and I.M. Stewart, Nature, 1966, 210, 522.

29. R. Beckett and B.F. Hoskins, J.C.S. Chem.Comm., 1967, 909.

30. R. Beckett and B.F. Hoskins, J.C.S. Dalton, 1974, 622.

Postgraduate Courses Attended

"Synchrotron Radiation and its Applications"

by Dr. I. Munro, Dr. C.D. Garner, Dr. P. Norman
Dr. J. Helliwell and Dr. I. Hillier

"Homogeneous Catalysis"

by Dr. T.A. Stephenson

"Cage and Cluster Compounds"

by Dr. A.J. Welch

"Interpreting the Results of Crystallography"

by Dr. R.O. Gould, Dr. M.D. Walkinshaw and
Dr. A.J. Welch

"Electrochemistry in and out of Mothballs"

by Dr. G.A. Heath

"Chemistry of the Photographic Process"

by Dr. L.A. Williams

"Pulse Sequences and their Applications to N.M.R. Spectroscopy"

by Dr. G.A. Morris

"History of the Chemistry Department"

by Dr. W.P. Doyle

Departmental and Research Seminars and Colloquia